

DTIC FILE

2

# NAVAL POSTGRADUATE SCHOOL

## Monterey, California

DTIC  
S ELECTE D  
JUN 06 1989  
D



AD-A208 483

# THESIS

AN INVESTIGATION INTO THE USE OF AN  
EXISTING SHOCK TUBE AS A DRIVER  
FOR A HYPERSONIC SHOCK TUNNEL

by

Michael H. Sherman

March 1989

Thesis Advisor:

Raymond P. Shreeve

Approved for public release; distribution is unlimited

89 6 05 136

## REPORT DOCUMENTATION PAGE

1a REPORT SECURITY CLASSIFICATION UNCLASSIFIED			1b RESTRICTIVE MARKINGS		
2a SECURITY CLASSIFICATION AUTHORITY			3 DISTRIBUTION/AVAILABILITY OF REPORT Approved for public release; distribution is unlimited		
2b DECLASSIFICATION/DOWNGRADING SCHEDULE			5 MONITORING ORGANIZATION REPORT NUMBER(S)		
4 PERFORMING ORGANIZATION REPORT NUMBER(S)			5 MONITORING ORGANIZATION REPORT NUMBER(S)		
6a NAME OF PERFORMING ORGANIZATION Naval Postgraduate School		6b OFFICE SYMBOL (If applicable) Code 67		7a NAME OF MONITORING ORGANIZATION Naval Postgraduate School	
6c ADDRESS (City, State, and ZIP Code) Monterey, California 93943-5000			7b ADDRESS (City, State, and ZIP Code) Monterey, California 93943-5000		
8a NAME OF FUNDING/SPONSORING ORGANIZATION		8b OFFICE SYMBOL (If applicable)		9 PROCUREMENT INSTRUMENT IDENTIFICATION NUMBER	
8c ADDRESS (City, State, and ZIP Code)			10 SOURCE OF FUNDING NUMBERS		
			PROGRAM ELEMENT NO.	PROJECT NO.	TASK NO.
			WORK UNIT ACCESSION NO.		
11 TITLE (Include Security Classification) AN INVESTIGATION INTO THE USE OF AN EXISTING SHOCK TUBE AS A DRIVER FOR A HYPERSONIC SHOCK TUNNEL					
12 PERSONAL AUTHOR(S) Sherman, Michael H.					
13a TYPE OF REPORT Master's Thesis		13b TIME COVERED FROM TO		14 DATE OF REPORT (Year, Month, Day) 1999, March	
15 PAGE COUNT 152					
16 SUPPLEMENTARY NOTATION The views expressed in this thesis are those of the author and do not reflect the official policy or position of the Department of Defense or the U.S. Government.					
17 COSATI CODES			18 SUBJECT TERMS (Continue on reverse if necessary and identify by block number)		
FIELD	GROUP	SUB GROUP	Shock Tube; Tailoring; Shock Tunnel		
19 ABSTRACT (Continue on reverse if necessary and identify by block number) Experiments were carried out using an existing tube alone, and with the tube connected to a two-dimensional wedge nozzle. The range of maximum dura- tion of steady reflected pressure from 3.5 to 5 milliseconds was achieved through tailored operation for incident shock strengths of 3.4 and 2.0, using pure Helium and a 70% Helium/30% Nitrogen mixture as the driver gas respectfully.  Spark and continuous light shadowgraph techniques were attempted using an optical window at the Mach 4.3 location. Results demonstrated that the short duration flow phenomena in a shock tunnel can be recorded successfully using existing equipment. Calculations showed that the addition of a Mach 10 nozzle and 15 m <sup>3</sup> (6' diameter x 15' long) dump chamber would provide a useful hyper- sonic facility for instruction and research.					
20 DISTRIBUTION/AVAILABILITY OF ABSTRACT <input checked="" type="checkbox"/> UNCLASSIFIED/UNLIMITED <input type="checkbox"/> SAME AS RPT <input type="checkbox"/> DTIC USERS			21 ABSTRACT SECURITY CLASSIFICATION Unclassified		
22a NAME OF RESPONSIBLE INDIVIDUAL Prof. Raymond P. Shreeve			22b TELEPHONE (Include Area Code) (408) 646-2165		22c OFFICE SYMBOL Code 67Sf

Approved for public release; distribution is unlimited

An Investigation into the Use of an Existing  
Shock Tube as a Driver for a Hypersonic Shock Tunnel

by

Michael H. Sherman  
Civilian, Naval Air Systems Command  
B.S., Pennsylvania State University, 1983

Submitted in partial fulfillment of the  
requirements for a degree of

MASTER OF SCIENCE IN AERONAUTICAL ENGINEERING

from the

NAVAL POSTGRADUATE SCHOOL  
March 1989

Author:

Michael H. Sherman  
Michael H. Sherman

Approved by:

Raymond P. Shreeve  
Raymond P. Shreeve, Thesis Advisor

David W. Netzer  
David W. Netzer, Second Reader

Anna F. Plotter  
for E. Roberts Wood, Chairman  
Department of Aeronautics and Astronautics

G.E. Schacher  
G.E. Schacher,  
Dean of Science and Engineering

### ABSTRACT

Experiments were carried out using an existing tube alone, and with the tube connected to a two-dimensional wedge nozzle. The range of maximum duration of steady reflected pressure from 3.5 to 5 milliseconds was achieved through tailored operation for incident shock strengths of 3.4 and 2.0, using pure Helium and a 70% Helium/30% Nitrogen mixture as the driver gas respectfully.

Spark and continuous light shadowgraph techniques were attempted using an optical window at the Mach 4.3 location. Results demonstrated that the short duration flow phenomena in a shock tunnel can be recorded successfully using existing equipment. Calculations showed that the addition of a Mach 10 nozzle and 15 m<sup>3</sup> (6' diameter x 15' long) dump chamber would provide a useful hypersonic facility for instruction and research.



Accession For	
NTIS CRA&I	<input checked="checked" type="checkbox"/>
DTIC TAB	<input type="checkbox"/>
Unannounced	<input type="checkbox"/>
Justification	
By	
Distribution /	
Availability Codes	
Dist	Avail and/or Special
A-1	

## TABLE OF CONTENTS

I.	INTRODUCTION -----	1
II.	THEORETICAL CONSIDERATIONS--A REVIEW -----	5
	A. BASIC SHOCK TUBE -----	5
	B. PERFORMANCE -----	8
	C. SHOCK TUNNELS -----	12
	D. TAILORED OPERATION -----	19
III.	NPS SHOCK TUBE -----	26
	A. STRUCTURE -----	26
	B. DIAPHRAGM CHAMBER -----	26
	C. NOZZLE ASSEMBLY -----	30
	D. INSTRUMENTATION -----	35
	E. OPTICAL MEASUREMENT SYSTEMS -----	41
IV.	EXPERIMENTAL PROCEDURE -----	47
	A. PREPARATION -----	47
	B. LOADING THE DRIVEN GAS -----	47
	C. LOADING THE DRIVER GAS AND FIRING -----	47
V.	EXPERIMENTAL RESULTS AND DISCUSSION -----	49
	A. TAILORING -----	49
	B. TIME OF STEADY PRESSURE -----	50
	C. PRESSURE RECOVERY -----	54
	D. REFLECTED TEMPERATURE -----	54
	E. SHOCK ATTENUATION -----	54
	F. OPTICAL MEASUREMENTS -----	58

VI.	SIZING CONSIDERATIONS FOR A HYPERSONIC TUNNEL ----	66
A.	NOZZLE THROAT SIZE -----	66
B.	DUMP CHAMBER SIZE -----	67
C.	HIGH ENTHALPY MODIFICATION -----	73
VII.	CONCLUSIONS AND RECOMMENDATIONS -----	74
APPENDIX A:	APPRAISAL OF THE PRESENT SHOCK TUBE -----	76
APPENDIX B:	ESTIMATION OF SHOCK TUNNEL NOZZLE THROAT AREA -----	80
APPENDIX C:	ESTIMATION OF THE REQUIRED DUMP CHAMBER VOLUME -----	84
APPENDIX D:	SUMMARY OF EXPERIMENTAL DATA -----	88
APPENDIX E:	COMPUTER PROGRAM FOR SHOCK TUNNEL EVALUATION -----	126
	LIST OF REFERENCES -----	137
	INITIAL DISTRIBUTION LIST -----	139

## LIST OF TABLES

1.	THEORETICAL PREDICTION OF TEST CONDITIONS FOR A HYPERSONIC NOZZLE ( $M_o = 10$ ) DRIVEN FROM THE REFLECTED REGION OF A SHOCK TUBE -----	16
2.	EXPERIMENTALLY TAILORED MACH NUMBERS FOR DRIVER GAS MIXTURES -----	25
3.	EXPERIMENTALLY DETERMINED REFLECTED PRESSURE MAGNITUDE AND DURATION AND CALCULATED TEMPERATURE (HE DRIVER/ $N_2$ DRIVEN) -----	56
4.	EXPERIMENTALLY DETERMINED PRESSURE MAGNITUDE AND DURATION AND CALCULATED TEMPERATURE (70% HE, 30% $N_2$ DRIVER/ $N_2$ DRIVEN) -----	56
5.	O-RING REPLACEMENT GUIDE -----	77
6.	TIME MEASUREMENT (70% HELIUM 30% NITROGEN DRIVER/ $N_2$ DRIVEN) -----	90
7.	TIME MEASUREMENT (HE DRIVER/ $N_2$ DRIVEN) -----	91

## LIST OF FIGURES

1. Ground Based Testing Facilities -----	2
2. Thermodynamic States in the Operation of a Shock Tube -----	6
3. Time History of Events after Diaphragm is Broken -----	7
4. Pressure Ratio ( $P_4/P_1$ ) Required to Generate a Given Shock Strength Using Various Gas Mixtures -----	9
5. Variation of Shock Strength as a Function of Speed of Sound -----	10
6. Reflected Pressure as a Function of Shock Strength for Equilibrium Air -----	13
7. Reflected Temperature as a Function of Shock Strength for Equilibrium Air -----	14
8. Evolution of a Shock Tunnel -----	15
9. Experimentally Determined Liquification Properties of Air and Nitrogen -----	17
10. Experimental Observation of the Three Types of Wave Interactions in the Reflected Region of a Shock Tube -----	21
11. Available Steady Pressure Time -----	23
12. Experimental Pressure Recovery for Different Driver Gases -----	23
13. Variation of Tailored Mach Number with Helium Fraction -----	24
14. 3" Diameter Shock Tube with Instrumentation Layout -----	27
15. Shock Tube Driver Section -----	28
16. Dual Diaphragm Chamber (Unbolted) -----	29
17. Two Dimensional Nozzle and Dump Chamber -----	31

18.	Assembled Dump Chamber, Model Support and Nozzle -----	32
19.	Dimensional Drawing of the Nozzle -----	32
20.	Optical Window Installation -----	33
21.	Views of the Nozzle and Model Support -----	34
22.	Thin Film Instrumentation Assembly -----	36
23.	Typical Polaroid Photograph of the Thin Film Response from Location B and the Output of the Original Pressure Transducer -----	38
24.	A Typical Recording Using the SD380 Signal Analyzer -----	39
25.	Scientific Atlanta SD380 Four Channel Signal Analyzer with Hard Disk Installed -----	42
26.	Optical Layout Sketch -----	43
27.	Constant Light Source and Lens Mounted on an Adjustable Optical Bench -----	44
28.	Spark Source with High Voltage Power Supply -----	44
29.	Spark Timing Delay Circuit and High Voltage Pulse Generator -----	46
30.	Hycam Movie Camera with Separate Pulse Generator -----	46
31.	Experimentally Determined Endwall Pressure Traces Using Helium as a Driver Gas -----	51
32.	Experimental Determined Endwall Pressure Traces Using a Mixture of 70% Helium and 30% Nitrogen as a Driver Gas -----	52
33.	Comparison of Steady Pressure Time Achieved in the NPS 3 Inch Shock Tube with Experimental Results of Pennelegion -----	53
34.	Comparison of Reflected Pressure Measurements in the NPS 3 Inch Shock Tube with Experimental Results of Pennelegion -----	55
35.	Variation in Shock Transit Times Between Measurement Stations -----	57

36.	Results Obtained Using Hycam Camera -----	60
37.	Spark Shadowgraph with No Flow Present -----	61
38.	Film Exposure without a Spark Source -----	62
39.	Time for Reflected Region Pressure to Drop to Half its Initial Value -----	68
40.	Calculated Time of Decay of Reflected Region Pressure for a 6.5mm Nozzle Throat -----	70
41.	Dump Chamber Volume Requirements -----	72
42.	Shock Strength vs. $P_4/P_1$ for Data Reduced from Polaroid Photographs -----	89
43.	SD380 Menu Selection Items of Interest -----	91

### LIST OF SYMBOLS

$a$	Speed of sound
$A$	Area
$A^*$	Throat area
$C$	Contact surface
$C_1$	Constant (defined in Equation B.3)
$D$	Tube diameter
$m$	Mass
$M$	Mach number
$P$	Pressure
$R$	Rarefaction, or expansion wave
$R_t$	Nozzle throat radius
$S$	Shock
$t$	Time
$t_{start}$	Starting time for the nozzle
$T$	Temperature
$U$	Gas velocity
$V$	Volume
$x_c$	Displacement of shock-contact surface intersection from the end of the tube

### Greek Symbols

$\beta$	Nozzle half angle
$\gamma$	Ratio of specific heats
$\rho$	Density

### Subscripts

D	Dump chamber
e	Exit of the nozzle
i	Region, defined in Figure 3 ( $i = 1-8$ )
S	Shock
t	Stagnation condition in reflected shock region
TE	Tailored condition, from experiment
0	Initial condition in the reflected shock region

### ACKNOWLEDGMENTS

Sponsorship--The Naval Air Systems Command Propulsion and Power Division and Naval Aviation Executive Institute whose dedication to the future needs of the Fleet made this educational opportunity possible.

Special thanks go to Professor R.P. Shreeve whose inspiration and professionalism created an enjoyable learning experience. Valuable insight was gained through his determination and ability to reveal the tools and techniques of experimental work. These lessons will have a positive influence on future analysis and decision making.

Special thanks go to Dr. Michael Jedwab whose assistance in the operation of the signal analyzer is greatly appreciated.

Thanks to Ted Best whose creative abilities in hardware adaptation provided all the equipment necessary for reactivation of the shock tube. Additional thanks to Jack King for his help in instrumentation layout and design.

Most of all I would like to thank my wife, Theresa, whose constant support and dedication to our two children enabled many nights and weekends to be devoted to this effort.

## I. INTRODUCTION

The simulation of flight conditions using ground based facilities has been an essential part of all aircraft development. Figure 1 illustrates the various types of facilities which have evolved to simulate flight at progressively higher speeds and altitudes. Increasing energy requirements led to blow-down wind tunnels. The need to avoid condensation in nozzle expansions required heaters. The very high stagnation enthalpies associated with hypersonic flight led to very short duration, intermittent techniques. Each of the types shown in Figure 1 was in operation more than 20 years ago. A renewed interest in hypersonic simulation has been generated by the National Aerospace Plane(NASP) program.

A recent review of facility requirements for hypersonic propulsion system testing by Dunn and Lori [Ref. 1] concludes that a single ground based facility will not be capable of providing the necessary testing to cover the NASP flight envelope. The planned use of Computational Fluid Dynamic (CFD) codes to bridge the gap left by inadequate ground based facilities will make CFD codes an essential part of the design process but, before confidence can be placed in these codes, fundamental experiments are needed to validate the models incorporated for real gas behavior.

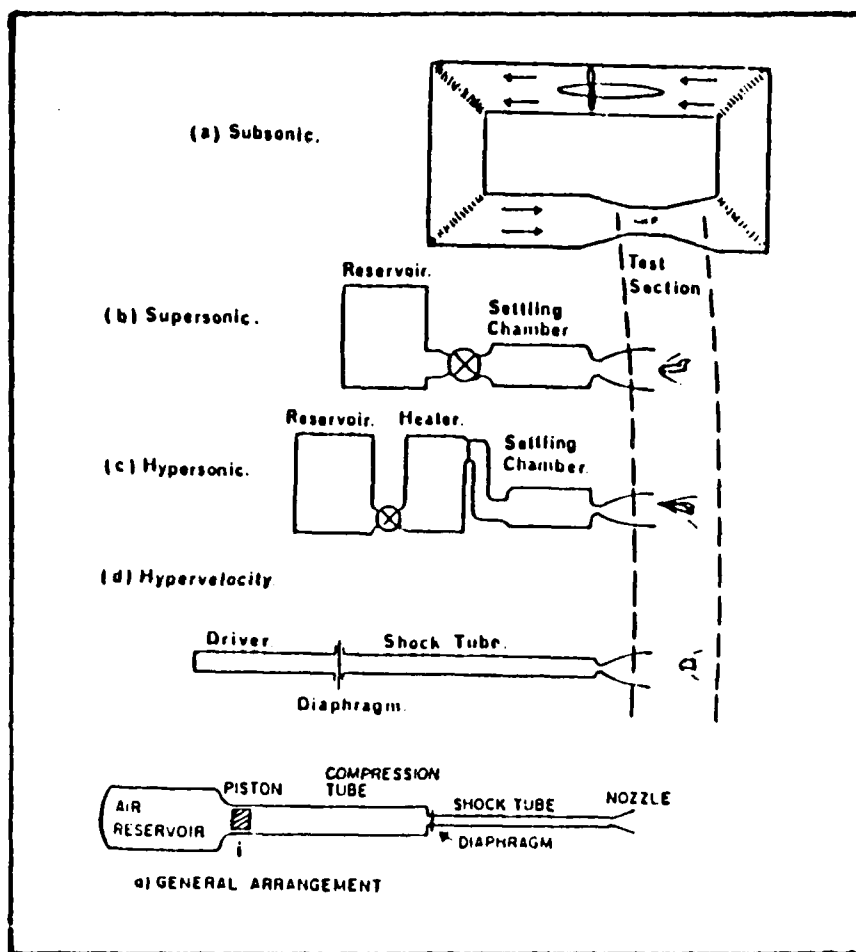


Figure 1. Ground Based Testing Facilities [Ref. 1]

Recognizing the need for CFD validation, the feasibility of establishing a shock tunnel capability by modifying the existing Naval Postgraduate School (NPS) three inch diameter shock tube, was examined in the present study. The time duration and magnitude of constant pressure available in the reflected region of the shock tube were evaluated. The concept of tailoring was examined using two types of driver gases, pure Helium (He) and a mixture of 70% Helium and 30% Nitrogen ( $N_2$ ), driven into Nitrogen as a test gas. An exploratory shock-tunnel nozzle experiment was conducted, and the capability of recording short-duration flow phenomena using available visualization techniques was demonstrated.

It was concluded that the development of an operational hypersonic shock tunnel was feasible and would provide the means for follow-on efforts in the area of CFD code validation. At the same time, such a facility would provide a useful illustration of hypersonic flow to aeronautical and space applications engineering students.

The following material is divided into three sections; 1) a review of shock tube and shock tunnel ideas, 2) a discussion of the experimental investigation including a description of the facilities, experimental procedure and results; and (3) an evaluation of nozzle throat and dump chamber sizing requirements for a hypersonic tunnel. Instrumentation modifications will be required in the

development of a hypersonic capability. Appendix A reviews the existing facility and provides recommendations for upgrading the current hardware and instrumentation. Simplified flow models are developed in Appendices B and C to enable the selection of nozzle throat diameter and dump chamber volume respectively. Experimental pressure and thin film traces obtained in the experimental program are contained in Appendix D together with predicted results obtained using a computer performance code, which is listed in Appendix E.

## II. THEORETICAL CONSIDERATIONS--A REVIEW

### A. BASIC SHOCK TUBE

A shock tube is an economical short duration test facility used in laboratory experiments in gas dynamics, aerodynamics and physics. The principles of shock tube operation, which are well documented in numerous texts, for example, Gaydon and Hurle [Ref. 2] and Owczarek [Ref. 3], are illustrated in Figures 2 and 3 [Ref. 4]. As shown in Figure 2, the device consists of a long tube divided into a high pressure and a low pressure section by a diaphragm. When the diaphragm separating the high pressure driver section, region 4, and the low pressure section, region 1, is ruptured, a series of compression waves coalesce into a single shock front (S) which compresses and heats the region 1 test gas to region 2 conditions. Simultaneously, a series of rarefaction (expansion) waves (R) travel into the high pressure section, region 4, cooling and expanding the driver gas to region 3 conditions.

Region 3 (the expanded driver gas) and region 2 (the compressed test gas) are separated by a contact surface (C). The gases on either side of the contact surface travel with the same velocity, and are at the same pressure, but are different in temperature. A time history of the process (time vs. distance) is shown in Figure 3.

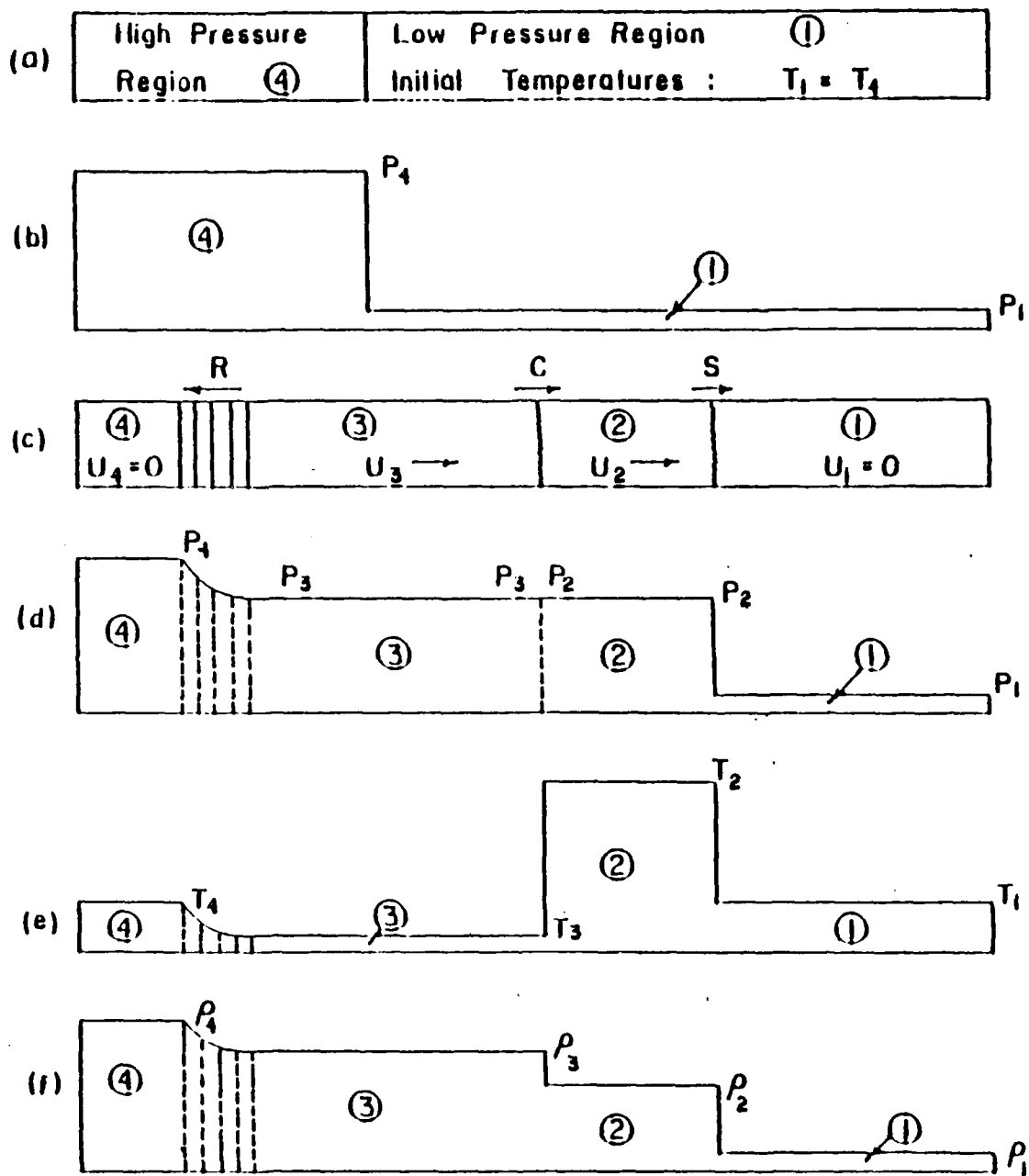


Figure 2. Thermodynamic States in the Operation of a Shock Tube [Ref. 4]

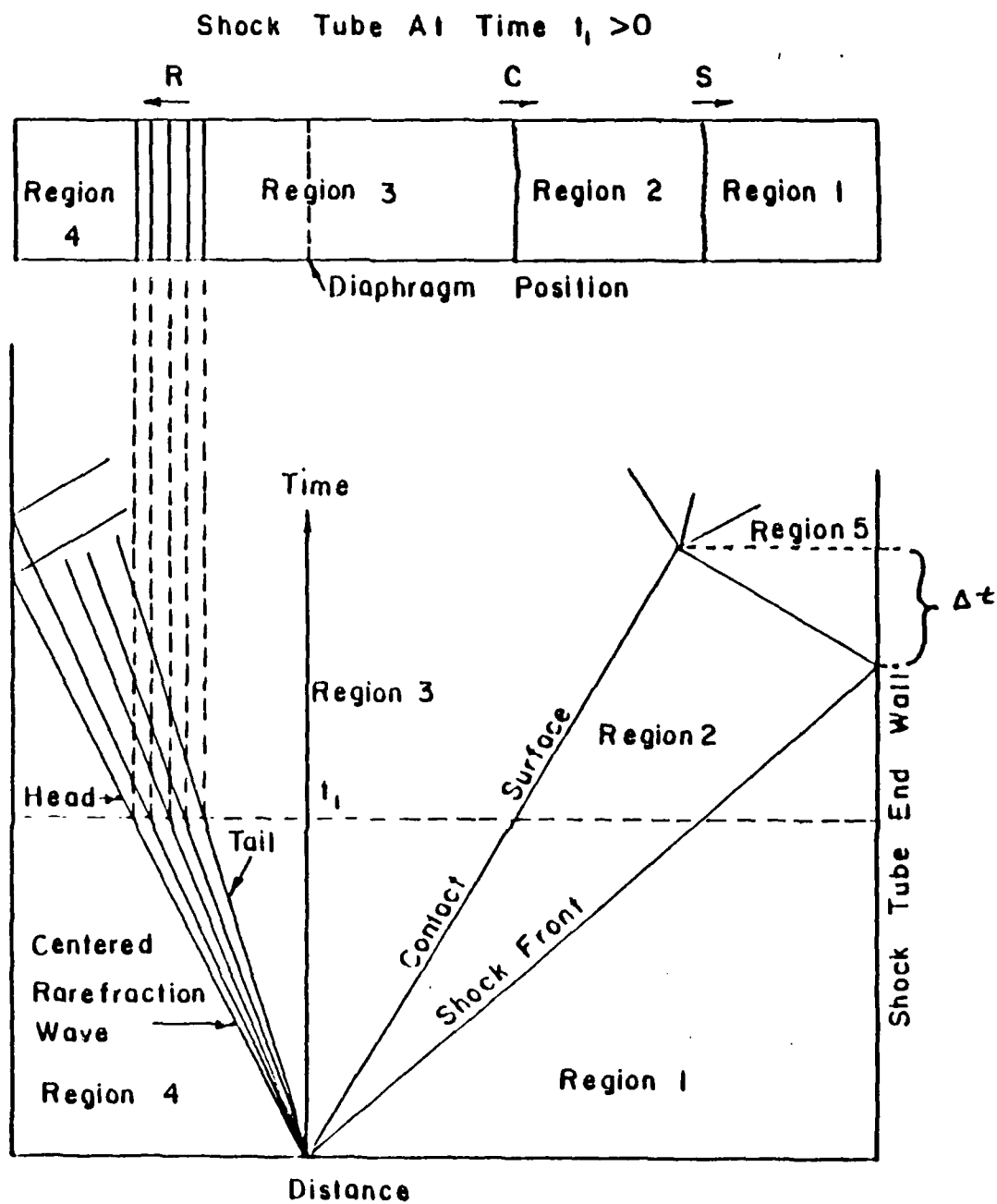


Figure 3. Time History of Events after Diaphragm is Broken [Ref. 4]

What is shown in Figure 3 can be determined accurately using the method of characteristics and shock theory (see [Ref. 3]). As the shock front reflects off the driven tube endwall, the region 2 gas is effectively shocked a second time, creating in region 5 stagnant gas at high pressure and temperature. This region may be used for high temperature gas dynamic studies or, when coupled to a nozzle, made to serve as a reservoir of compressed and heated gas for a hypersonic wind tunnel.

#### B. PERFORMANCE

The strength of the generated shock ( $M_s$ ) is related to the pressure ratio ( $P_4/P_1$ ) across the diaphragm and the speed of sound in the undisturbed gases through the equation given by Gaydon [Ref. 2].

$$\frac{P_4}{P_1} = \frac{2\gamma_1 M_s^{-(\gamma_1-1)}}{(\gamma_1+1)} \left\{ \left( \frac{\gamma_1-(\gamma_4-1)}{(\gamma_1+1)} \frac{a_1}{a_4} \right) \left( \frac{M_s-1}{M_s} \right) \right\}^{-\left(\frac{2\gamma_4}{\gamma_4-1}\right)} \quad (1)$$

Figures 4 [Ref. 5] and 5 [Ref. 6], which illustrate Equation (1), show that the strongest shocks are generated by using high pressure ratios and by using driver gases with high speeds of sound and low ratios of specific heats.

As the desired shock strength increases, the required  $P_4/P_1$  increases significantly. To achieve stronger shocks several approaches are possible. The most common include

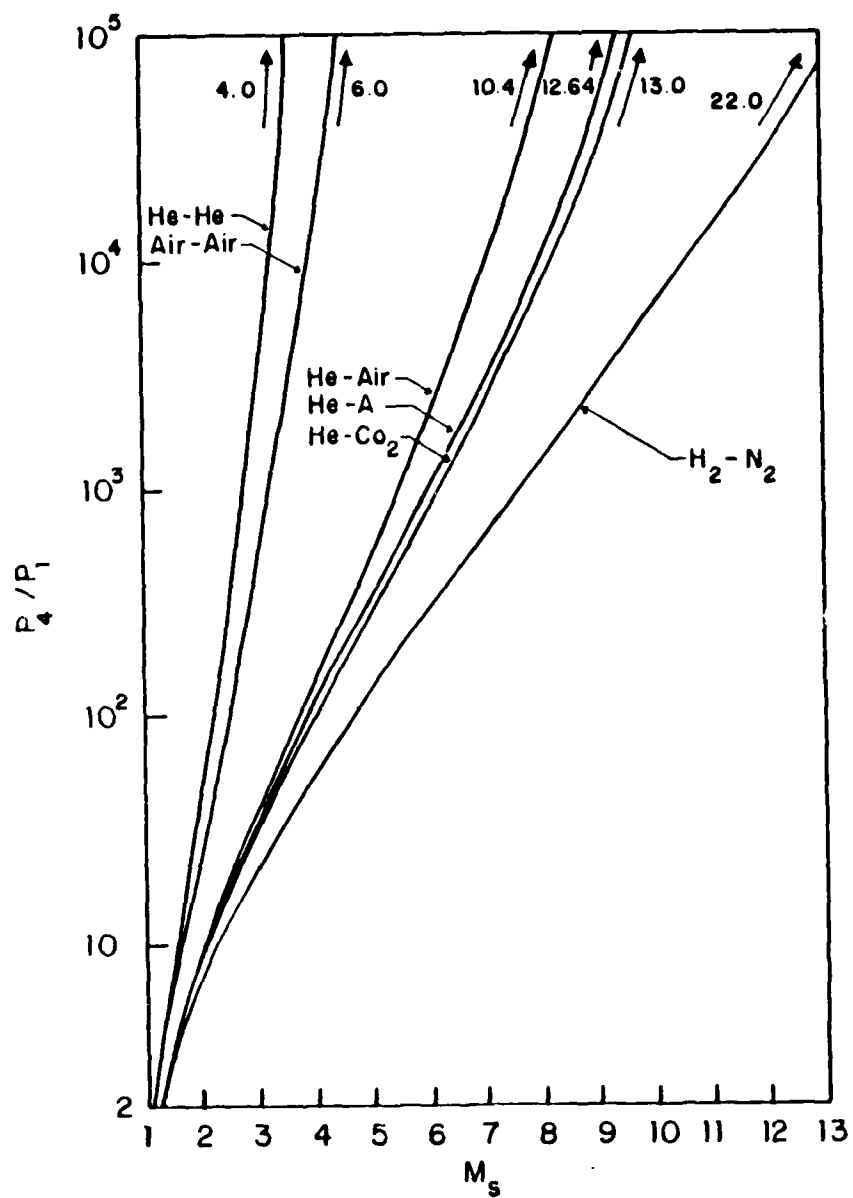
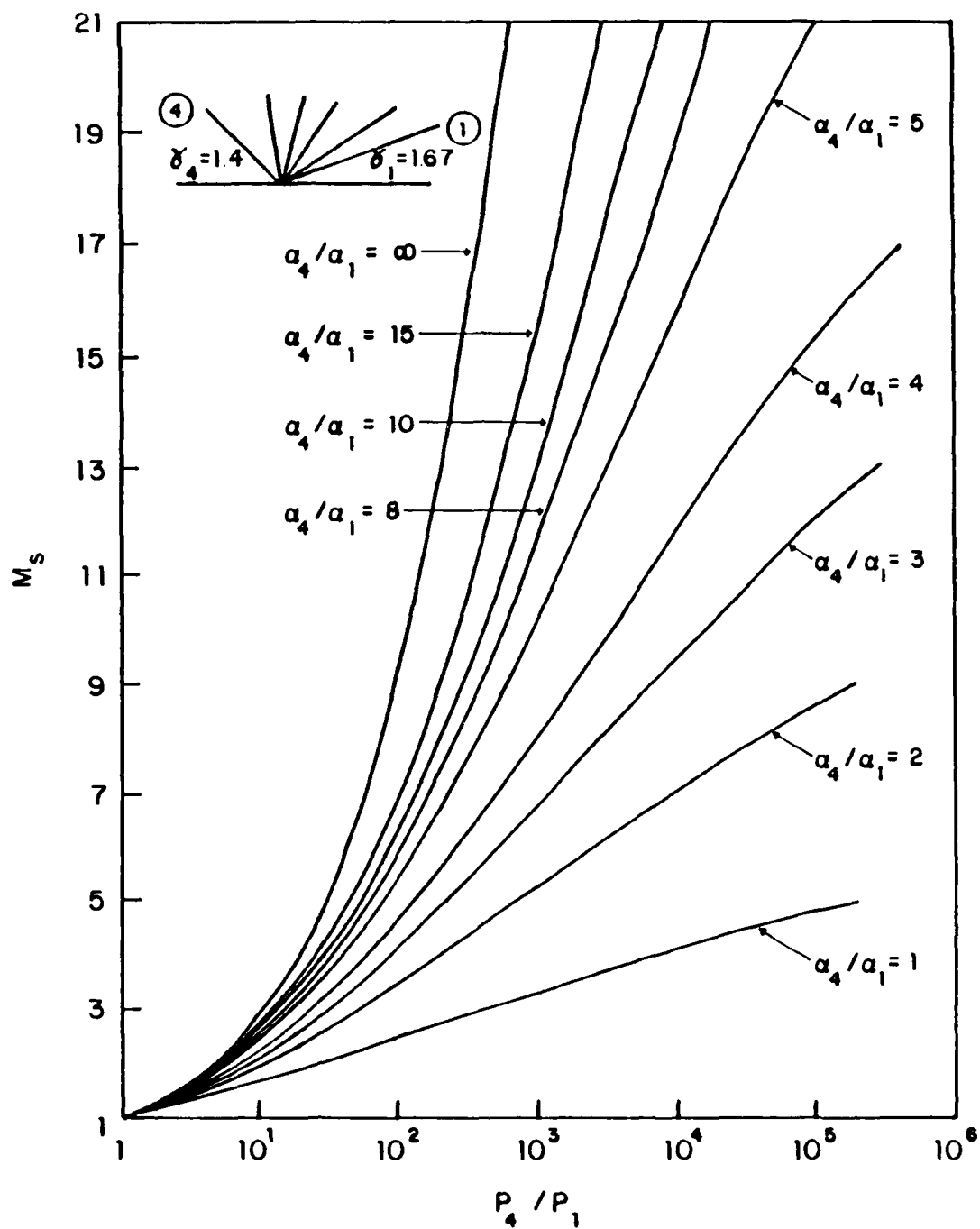
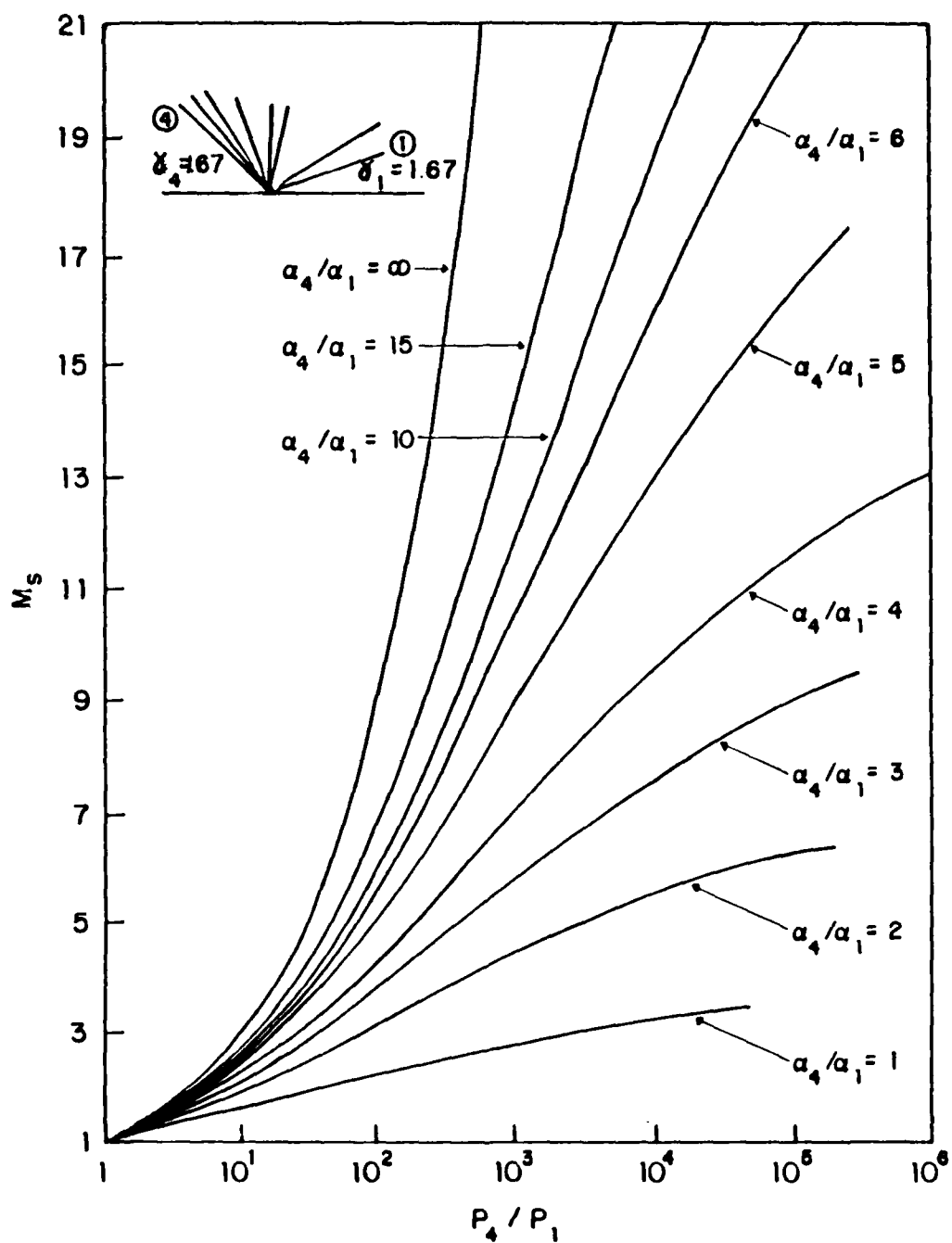


Figure 4. Pressure Ratio ( $P_4/P_1$ ) Required to Generate a Given Shock Strength Using Various Gas Mixtures [Ref. 5]



(a) Driver Gas Specific Heat of 1.4 and a Driven Gas Specific Heat of 1.67

Figure 5. Variation of Shock Strength as a Function of Speed of Sound



(b) Driver Gas Specific Heat of 1.67 and a Driven Gas Specific Heat of 1.67

Figure 5 (CONTINUED)

the use of an area reduction between the driver and driven sections [Ref. 5], the use of multiple diaphragms with a buffer gas in the driver [Ref. 5], and heating the driver gas through combustion or electrical discharge techniques [Ref. 6]. Figures 6 and 7 [Ref. 7] show the relationship between shock strength ( $M_s$ ) and reflected region 5 conditions for equilibrium air.

### C. SHOCK TUNNELS

The reflected region 5 pressure and temperature may be used to supply a supersonic or hypersonic nozzle if the nozzle throat is made sufficiently small to ensure full reflection of the incident shock. The evolution of this arrangement is shown schematically in Figure 8. To maximize test time and minimize the nozzle starting time, often a diaphragm separates the nozzle and dump chamber from the driven end of the shock tube. The dump chamber is sized and evacuated to a level which ensures that, when the tube is fired, the pressure in the chamber remains below the static pressure at the nozzle exit for the duration of steady flow. [Ref 8:pp. 624-640]

For hypersonic applications a conical nozzle is often used. Table 1 provides calculated test conditions for various flow expansions using ideal gas theory. The computer program used for the calculations is described in Appendix E. Since, in an isentropic expansion, static

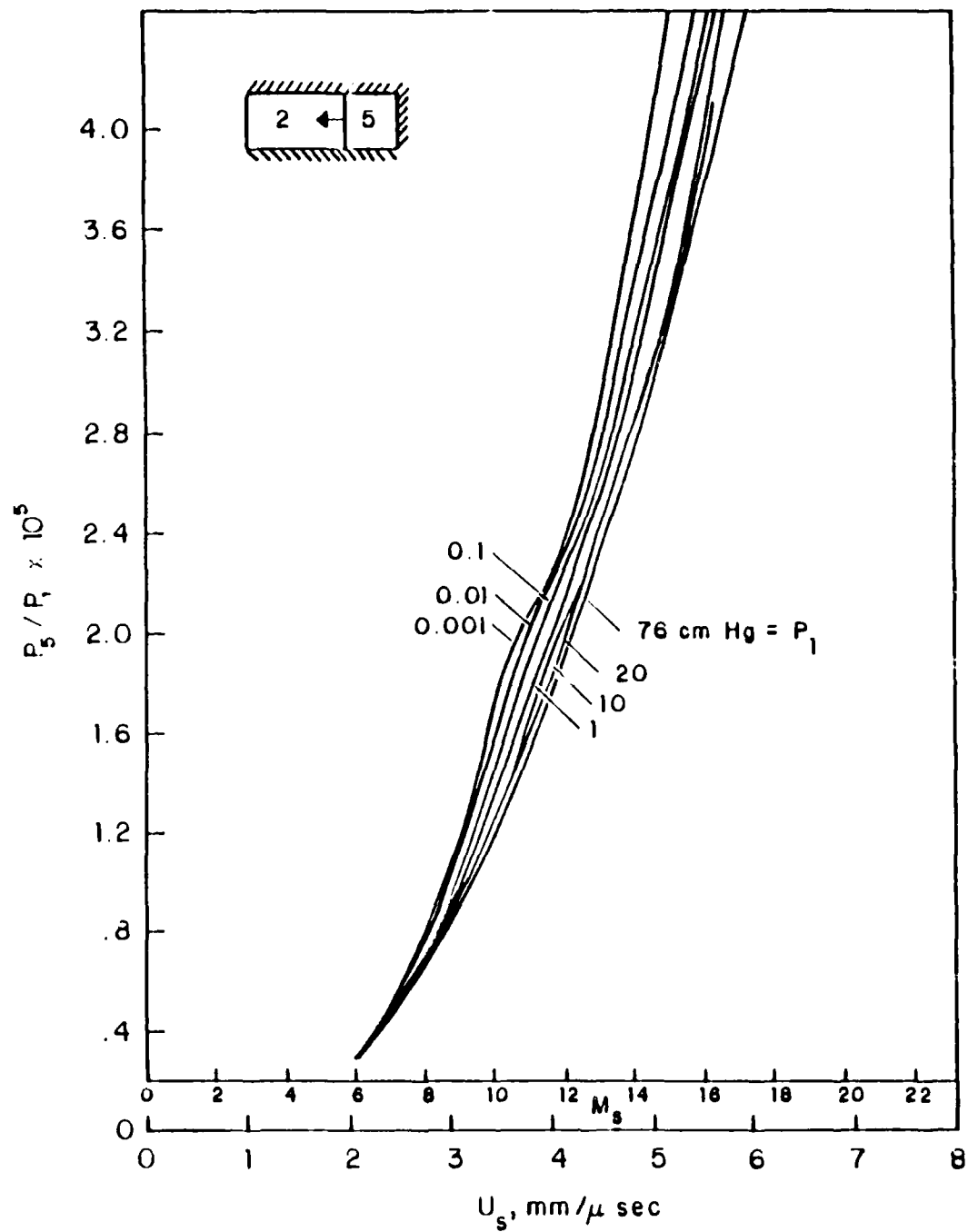


Figure 6. Reflected Pressure as a Function of Shock Strength for Equilibrium Air [Ref. 7]

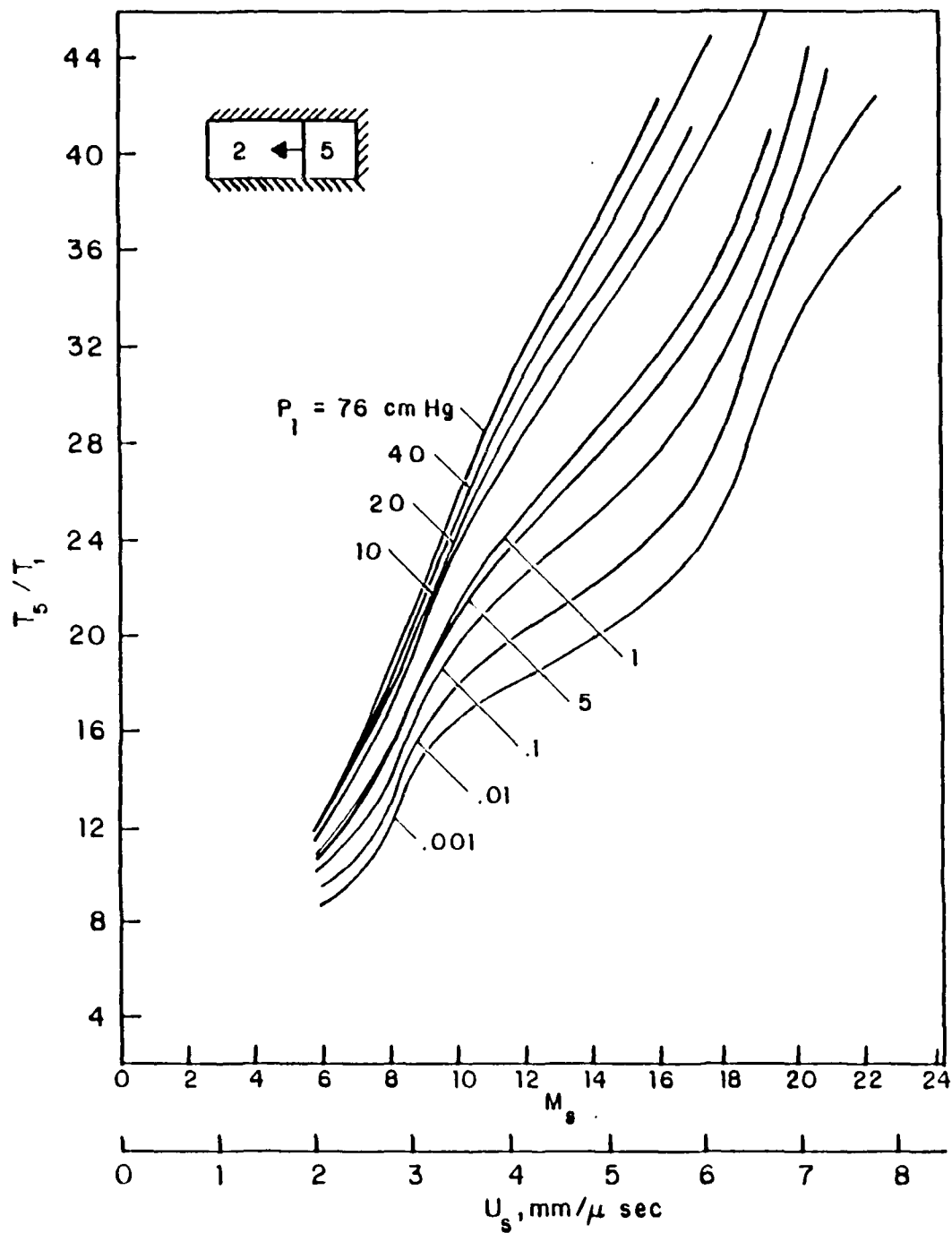


Figure 7. Reflected Temperature as a Function of Shock Strength for Equilibrium Air [Ref. 7]

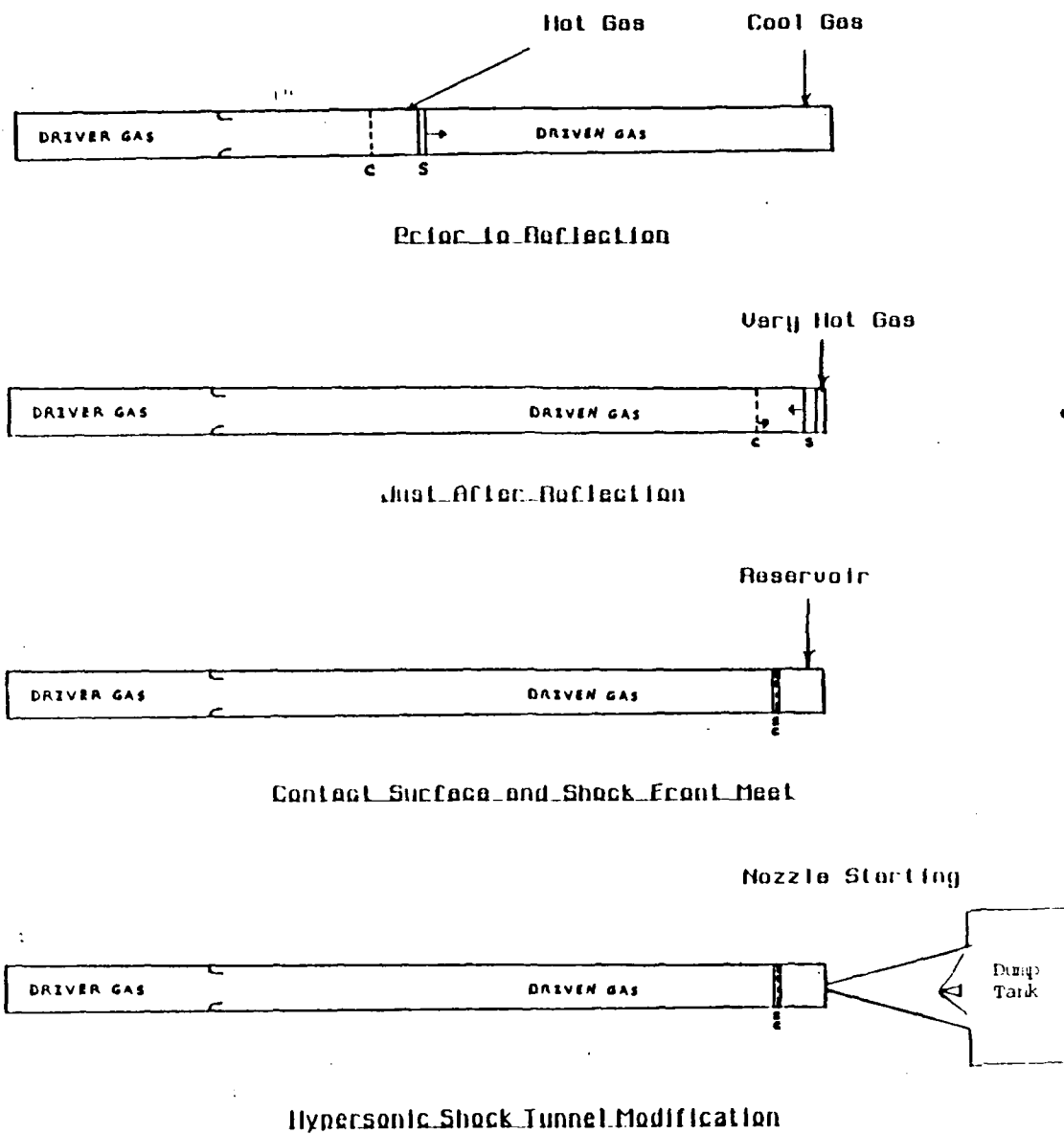


Figure 8. Evolution of a Shock Tunnel

TABLE 1

THEORETICAL PREDICTION OF TEST CONDITIONS FOR A HYPERSONIC  
NOZZLE ( $M_e = 10$ ) DRIVEN FROM THE REFLECTED REGION  
OF A SHOCK TUBE

Driver Gas	$M_s$	$P_5$ (Atm)	$T_5$ (°K)	$P_e$ (mm Hg)	$T_e$ (°K)	$t_{start}$ (msec)
Helium	2.4	58	973	1.02	50	.041
	3.7	32	2000	.55	94	.029
	4.2	23	2460	.41	116	.026
	4.5	19	2700	.33	131	.024
Nitrogen	1.8	23	632	.4	30	.051
	2.4	9.7	971	.169	50	.041
	2.6	6.7	1110	.118	52	.038
	2.8	5.3	1200	.09	56	.037

temperature decreases as the Mach number (of the test section) increases, liquefaction of the test gas becomes an issue. Since nitrogen closely matches the aerodynamic properties of air, but liquefies at a lower temperature, it is preferred for hypersonic facilities in which simulated real gas effects are not required. This is illustrated in Figure 9 which also shows the interesting results of wind tunnel experience [Ref. 9]. In practice, condensation is observed to occur at temperatures which are lower than the saturation temperature, thereby reducing somewhat the

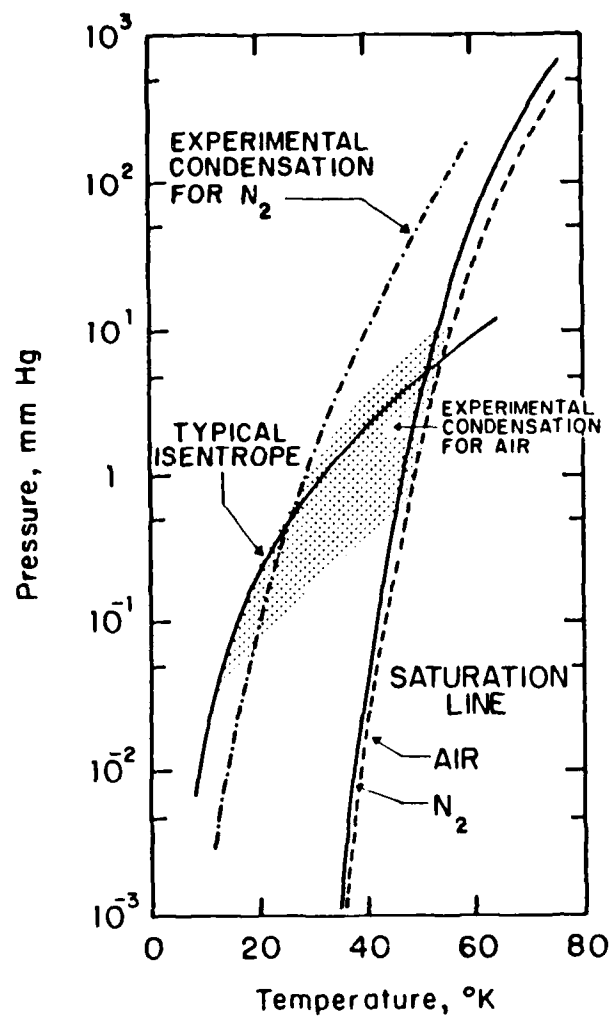


Figure 9. Experimentally Determined Liquification Properties of Air and Nitrogen [Ref. 9]

stagnation temperature requirements to reach a given Mach number.

Given the extremely short test time available in a shock tube, any coupling to a hypersonic nozzle must be done in such a way so as to minimize nozzle starting transients and provide the maximum available steady flow in the test section. The starting time, defined as the time to approach steady flow through a hypersonic conical nozzle ( $\gamma_1 = 7/5$ ), is given by Smith [Ref. 8] as

$$t_{\text{start}} = \frac{.76R_t}{\beta a_5} [M_e^{1/2} (1 - \frac{1}{M_e}) + \frac{1}{15} (M_e^{3/2} - 1) + \frac{1}{25} (M_e^{5/2} - 1)] \quad (2)$$

A reduction in starting time may be achieved by using a large nozzle angle ( $\beta$  = nozzle half angle), a small throat radius ( $R_t$ ) and a high stagnation temperature in the reflected region. [Ref. 8:pp. 625-640] The variation in starting time with increasing incident shock strength for a conical nozzle with  $\beta = 30$  degrees is shown in Table 1.

After the unsteady starting process, the useful test flow will continue as long as a sufficiently high pressure ratio is maintained across the nozzle. The steady flow process will be a function of only the upstream reflected stagnation conditions as long as the dump chamber has sufficient volume. Ideally, uniform reservoir stagnation conditions will end when the reflected region conditions are changed by a wave emanating from the interaction of the

contact surface and the head or tail of the reflected expansion wave (Figure 2). The useful test time in the nozzle ends when the reflected pressure drops below the level required to maintain the static pressure at the nozzle exit above the back pressure in the dump chamber. Thus the useful test time will depend on the nozzle throat size, which governs the flow rate out of the tube, and the size of the dump chamber, which determines the rate at which the back pressure builds up.

#### D. TAILORED OPERATION

##### 1. Tailoring

The fundamental limitation of a shock tube is the available test time. Considerable effort has gone into trying to extend shock tube test times [Ref. 10]. Test times can be lengthened by as much as a factor of ten by "tailoring," which means adjusting conditions so that the ratio of the speed of sound and specific heat behind the reflected shock matches those in the region behind the contact surface. When this tailored condition is present, the reflected shock passes through the contact surface bringing it to rest. A Mach wave is reflected forwards off the contact surface and generates no additional disturbances as it passes through region 5. In the untailored condition, the wave reflected forward from the contact surface is not a Mach wave but a rarefaction wave when  $a_1 < a_3$ , and a shock

wave when  $a_1 > a_3$ . The reflected waves cause conditions in region 5 to change. Experimental evidence of the effect of the wave interactions obtained by Pennelegion [Ref. 10] are shown in Figure 10. Pennelegion's research fully explored tailoring analytically and provided supporting experimental evidence. His findings and experimental techniques were followed in the experiments undertaken in the present study. The tailored interface technique requires that the following equation be satisfied [Ref.10:p. 4];

$$\frac{a_2}{a_3} = \frac{\gamma_1}{\gamma_4} \left[ \frac{1 + \left(\frac{\gamma_1+1}{2\gamma_1}\right) \left(\frac{P_5}{P_2} - 1\right)}{1 + \left(\frac{\gamma_4+1}{2\gamma_4}\right) \left(\frac{P_5}{P_2} - 1\right)} \right]^{1/2} \quad (3)$$

A unique tailored condition (shock Mach number), exists for every combination of driver and driven gas. The duration of constant pressure in region 5 lasts until the rarefaction wave reflects from the driver endplate and returns to meet the contact surface. For low incident shock strengths it is the head of the rarefaction wave, and for high incident shock strengths it is the tail of the rarefaction wave which terminates the constant pressure.

The tailored interface technique for producing extended periods of constant reflected pressure and temperature was demonstrated experimentally for Mach numbers below 3.4. When the technique was applied to shocks of Mach

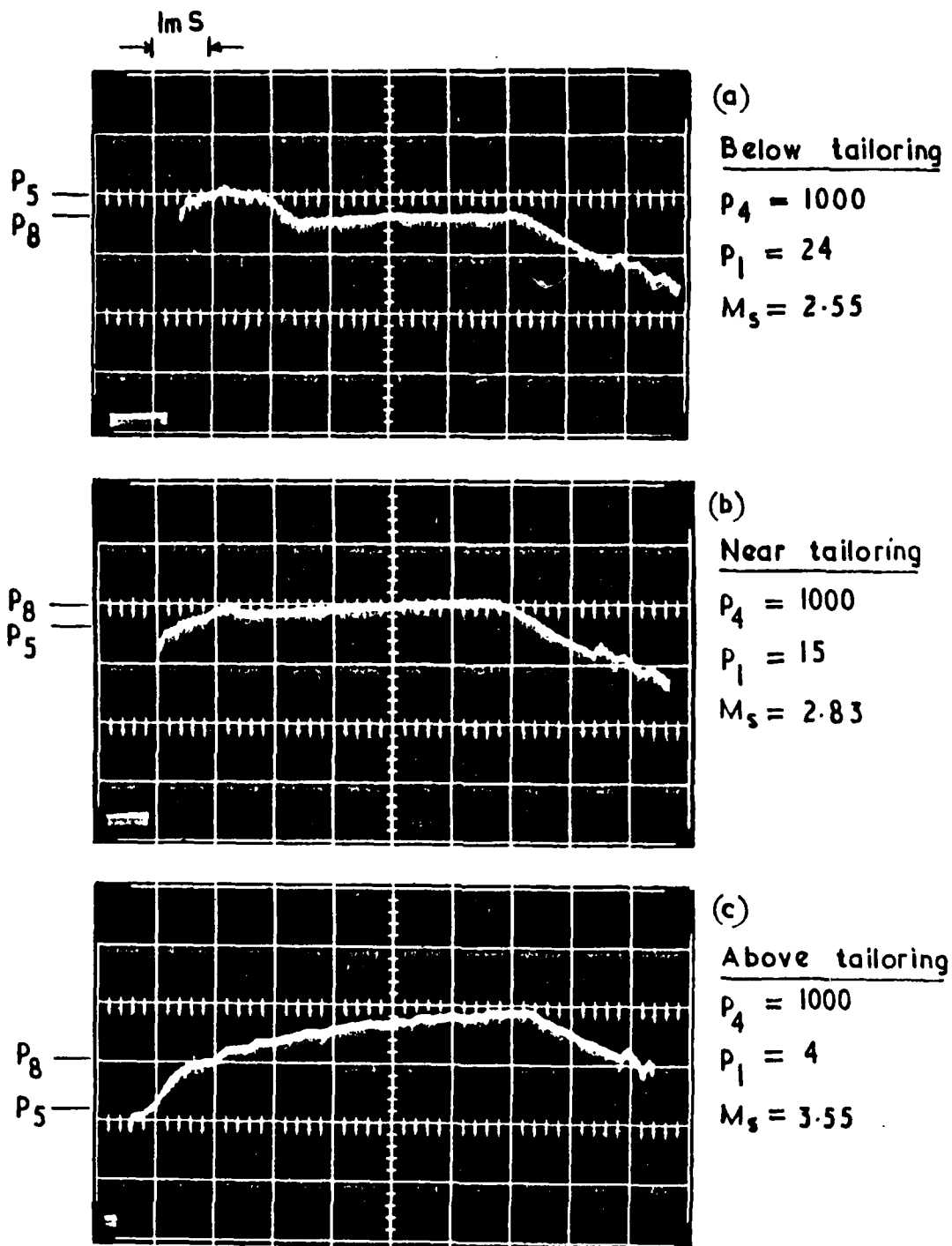


Figure 10. Experimental Observation of the Three Types of Wave Interactions in the Reflected Region of a Shock tube [Ref. 10]

number greater than 3.8, there was a significant drop in test time due to boundary layer interaction. In the under-tailored condition the reflected conditions showed an initial fall in temperature and pressure, followed by a slow rise in pressure and continued drop in temperature. The overtailored condition revealed a pressure rise from the reflection from the contact surface followed by a rapid drop in temperature. In all cases with strong incident shock waves, the real gas effects caused significant variation in the reflected region conditions. [Ref. 10]

## 2. Mixing of Driver Gases (He and N<sub>2</sub>)

The application of tailoring to increase test time in a hypersonic shock tunnel allows more accurate measurements of force and pressure to be made on test models. As desired test section Mach number increases there is a significant decrease in working section static pressure. It is therefore desirable to have reflected region pressures as steady and as high as possible. Pressure recovery, defined as the ratio of the initial step in the reflected pressure ( $P_5$ ) to driven pressure ( $P_4$ ), may be increased by increasing the speed of sound of the driver if some test time is sacrificed. The combination of a driver of Helium (He) and Nitrogen (N<sub>2</sub>) can provide an improvement in test time and pressure recovery over a driver of N<sub>2</sub> alone. Experimental evidence of this is shown in Figures 11 and 12 from Pennelegion [Ref. 10]. From the same study,

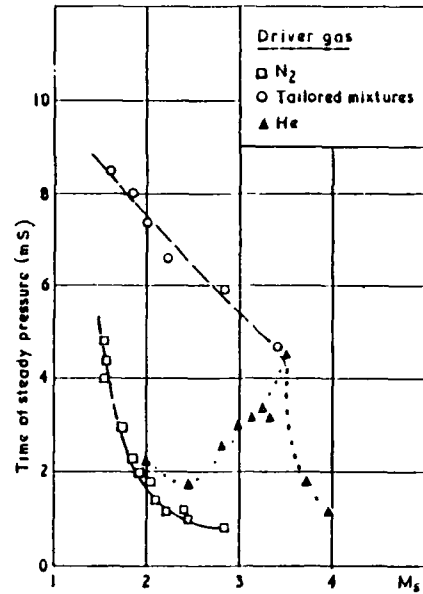


Figure 11. Available Steady Pressure Time [Ref. 10]

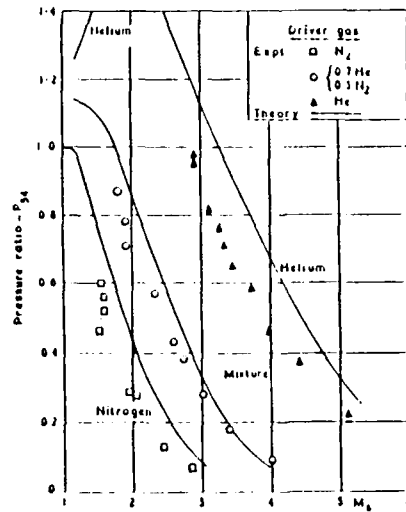


Figure 12. Experimental Pressure Recovery for Different Driver Gases [Ref. 10]

Figure 13 and Table 2 show tailoring using various mixtures of He and N<sub>2</sub> to generate shocks in the range  $1 < M_s < 3.4$ . The tailoring shock Mach number may be selected to provide the required stagnation temperature to prevent liquefaction and maximize test time for hypersonic nozzles with various Mach numbers. Pennelgion [Ref. 10], provided the method for calculating tailored conditions for He, N<sub>2</sub> mixtures.

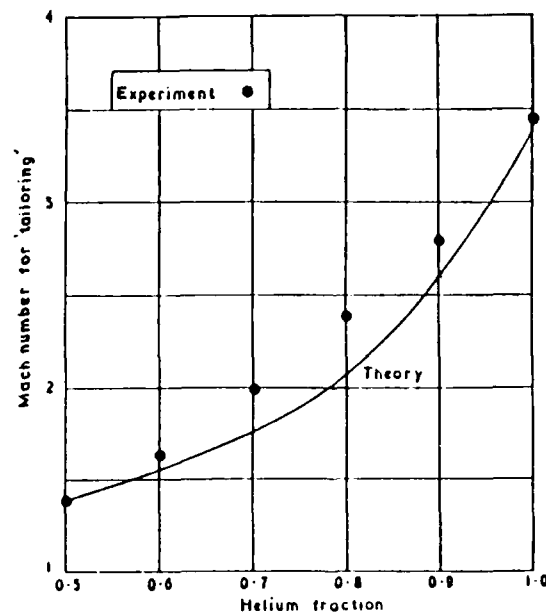


Figure 13. Variation of Tailored Mach Number with Helium Fraction [Ref. 10]

TABLE 2  
EXPERIMENTALLY TAILORED MACH NUMBERS FOR DRIVER  
GAS MIXTURES [REF. 10]

He Fraction	$M_{TE}$	$P_4/P_1$	Time Steady Pressure (msec)	$T_5$ (°K)
0.7	2.0	24	6.5	714
0.8	2.7	60	6.0	1096
0.9	2.8	70	4.7	1159
1.0	3.4	124	4.3	1553

### III. SHOCK TUBE

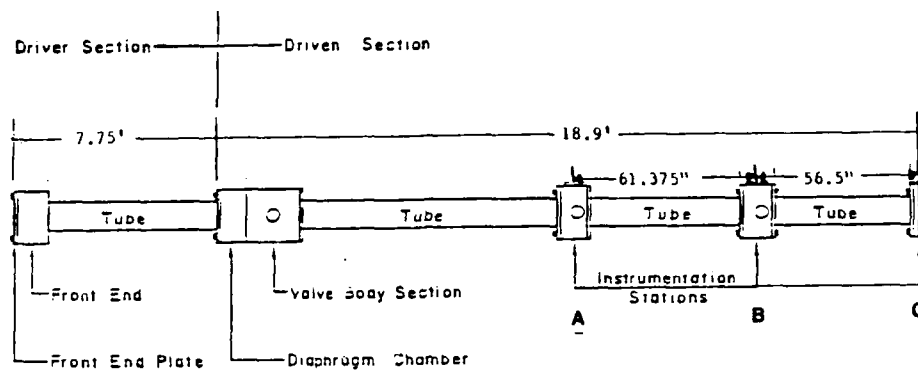
In this section the existing shock tube and instrumentation, and the modifications made during the course of the present experiments, are described.

#### A. STRUCTURE

The three inch diameter shock tube at the Naval Postgraduate School Aeropropulsion Laboratories is shown in Figure 14. A detailed description is given in Penaranda [Ref. 4]. The tube, constructed of highly polished 303 stainless steel consists of a driver section 7.75 feet long, shown in detail in Figure 15, and a driven section 18.9 feet long.

#### B. DIAPHRAGM CHAMBER

The tube incorporates a double diaphragm arrangement to maintain precise and repeatable diaphragm bursting pressure ratios ( $P_4/P_1$ ). The tube currently is fitted with diaphragms designed to burst using a constant driver pressure of 600 psi. Scored brass diaphragms designed to rupture at 400 psi are inserted. Variation in shock speed is obtained through adjustment of the downstream pressure ( $P_1$ ). To obtain the desired pressure ratio, the 2.5 inch long diaphragm chamber (Figures 15 and 16) and the driver chamber are simultaneously filled to one half of the desired  $P_4$  pressure (300



### Pressure Transducer

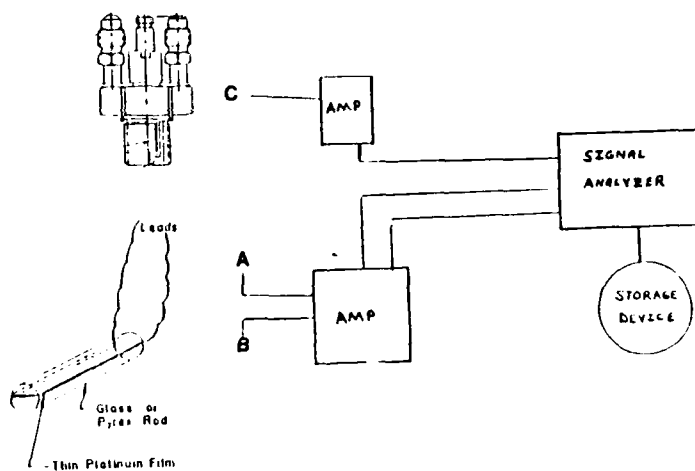


Figure 14. 3" Diameter Shock Tube with Instrumentation Layout

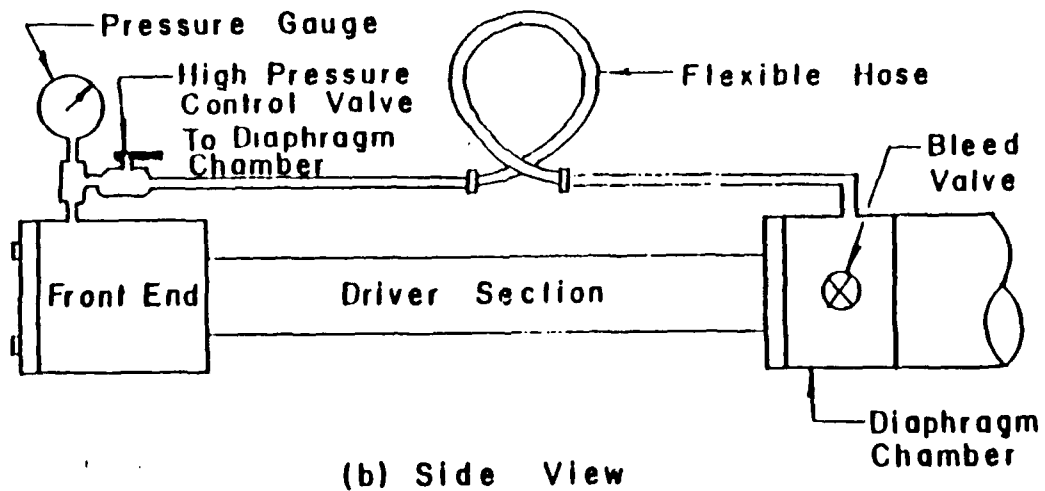
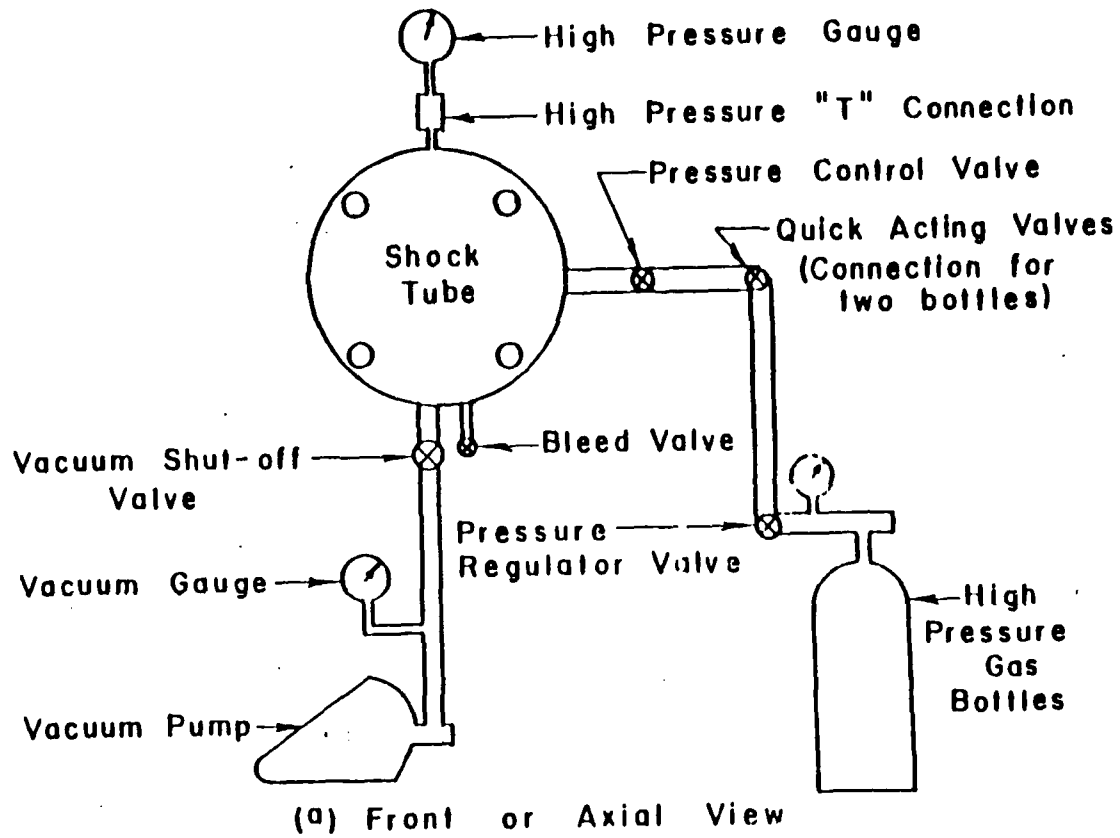


Figure 15. Shock Tube Driver Section [Ref. 4]

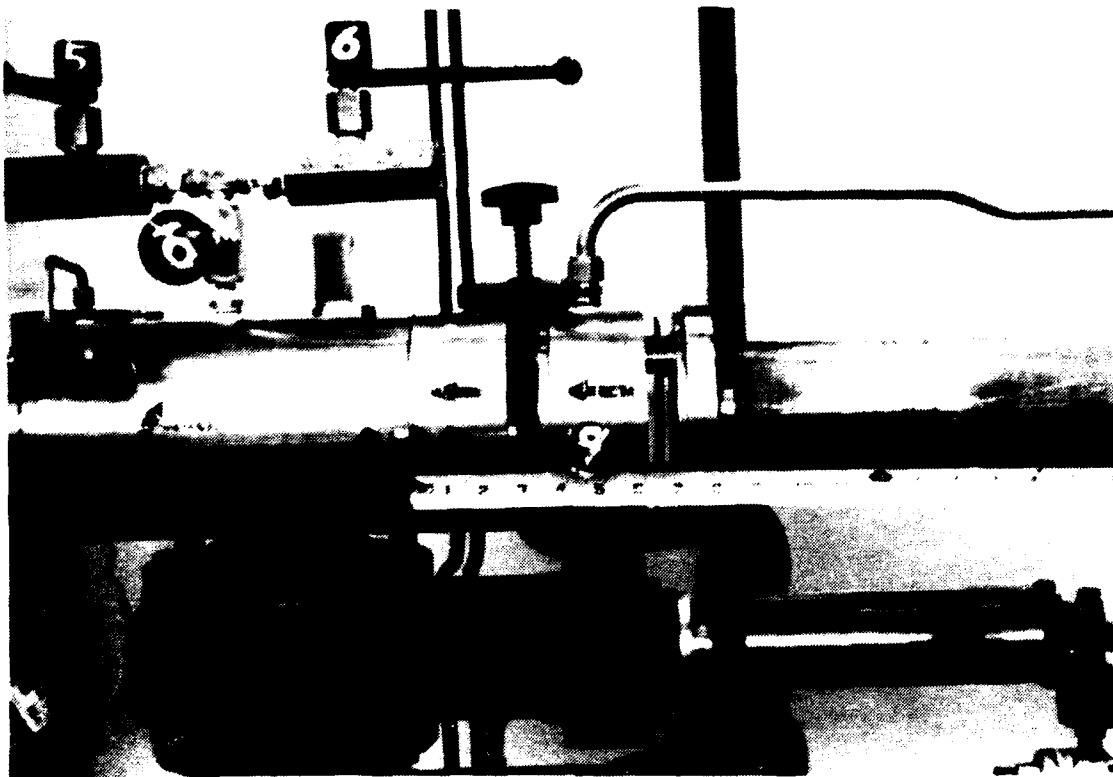


Figure 16. Dual Diaphragm Chamber (Unbolted)

psi). A diverting valve is closed to isolate the diaphragm chamber at 300 psi. The driver section pressure is then raised to the desired  $P_d$  pressure (600 psi). To fire the tube, a diverting valve is opened and some of the driver gas at 600 psi is dumped into the diaphragm chamber causing the first diaphragm to break. The second diaphragm breaks immediately, as the pressure on the driven face of the diaphragm rapidly falls.

The dual diaphragm arrangement minimizes bursting pressure fluctuations due to inconsistencies in the material of the diaphragms. By applying a pressure of 200 psi above the design bursting pressure of the first diaphragm, rupture of the two diaphragms is ensured with a precise value of  $P_4$ . In shock tubes using a single diaphragm arrangement, precise bursting pressures cannot be repeated unless the complexity of a diaphragm puncturing device is used. Without a puncture device, the bursting pressure fluctuations remain a function of the uniformity of the diaphragm material.

#### C. NOZZLE ASSEMBLY

An existing two dimensional stainless steel nozzle designed for an exit Mach number of 5.72 ( $A/A^* = 43.7$ ) and a rectangular dump chamber to which it bolted were available for the present study. The assembly is shown in Figure 17. For the present experiments two 1" diameter window ports were installed to allow optical measurement techniques to be exercised, and a model support was constructed to position a 3/8" axisymmetric model on the nozzle centerline in line with the window, where the Mach number was about 4.3. The final assembly is shown in Figure 18. The dimensions of the nozzle are given in Figure 19 and the design of the window installation is shown in Figure 20. Views of the nozzle and model support are shown in Figure 21. Since the nozzle and dump tank existed (from a previous gas dynamic laser

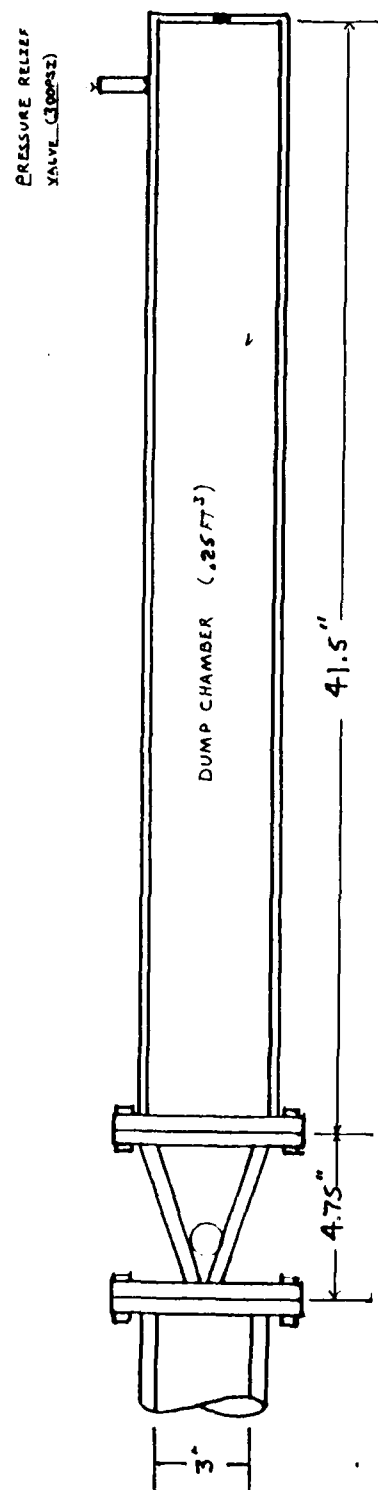


Figure 17. Two Dimensional Nozzle and Dump Chamber

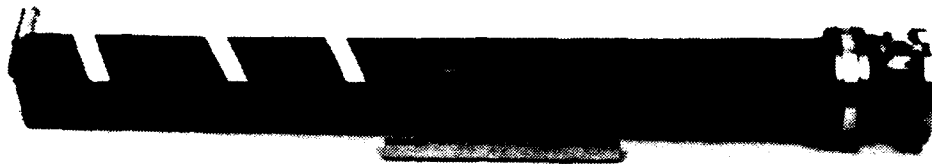


Figure 18. Assembled Dump Chamber, Model Support and Nozzle

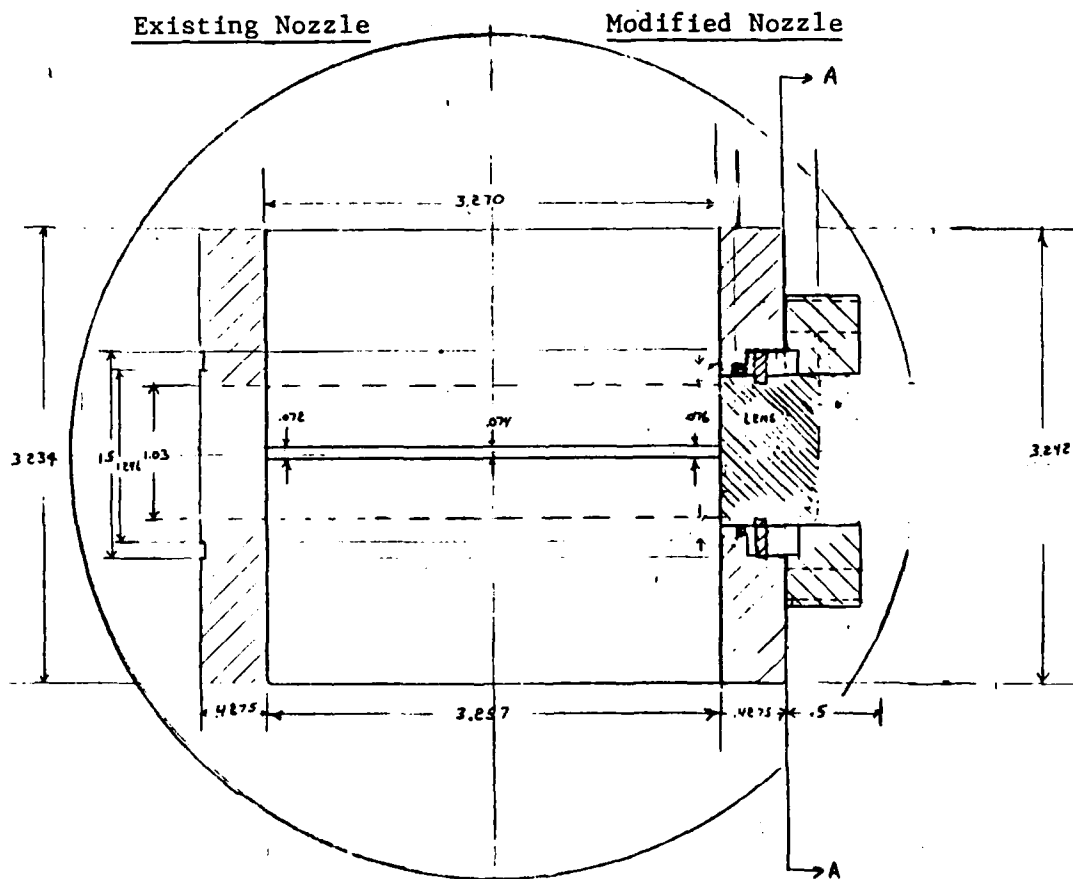
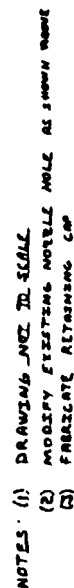


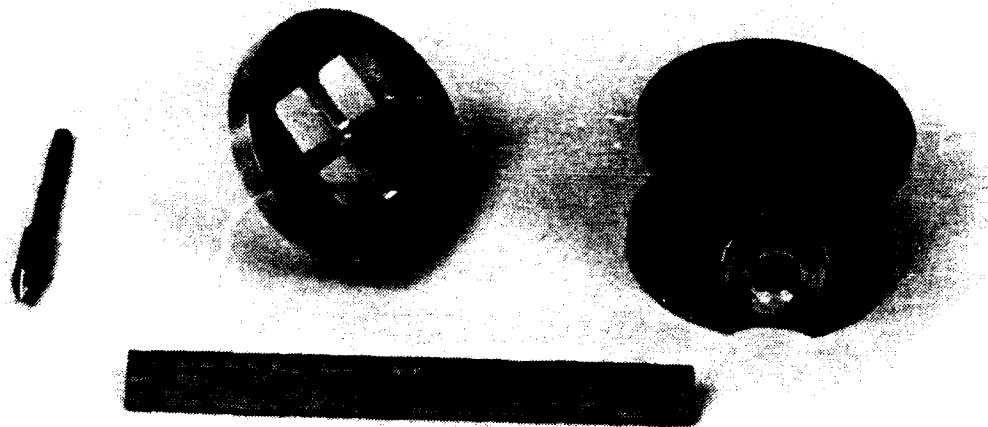
Figure 19. Dimensional Drawing of the Nozzle



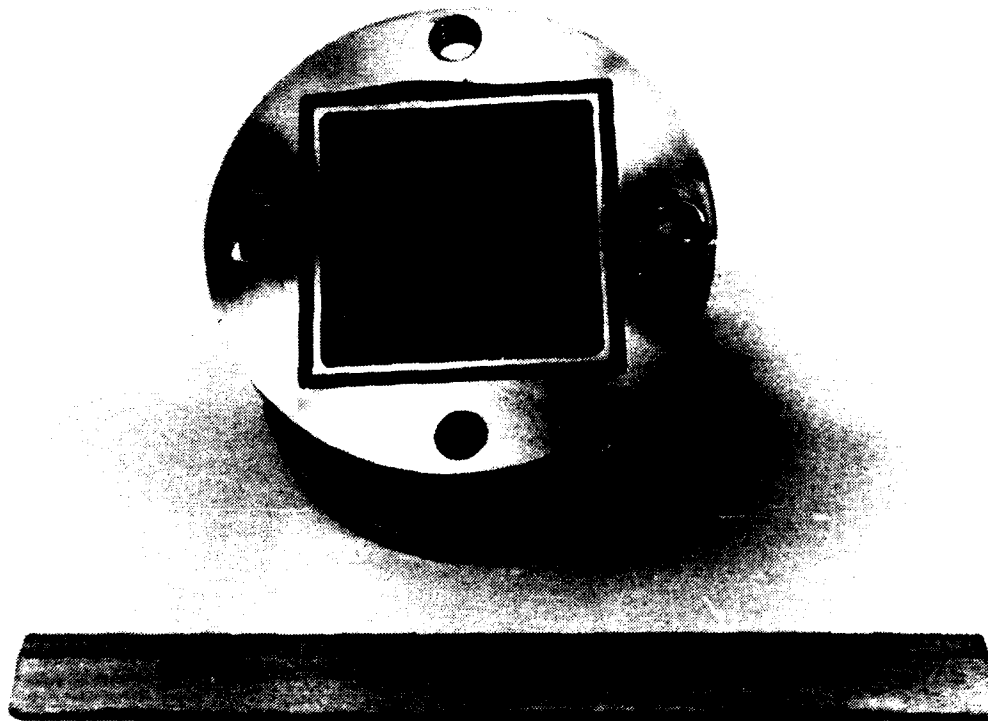
(2) MODIFY EXISTING NOVELL  
(2) FABRICATE ALUMINUM CAP

Prepared by M. N. SHEPARD

Figure 20. Optical Window Installation



(a) Model, Model Support and Nozzle



(b) Nozzle Exit

Figure 21. Views of the Nozzle and Model Support

investigation), location and sizing of the window as well as the maximum flow duration were limited by the existing hardware.

#### D. INSTRUMENTATION

##### 1. Shock Speed

Shock speed was determined by measuring the time for the shock to travel between thin film gauges located at positions A and B and from B to the pressure transducer at C (Figure 14). The locally manufactured thin film gauges shown in Figure 22, consist of a 0.25" diameter pyrex rod coated with a 1/32" wide thin film of platinum giving a cold resistance of 100 ohms. [Ref. 4:p. 23] As the region of hot gas immediately behind the shock front passes over the platinum, its temperature and resistance change and a voltage pulse is generated. In the present work the signals from the thin films were amplified and recorded for analysis. The thin films at location A also served as a trigger for the digital counter and shadowgraph spark source.

Shock speed was determined in different ways. The pre-existing techniques involved using oscilloscope records of thin film and pressure transducer outputs, and also the output of a digital counter triggered on and off by the thin films at A to B respectively. In the present work, in runs 1 through 49 shock speeds were determined from a Polaroid

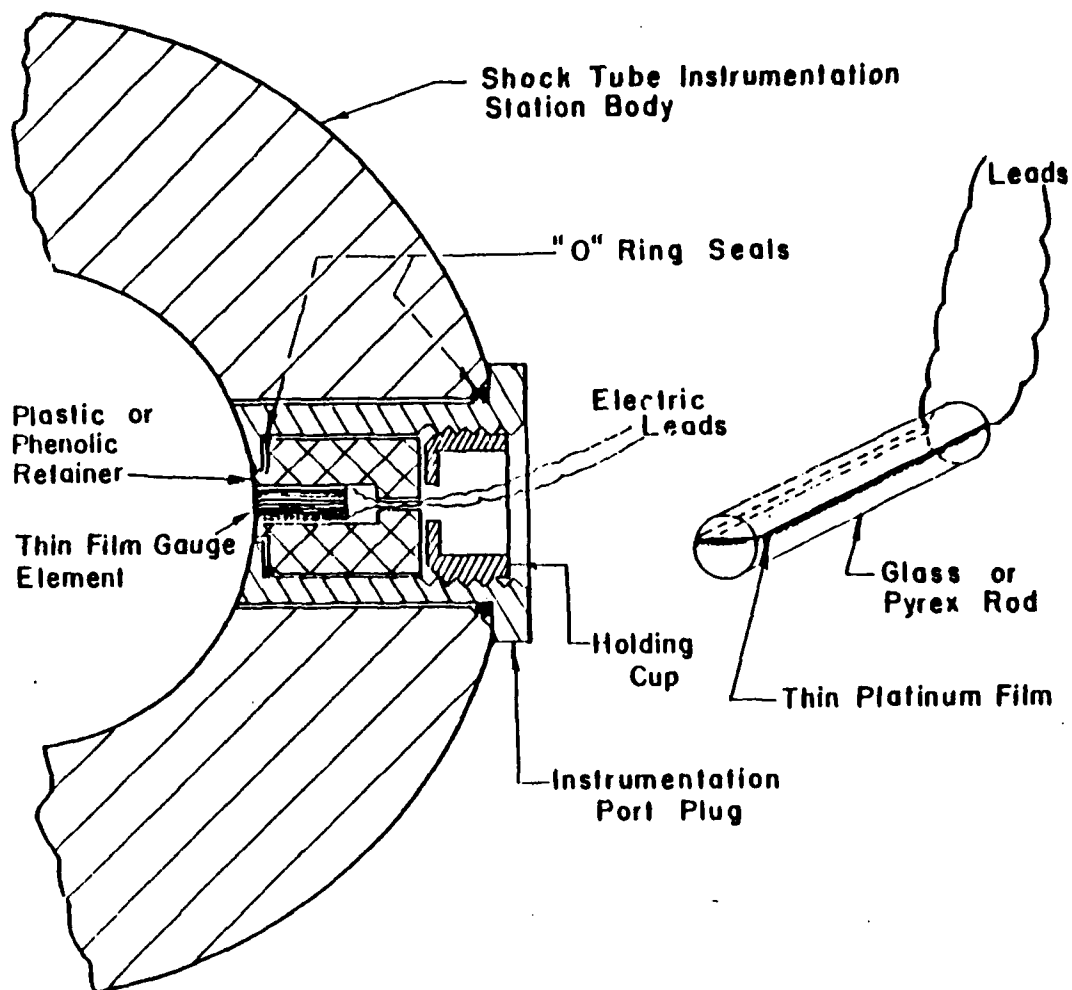


Figure 22. Thin Film Instrumentation Assembly  
[Ref. 4]

photograph of the oscilloscope, such as is shown in Figure 23, and from the digital counter. Both techniques were identical to those used in the late 1960's.

In runs 50-85, the outputs of the three traces were recorded digitally on three of the available four channels of a Scientific Atlanta SD380 Spectrum Analyzer. Data were recorded at .019 and .039 msec intervals depending upon the time scale selected. An example is shown in Figure 24. The shock speeds were determined during postprocessing of the data.

## 2. Driver Tube Pressure

A dial gauge with 10 psi pressure increments was used to determine when the constant 600 psi driver pressure was reached. A dead weight tester was used to calibrate the gauge.

## 3. Driven Tube Pressure

Two calibrated Wallace and Tiernan Bourdon tube gauges were used to determine the driven tube pressures. In the range from 0 to 50mm Hg, a gauge with increments of .2 mm Hg was used. For higher driven pressures, a second gauge with a range from 0 to 35 psi in increments of .05 psi was used.

## 4. Driven Tube Temperature

A Type K (chromel-alumel) thermocouple, connected to a Daigger Scientific Digital Panel Meter using matched

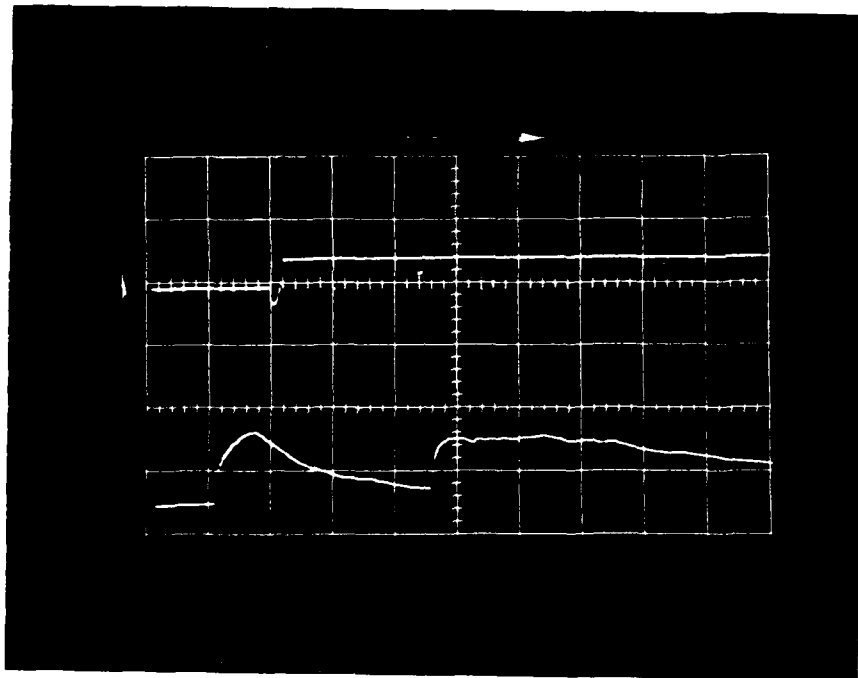


Figure 23. Typical Polaroid Photograph of the Thin Film Response from Location B and the Output of the Original Pressure Transducer

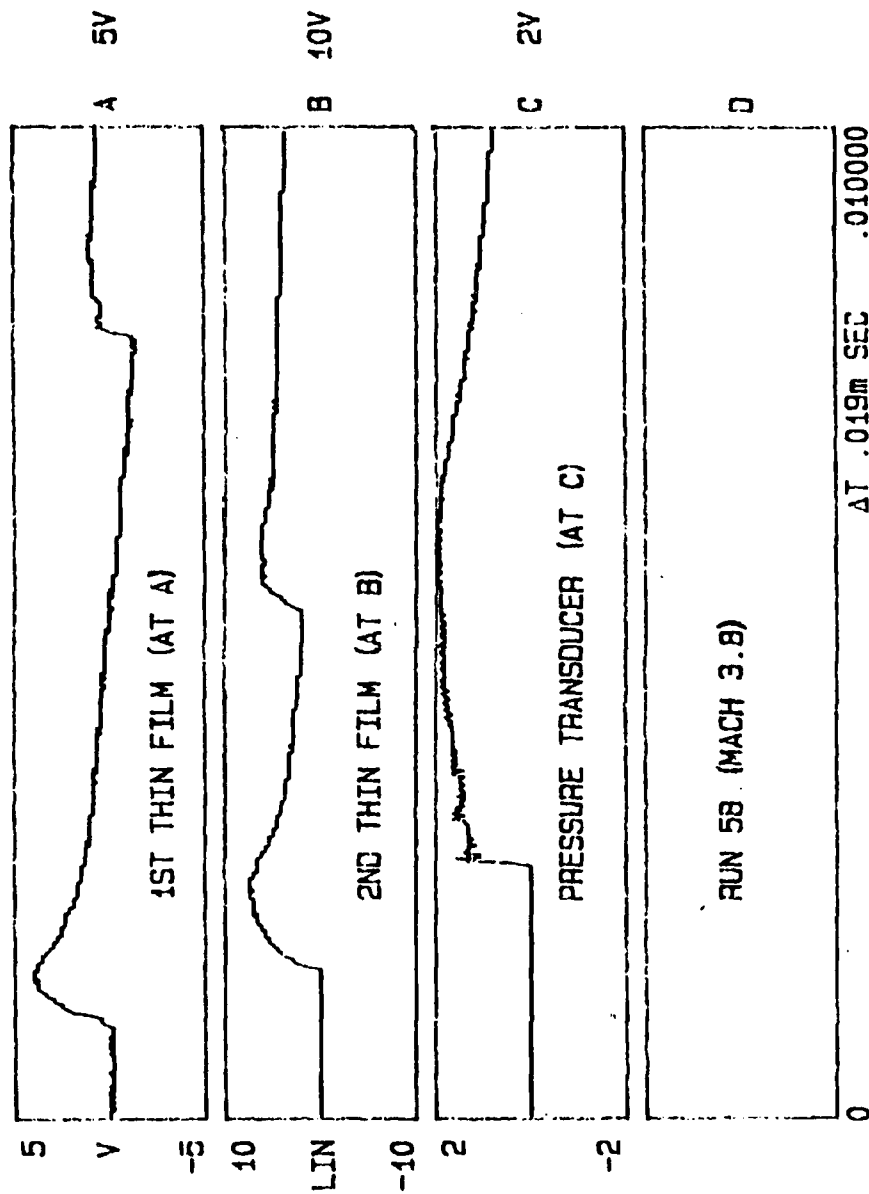


Figure 24. A Typical Recording Using the SD380 Signal Analyzer

extension wires, was mounted in the driven end of the tube. The digital readout was recorded prior to every run.

#### 5. Reflected Pressure and Test Duration

A piezoelectric pressure transducer, Endevco model 2501, a charge amplifier, Endevco model 2700, and a Tektronics 551 oscilloscope were initially used to record the transient region 5 pressure. The lack of resolution and strange qualitative behavior observed in the results (Figure 23), led to the mounting of an improved transducer.

A PCB Piezotronics, Inc. Model 124A pressure transducer connected to a model 504A dual gain charge amplifier were used in runs 50 through 75. The system was calibrated using a standard static calibration feature described in the manufacturer's manuals [Refs. 11,12]. The transducer provided a response of 240 psi/volts. Experimental traces obtained are given in Appendix D.

#### 6. Oscilloscopes

Two Tektronics oscilloscopes, models 549 and 551, fitted with Polaroid cameras were used for runs 1 through 49. The capability of the scopes are fully described in the associated manuals [Refs. 13,14]. Time measurements to determine shock speed, and voltage levels to determine pressure, were determined by overlaying a scale on the Polaroid photographs.

## 7. Signal Analyzer

A Scientific Atlanta SD380 four channel signal analyzer (Figure 25) equipped with a hard disk and plotter was used to record and process data from runs 50 through 85. The independent channel trigger delays ( $\pm$ ), adjustable scales and post-processing capabilities of the digitized data (in contrast to photographing oscilloscopes), is evidence of the advances in measurement capabilities over the past 20 years. A full description of capabilities of the analyzer is given in the instrument manual. [Ref. 15]

## E. OPTICAL MEASUREMENT SYSTEMS

A simple shadowgraph arrangement was generated from the components of a 6" schlieren system. The optical layout is shown in Figure 26 [Ref. 16]. The spark source was used with Polaroid film in a camera back attached to the nozzle window. The continuous source was used with a Hycam movie camera.

### 1. Light Sources

#### a. High Pressure Mercury Arc Lamp

A high pressure mercury arc lamp (Per Type 112-5145) constant light source was used with a six inch achromatic convex lens with a focal length of 60 inches. The arrangement, mounted on an adjustable bench (Figure 27), provided a parallel light beam through the nozzle windows.

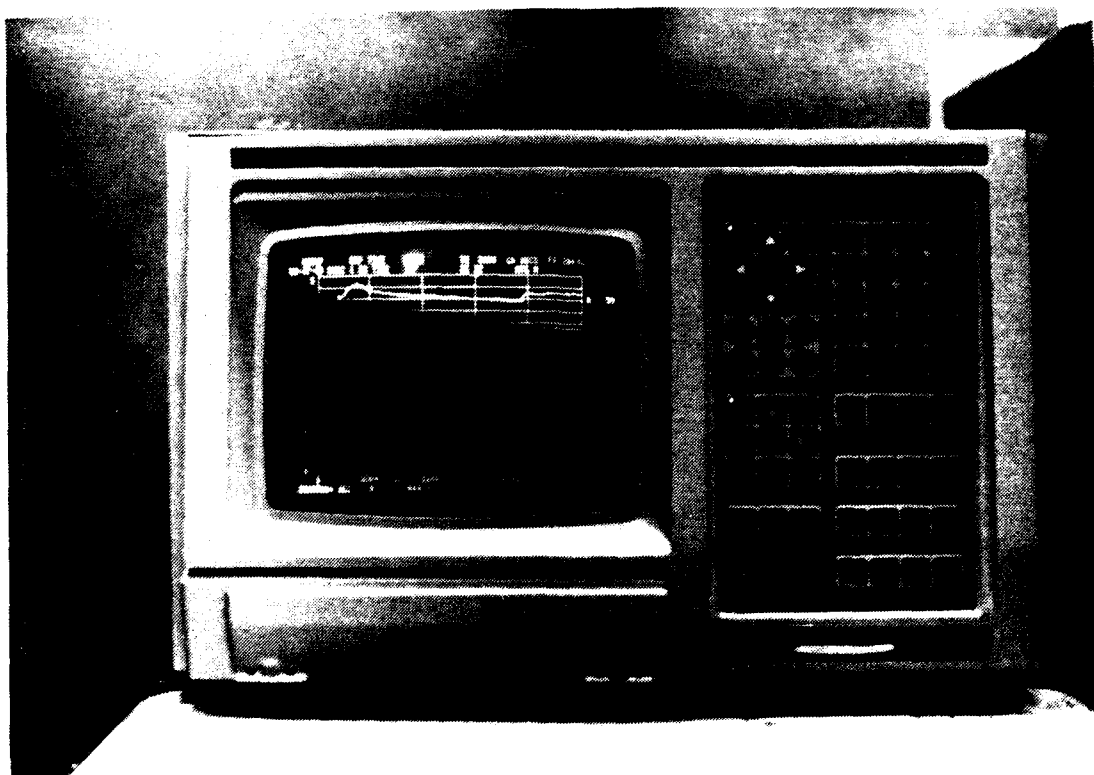


Figure 25. Scientific Alanta SD380 Four Channel Signal Analyzer with Hard Disk Installed

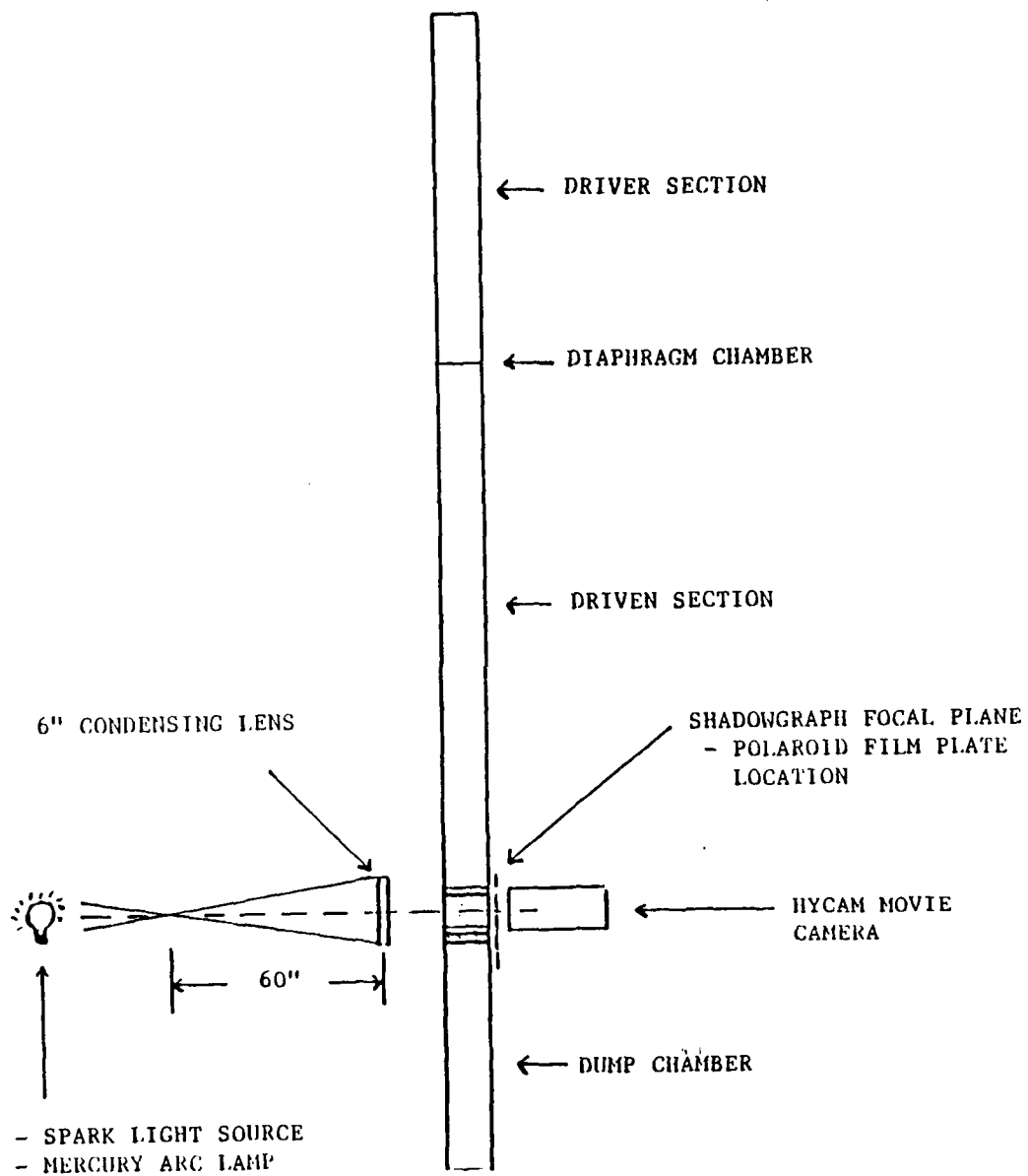


Figure 26. Optical Layout Sketch

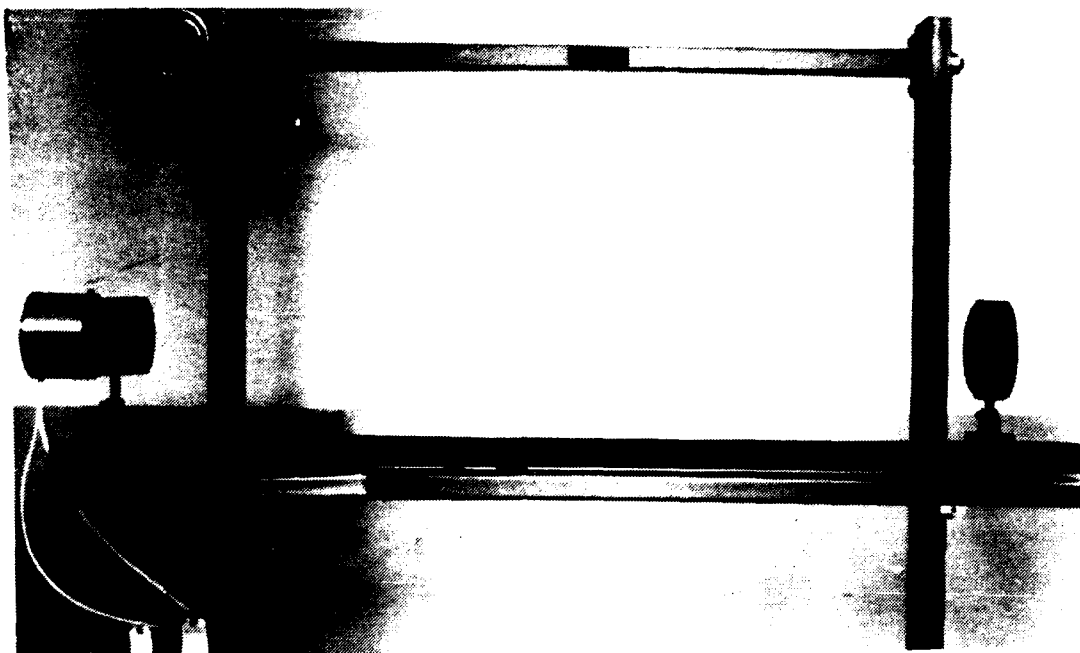


Figure 27. Constant Light Source and Lens Mounted on an Adjustable Optical Bench

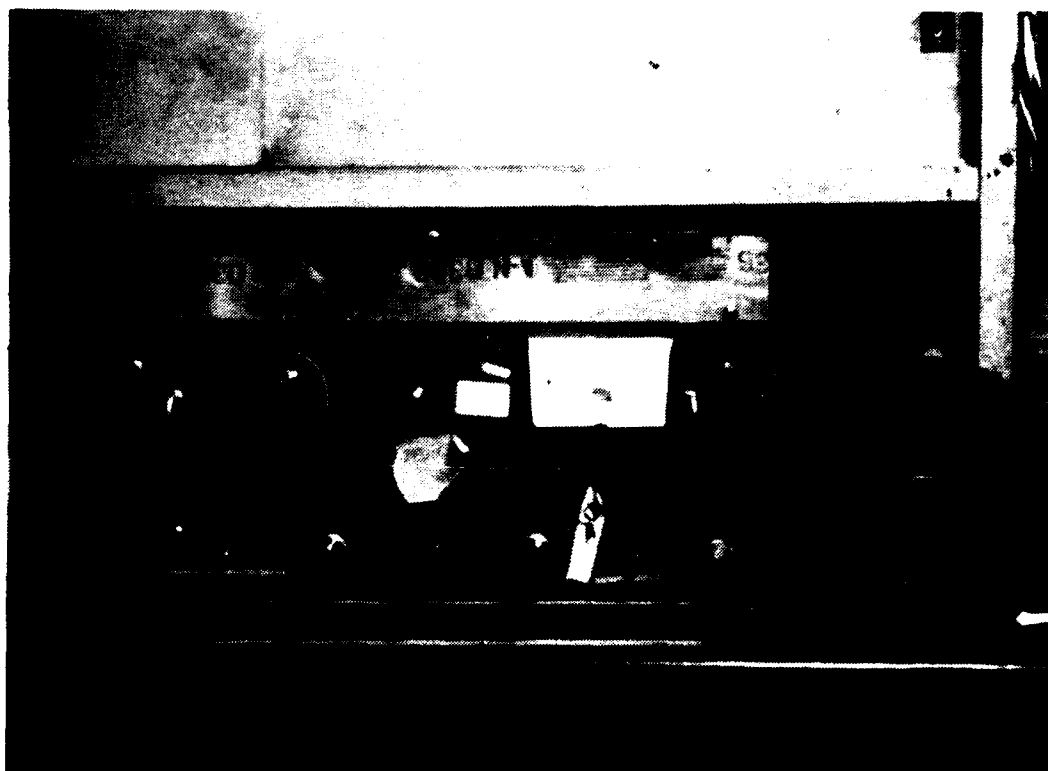


Figure 28. Spark Source with High Voltage Power Supply

The beam was adjusted by the procedures described in the associated manual [Ref. 16].

b. NASA 229-D Spark Light Source

A NASA 229-D spark light source (Figure 28) provided a nanosecond spark for shadowgraph pictures taken with Polaroid film. The spark was triggered from a thin film connected through the delay and voltage circuits shown in Figure 29. The timing for the spark source was determined experimentally.

2. Camera Systems

a. Hycam Movie Camera

A Hycam movie camera [Ref. 17] with a framing rate on the order of 6000 pictures per second at runout of a 400 ft roll of film, was used. The camera was equipped with a Nikon 55mm lens and ASA 250 black and white film. A time reference was provided on the edge of the film by a strobe light pulsing at 1000 pulses per second. The camera was triggered manually. The camera was mounted on a second adjustable bench as shown in Figure 30.

b. Spark Shadowgraphs

Spark shadowgraphs were taken using a Polaroid Land Film Holder with Type 52 ASA 400 Black and White film, held directly behind the optical windows. To eliminate stray light, the mounting arrangement was contained in a cardboard box, and tests were conducted after dark.

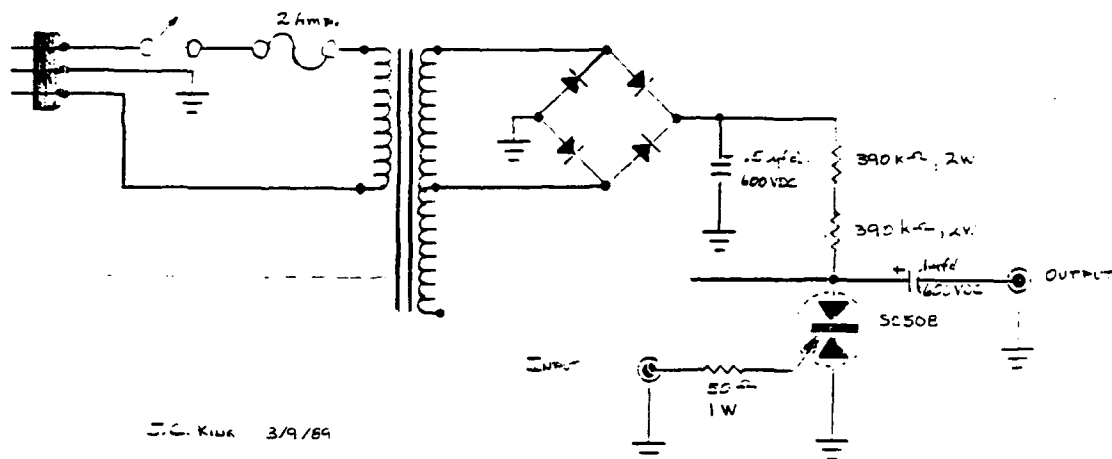


Figure 29. Spark Timing Delay Circuit and High Voltage Pulse Generator



Figure 30. Hycam Movie Camera with Separate Pulse Generator

#### IV. EXPERIMENTAL PROCEDURE

##### A. PREPARATION

Prior to testing, with the driven endplate removed and the diaphragm chamber opened, a cloth lightly dampened with Acetone was pulled through the driver and driven sections. O-ring grooves of the opened sections were thoroughly cleaned and a thin coating of vacuum grease was applied to the rubber O-rings. Diaphragms were wiped clean of visible dirt and the system reassembled. The cleaning procedure was repeated after approximately 15 runs. Using a roughing pump, a clean-tube vacuum pressure of 3 mm Hg was routinely achieved.

##### B. LOADING THE DRIVEN GAS

Prior to loading to the desired test pressure ( $P_1$ ), the driven section was purged. To purge, the tube was evacuated to 3 mm Hg and then isolated from the roughing pump. Nitrogen was introduced to a pressure 1 to 4 psi. The tube was then evacuated a second time and repressurized to the desired test condition.

##### C. LOADING THE DRIVER GAS AND FIRING

The driver assembly is designed to operate at 600 psi with single or dual gas combinations. To purge the driver section and diaphragm chamber, the system was pressurized to

approximately 30 psi and then vented to atmospheric pressure. The system was then pressurized to 600 psi with the diverter valve to the diaphragm chamber being closed at 300 psi. When the 70% He and 30% N<sub>2</sub> driver mixture was used, the system was pressurized to 420 psi with He and then to 600 psi with N<sub>2</sub>.

The tube was fired by opening the diverter valve to the diaphragm chamber. Some seepage from the driver section was evident. To minimize this effect the tube was fired immediately after reaching the 600 psi level. Replacement of O-rings would minimize this problem. Seepage into the driven section was not evident.

## V. EXPERIMENTAL RESULTS AND DISCUSSION

A series of experiments was conducted to gain experience with the shock tube. The study consisted of approximately 85 shots involving the use of He and a 70% He/30% N<sub>2</sub> mixture as driver gases, driven into a N<sub>2</sub> test gas. Studies with the shock tube assembled with the pressure transducer mounted in the end of the driven tube, were concentrated on investigating the concept of tailoring to maximize the magnitude and duration of steady pressure in the reflected region. While more than 75 shots were made in this configuration, the replacement of the pressure transducer and postprocessing of data taken with the SD380 greatly enhanced the results. For this reason, only data taken after run 50 using the SD380 are presented. Studies with the nozzle attached at the end of the driven tube were exploratory attempts to obtain flow visualization in a shock tunnel configuration. The results of the two series of experiments are discussed in the following sections.

### A. TAILORING

Using the nomenclature of Glass [Ref. 18], a tailored condition is defined as the condition when a Mach wave is reflected off the contact surface and causes no change in the reflected pressure ( $P_5$ ). This can be identified

experimentally (Figure 10) as the condition when the ratio of the initial reflected pressure ( $P_5$ ) and the pressure after the wave interaction at the contact surface reflects off the endplate ( $P_8$ ) being equal to one. Figure 31 shows examples of results in the present study for the end wall pressure untailored and tailored conditions using He with an incident shock strength,  $M_s = 3.4$ . Similar traces for near to a tailored mixture (.7 He and .3  $N_2$ ) with  $M_s = 2.0$  are shown in Figure 32. These results are in complete agreement with Pennelegion [Ref. 10].

#### B. TIME OF STEADY PRESSURE

It was experimentally determined in the present study that a tailored mixture as a driver gas produced a longer duration of steady pressure than that of a pure He driver. The time of steady pressure for the existing NPS shock tube using He as a driver was approximately 3.6 milliseconds while the mixture extended the test time duration to 5 milliseconds. A comparisons of the test times obtained in the present study with those of Pennelegion [Ref. 10] is shown in Figure 33. The trends are seen to be similar. Since the work of Pennelegion [Ref. 10] was performed at a constant driver pressure of 1000 psi in a N.P.L. 2" shock tube with a 10 ft driver and a 12 foot driven section some differences in the magnitudes of the test times are to be expected.

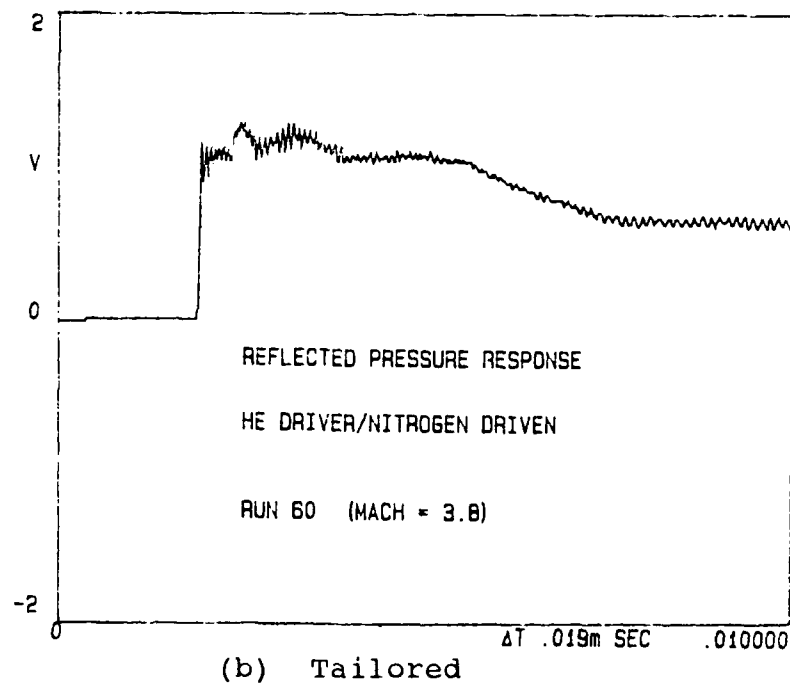
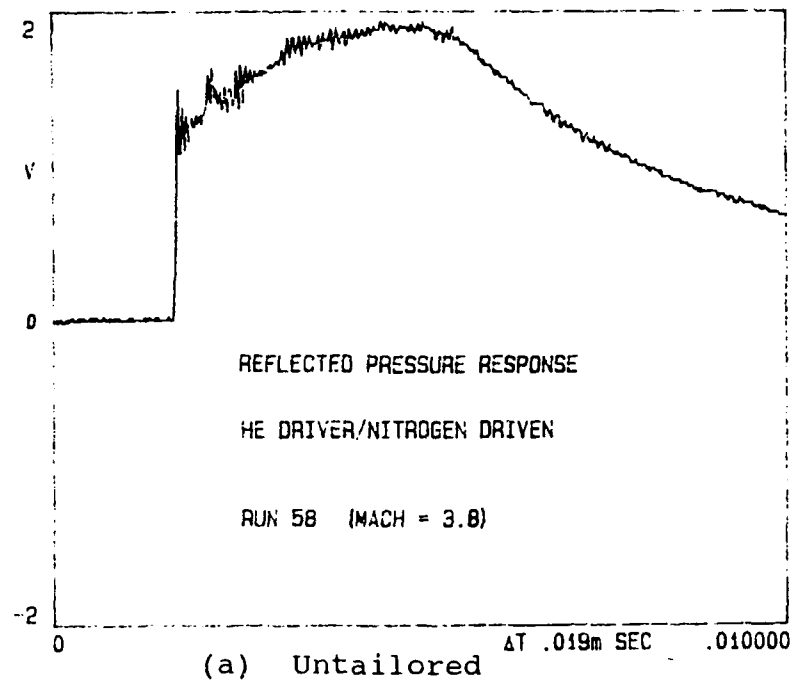
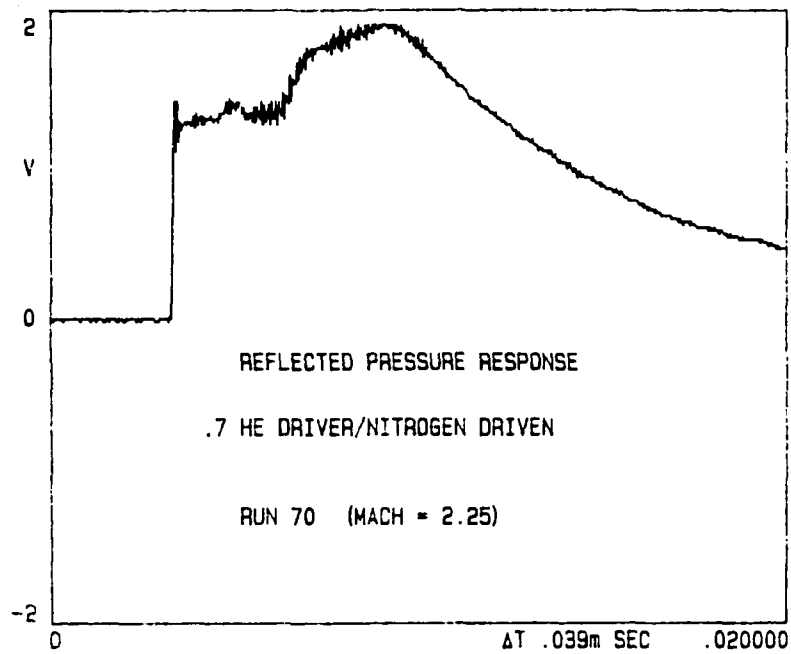
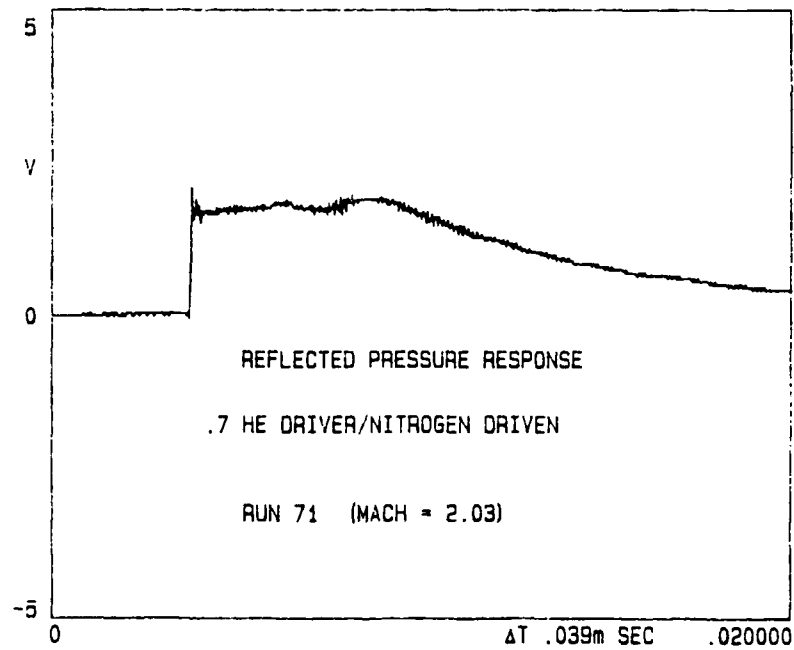


Figure 31. Experimentally Determined Endwall Pressure Traces Using Helium as a Driver Gas



(a) Untailored



(b) Tailored

Figure 32. Experimentally Determined Endwall Pressure Traces Using a Mixture of 70% Helium and 30% Nitrogen as a Driver Gas

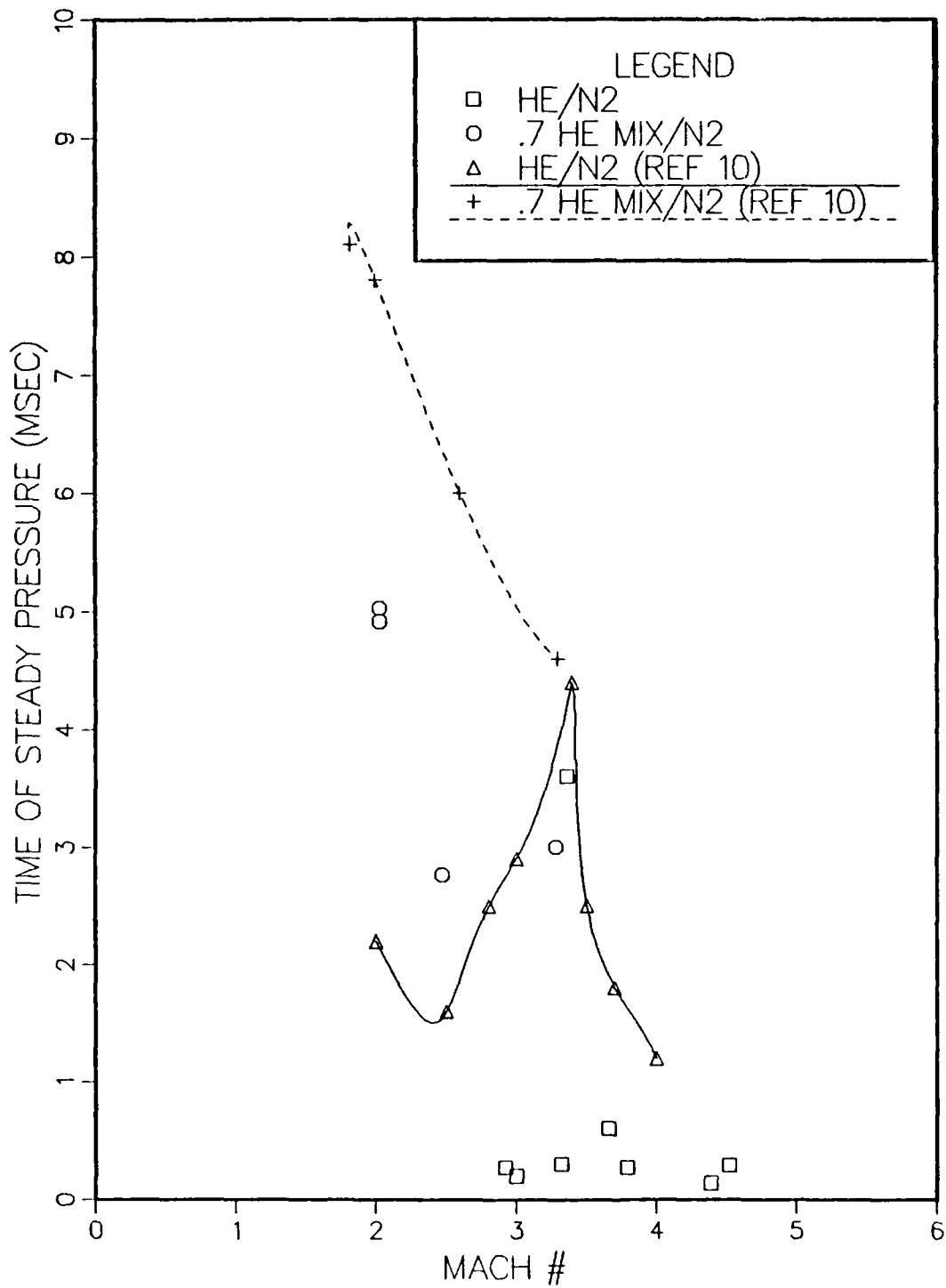


Figure 33. Comparison of Steady Pressure Time Achieved in the NPS 3 Inch Shock Tube with Experimental Results of Pennelegion [Ref. 10]

For low strength shocks the head of the expansion wave causes an early degradation of the reflected pressure in the NPS tube. The longer driver section in the N.P.L. tube is responsible for the difference.

#### C. PRESSURE RECOVERY

Figure 34 shows the fraction of initial driver pressure available in the reflected region as a function of shock Mach number. The data show that as shock strength increases pressure recovery decreases for both He and mixed driver gases. The data are in good agreement with the results of Pennelegion [Ref. 10]. The measured values of the reflected shock pressure, which are the pressures available to drive a hypersonic tunnel, are given in Tables 3 and 4.

#### D. REFLECTED TEMPERATURE

The reflected temperature was not determined experimentally. Instead, shown in Table 2 are values of stagnation temperatures calculated for shock strengths in the range from 2.0 to 3.4. These values were taken from the tabulated solutions (based on equilibrium chemistry) of Bernstein [Ref. 19:pp. 32-43].

#### E. SHOCK ATTENUATION

A representative illustration of measured shock attenuation for both a pure gas driver and the driver gas mixture is shown in Figure 35. Velocity can be inferred

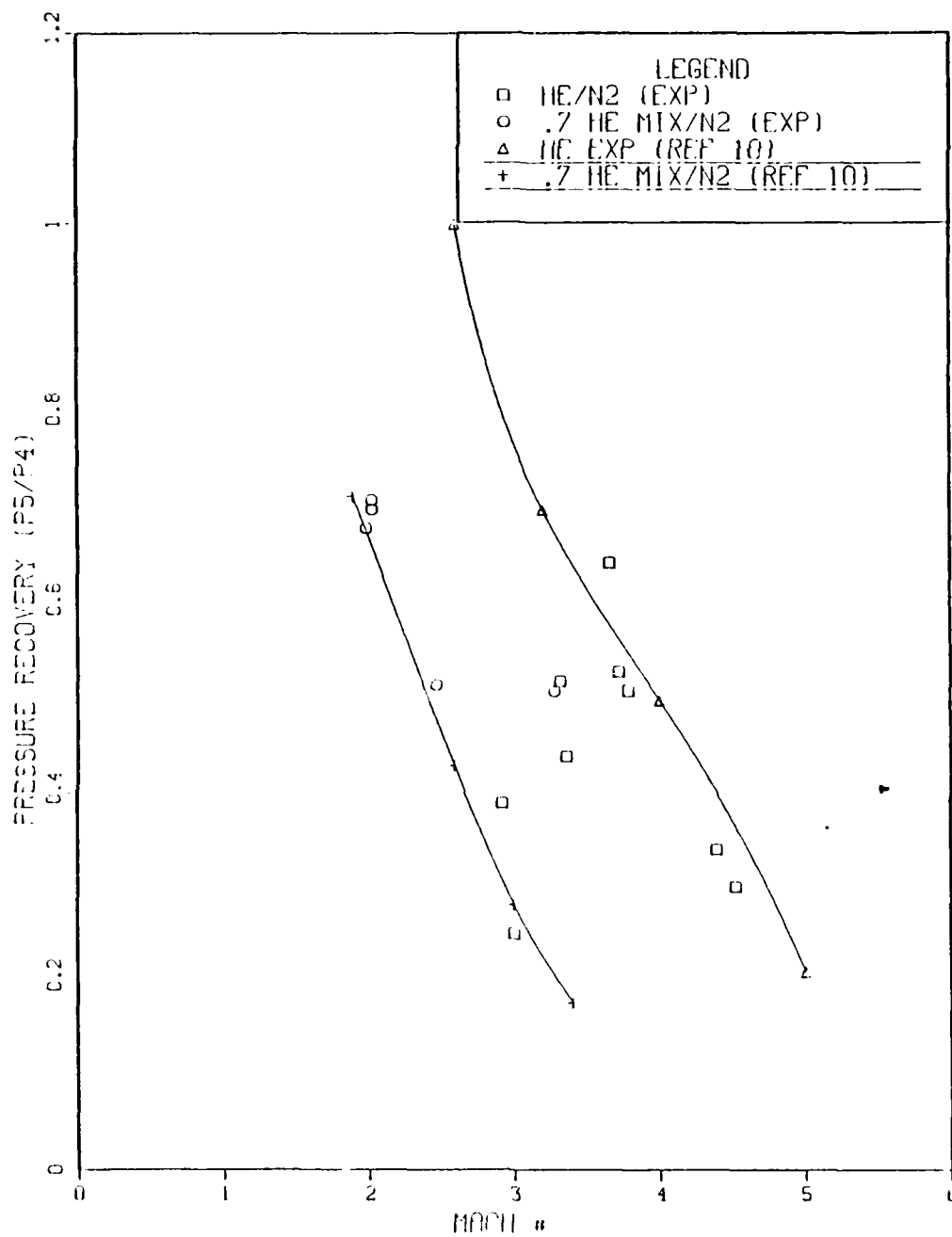


Figure 34. Comparison of Reflected Pressure Measurements in the NPS 3 Inch Shock Tube with Experimental Results of Pennelegion [Ref. 10]

TABLE 3

EXPERIMENTALLY DETERMINED REFLECTED PRESSURE MAGNITUDE  
AND DURATION AND CALCULATED TEMPERATURE (HE DRIVER/N<sub>2</sub> DRIVEN)

Run #	M <sub>s</sub>	P <sub>4</sub> /P <sub>1</sub>	P <sub>5</sub> (psi)	P <sub>8</sub> /P <sub>5</sub>	Time of Steady P <sub>5</sub> (msec)
50	3.08	994	150	1.79	1.3
51	2.92	353	235	1.23	1.2
52	4.39	414	207	1.38	1.9
53	3.32	93	312	1.42	1.5
57	4.52	500	183	1.25	0.3
58	3.79	207	304	1.23	0.3
59	3.66	148	386	1.13	1.6
60	3.36	169	264	1.13	3.6
61	3.72	167	317	1.23	0.5
64	3.42	164			--
65	3.65	158			--
66		184			
67	3.77	173			
68	3.81	400			
74	4.50	667			
75	4.10*	1240			

\* Estimated Value

TABLE 4

EXPERIMENTALLY DETERMINED PRESSURE MAGNITUDE AND DURATION  
AND CALCULATED TEMPERATURE (70% HE, 30% N<sub>2</sub> DRIVER/N<sub>2</sub> DRIVEN)

Run #	M <sub>s</sub>	P <sub>4</sub> /P <sub>1</sub>	P <sub>5</sub> (psi)	P <sub>8</sub> /P <sub>5</sub>	Time of Steady P <sub>5</sub> (msec)
62	2.40	50	317	1.10	2.8
63	2.66	51	310	1.23	1.5
69	2.47	50	310	1.09	2.5
70	2.25	50	305	1.11	3.3
71	2.03	24	427	1.02	4.9
72	2.03	22	422	1.08	5
73	1.99	21	410	1.13	2
77					
78		155			
79	3.0*	171			
80	3.4*	638			

\* Estimated Value

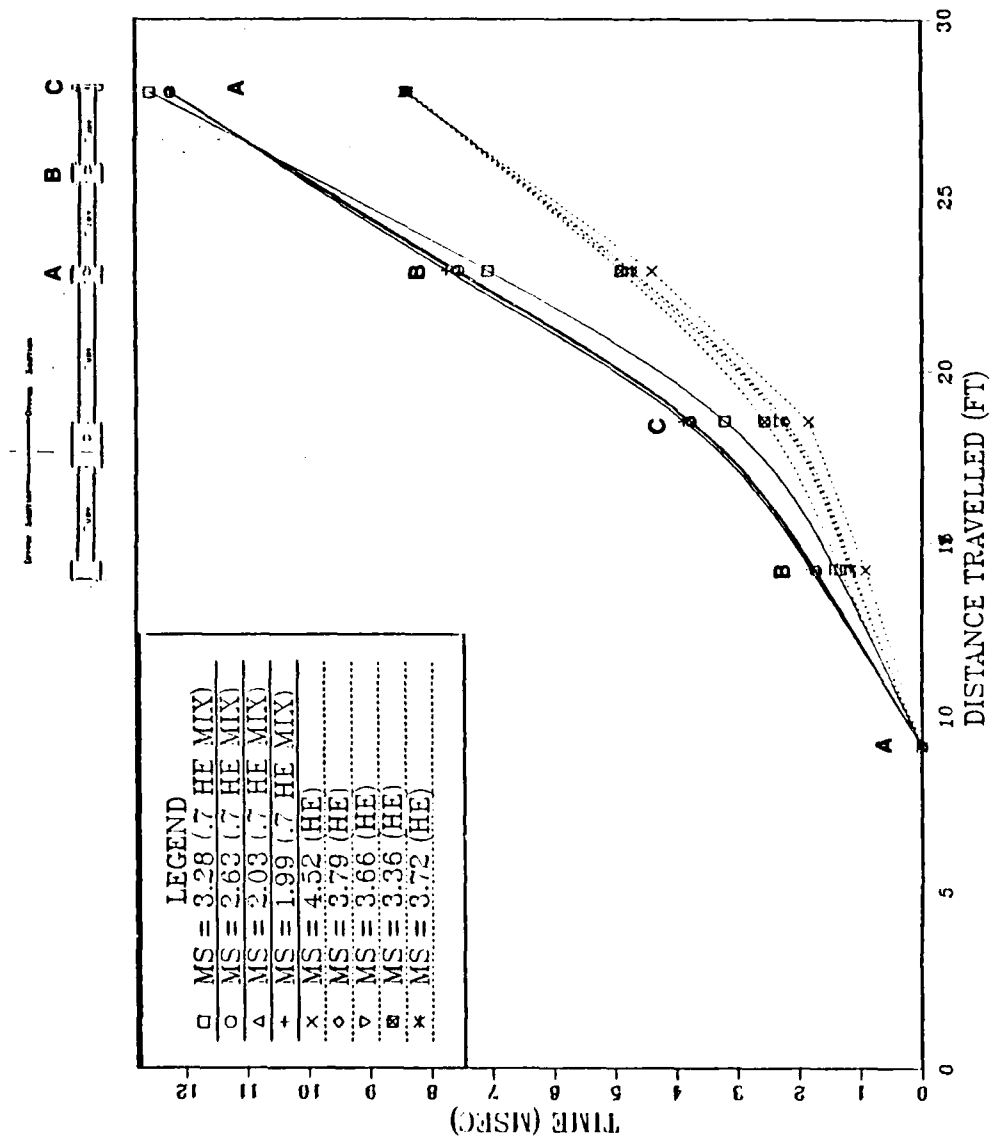


Figure 35. Variation in Shock Transit Times Between Measurement Stations

from the slope of the lines between the thin films A and B and between B and the pressure transducer at C. An increasing slope indicates a slower speed. The general trend is that for a given gas mixture, the stronger the shock strength the smaller the attenuation between B and C. Reflected velocity is of the order of one half the incident velocity. Tabulated results for all runs are found in Appendix D.

#### F. OPTICAL MEASUREMENTS

Before attempting to obtain photographs during the firing of the shock tube, a small freejet from a 1/4" flattened copper tube, powered by shop air, was installed in the model location, the spark light was adjusted using a neutral filter and a successful shadowgraph was taken.

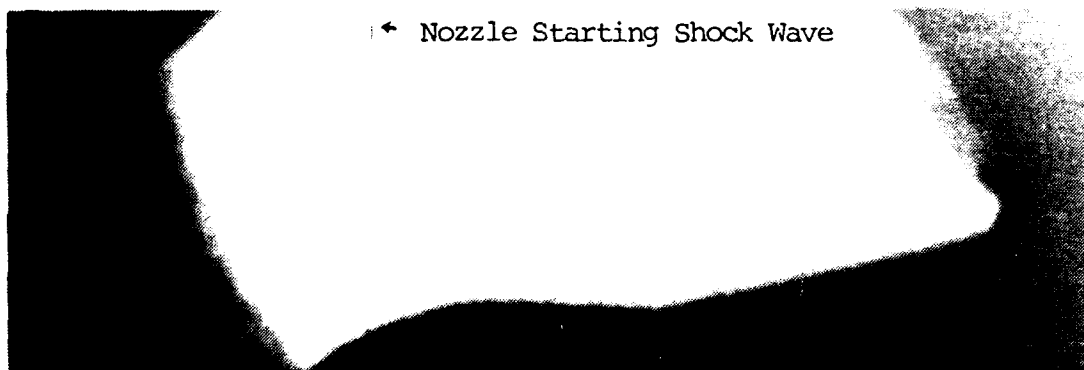
##### 1. Shadowgraph Using Hycam Camera

The Hycam Movie camera was triggered manually either one or two seconds before the diaphragm was ruptured. The 400 ft rolls of ASA 250 speed film provided approximately one second for the camera to accelerate, and a three second window to capture the event. It was found that all the available light was needed to obtain a correct exposure and the camera was focused on the outside surface of the window. The shadowgraph was made visible by the faint film which by then had deposited on the inside of the window. The result was successful.

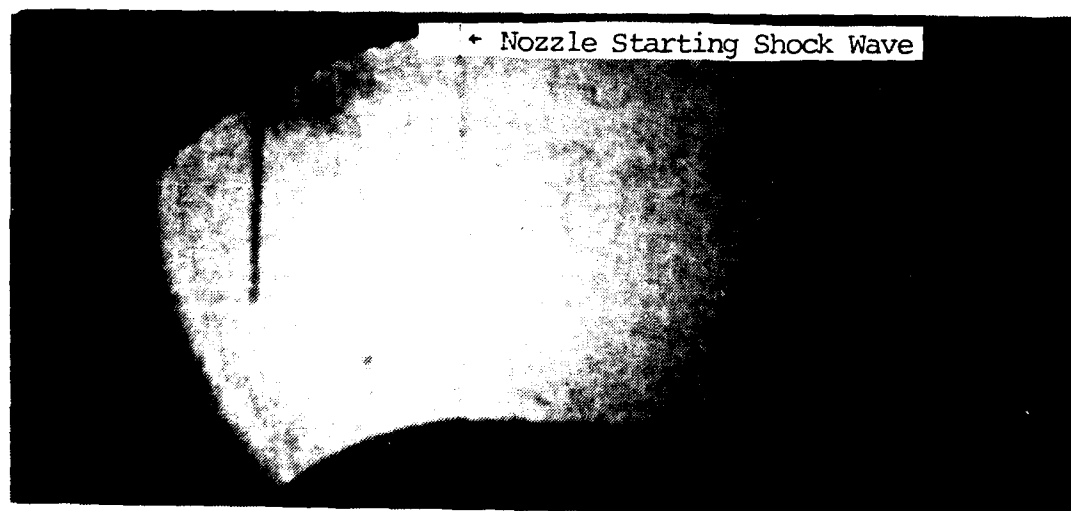
With the blunt body shown in Figure 21(a) installed, the nozzle starting Mach wave (Figure 36(a) and (b)), and the establishment of steady flow with an oblique shock visible (Figure 36(c)), were successfully recorded. Steady flow (started) conditions lasted a brief time until dump chamber back pressure unstated the nozzle. Incident shock strength was estimated to be  $M_s = 3.8$  providing a peak pressure in the reflected region of approximately 460 psi. The actual shock speed was not measured during the test since the starting of the camera caused premature triggering of the spectrum analyzer. However the initial conditions, and therefore the reflected pressure, were the same as in run 58. A complete record of this run given in Appendix D.

## 2. Spark Shadowgraph

Before firing the shock tube, the correct exposure for the expected shadowgraph was verified by opening the film and firing the spark source. The result is shown in Figure 37. It was subsequently found that when the shock tube was fired, the thin film signal failed to trigger the spark, and thus any exposure on the film was the result of light produced from within the tube. The results of exposing the film without discharging the spark as the shock Mach number was progressively increased, are shown in sections (a) to (e) of Figure 38. A faint glow appeared first at a  $M_s = 3.6$ . As  $M_s$  was increased for both a pure He driver and mixed driver gases, the luminosity increased.



(a) Nozzle Starting Shock Wave



(b) Nozzle Starting Shock Wave



(c) Oblique Shock

Figure 36. Results Obtained Using Hycam Camera

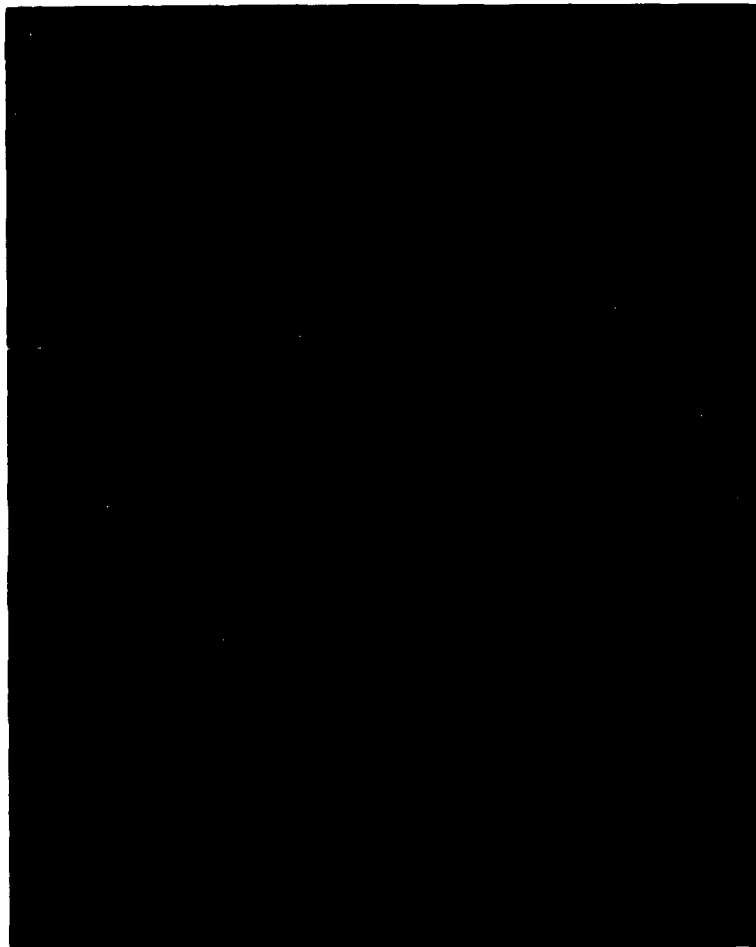
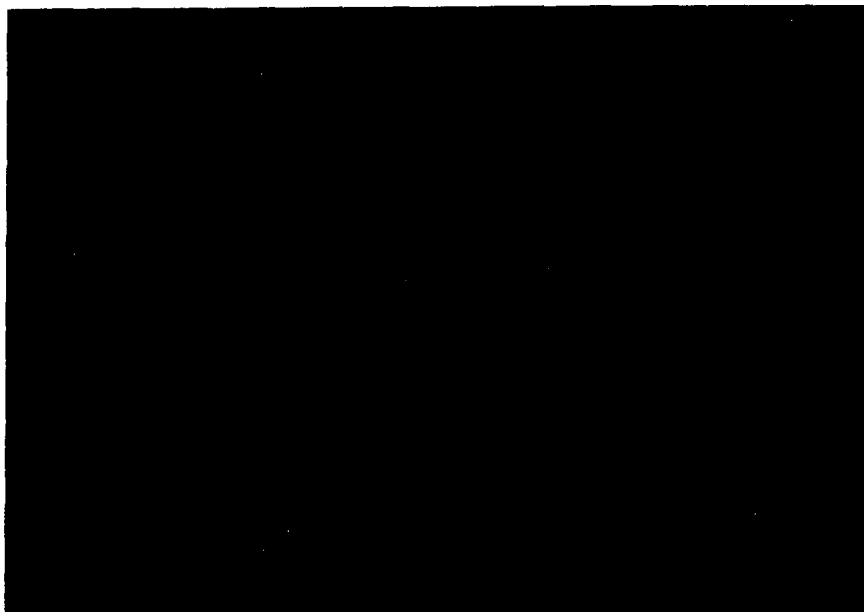
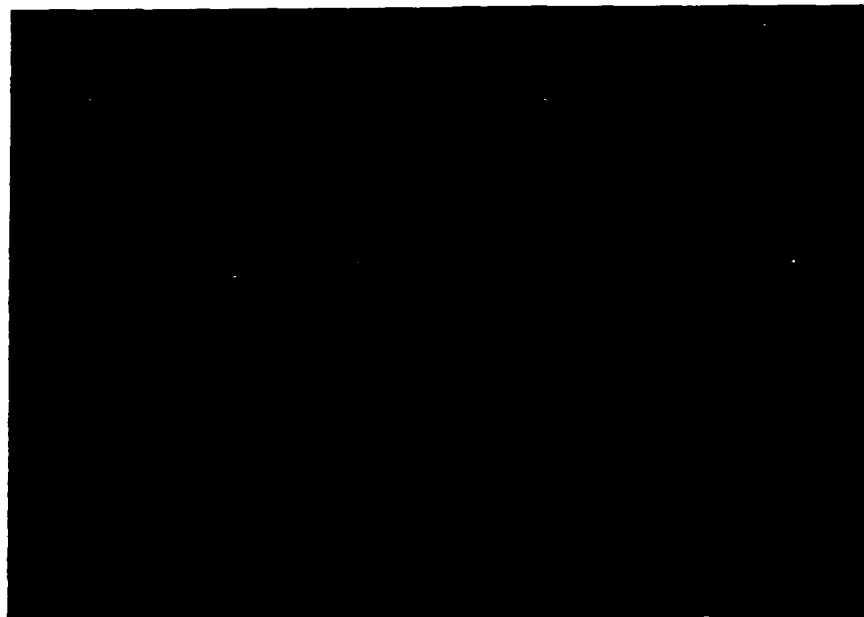


Figure 37. Spark Shadowgraph with No Flow Present

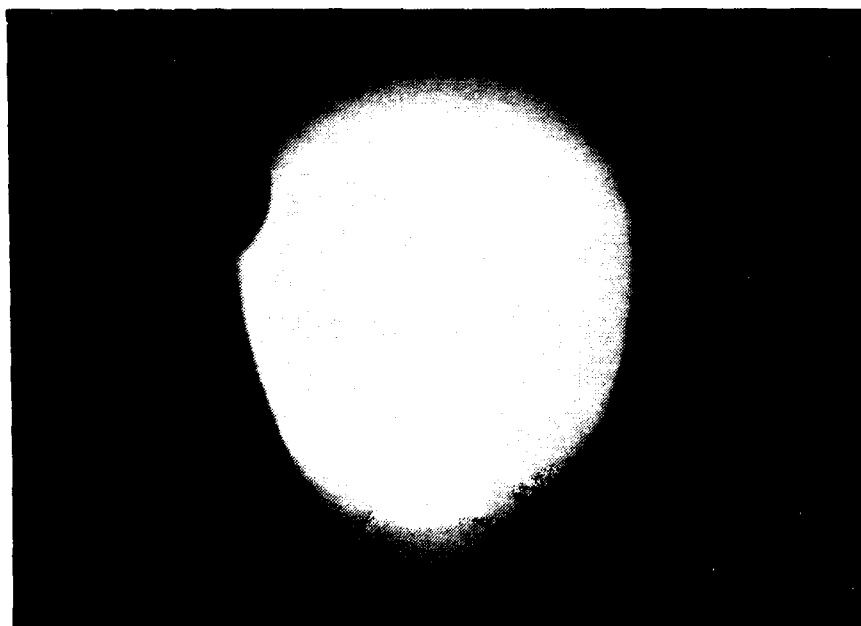


(a)  $M_S \approx 3.0$   
( $T_5 \approx 1200K$ )



(b)  $M_S \approx 3.6$   
( $T_5 \approx 1500K$ )

Figure 38. Film Exposure without a Spark Source

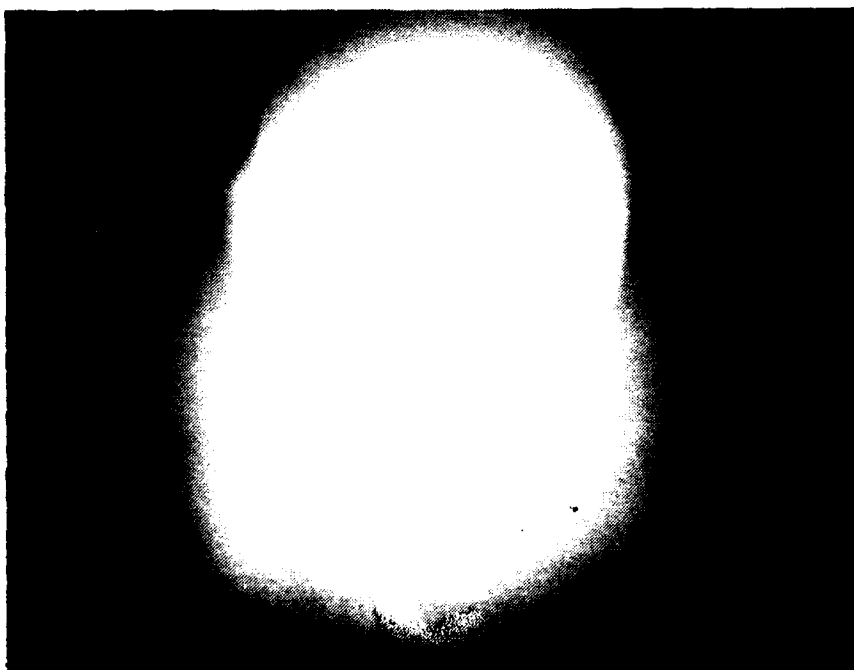


(c)  $M_S \approx 3.9$   
( $T_5 \approx 2000K$ )



(d)  $M_S \approx 4.1$   
( $T_5 \approx 2180K$ )

Figure 38. (CONTINUED)



(e)  $M_S \approx 4.5$   
( $T_5 \approx 2400K$ )

Figure 38. (CONTINUED)

The source of the light requires further investigation, but it is clear that some contamination must be present since the driver and driven gases, if pure, would not be excited at the temperature produced in the firing process.

## VI. SIZING CONSIDERATIONS FOR A HYPERSONIC TUNNEL

The experimental program showed that the basic shock tube gave reliable and repeatable results and, following the upgrading recommendations detailed in Appendix A, it could well serve as a driver for a hypersonic tunnel. Having experimentally defined the stagnation temperature and pressure available to drive such a facility, it only remained to arrive at a nozzle and a dump chamber configuration suitably matched to the tube. Simplified models were therefore developed to, first, calculate the effect of nozzle throat diameter on the available steady flow time and, second, to determine a suitable dump chamber size. The two calculations are detailed in Appendix B and Appendix C respectively.

### A. NOZZLE THROAT SIZE

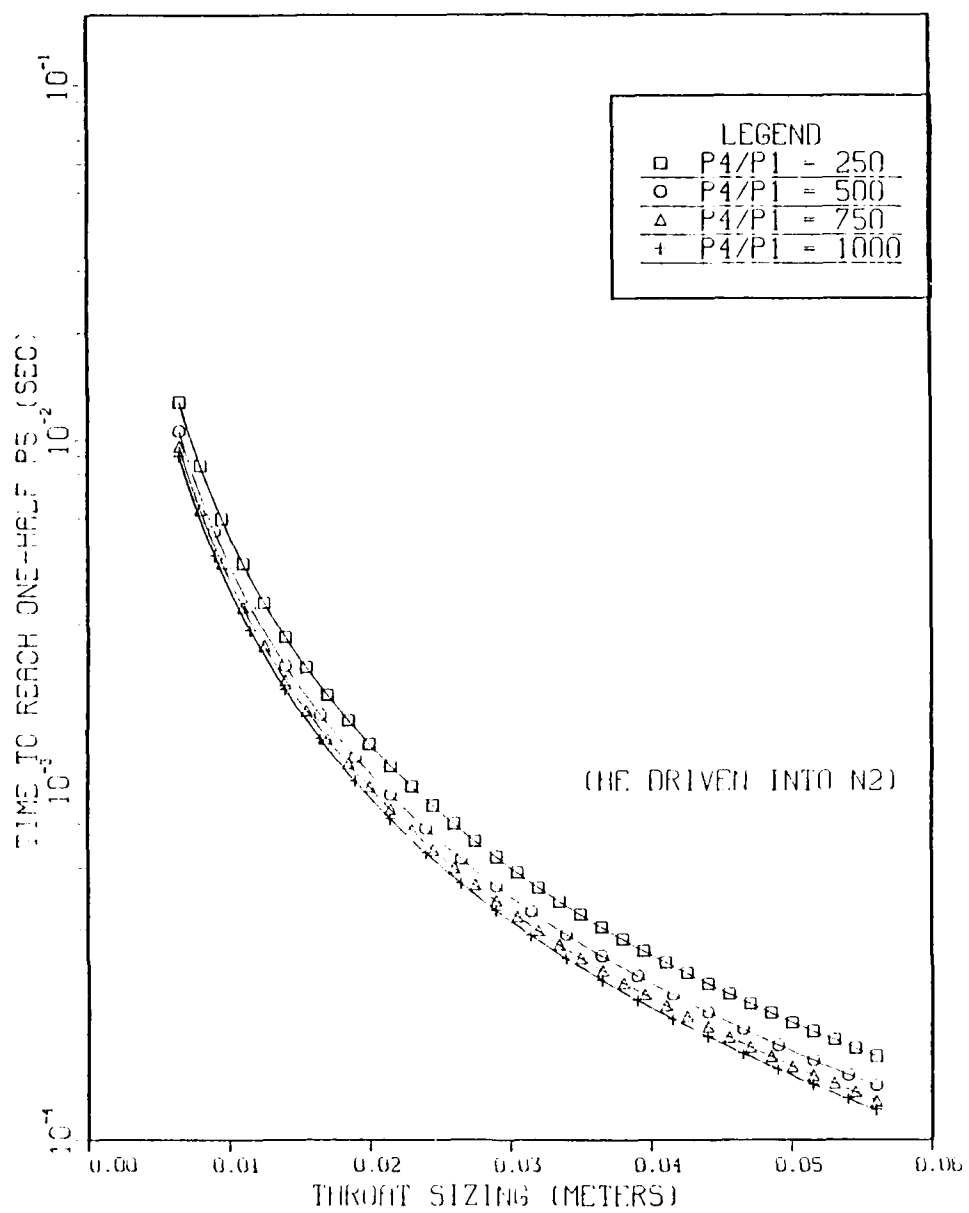
The nozzle throat diameter must be sized such that the time for which conditions in the reflected region are steady must be greater than the time required for the compressed mass of gas to exhaust through the nozzle. The model described in Appendix B estimates the time in relation to the falling pressure in the reflected region to be given by

$$t = \frac{m_0 \sqrt{T_5}}{C_1 A^* P_5} \left( \frac{2}{\gamma_5 - 1} \right) \left[ \frac{1}{\frac{\gamma_5 - 1}{2\gamma_5}} - 1 \right] \frac{P_t}{P_5} \quad (B.10)$$

If it is assumed the supply pressure can drop to half its initial value, the time required can be calculated using Equation (B.10) for different driver gases and shock strengths. Through the ratio  $m_0/\dot{m}_0$ , the calculated time is implicitly a function of the throat diameter. Results of such calculations are shown in Figure 39(a) and (b). The four curves shown illustrate the dependence of useful time on the shock strength and throat diameter. Clearly, the shock strength is less important than the throat area. Based on these results, a throat diameter 6.5mm (.025 inches) was selected. This choice made best use of the steady flow time which was experimentally determined to be from 3.5 to 5 milliseconds using tailored conditions. For the 6.5mm throat, Equation (B.10) was used to calculate the time for the reflected shock region pressure to decay to various fractions of its initial magnitude. The results are shown in Figure 40. Clearly, for even the strongest shock, the time for the pressure to decay to 80% of its initial value is longer than its experimentally determined tailored test time of 5 msecs.

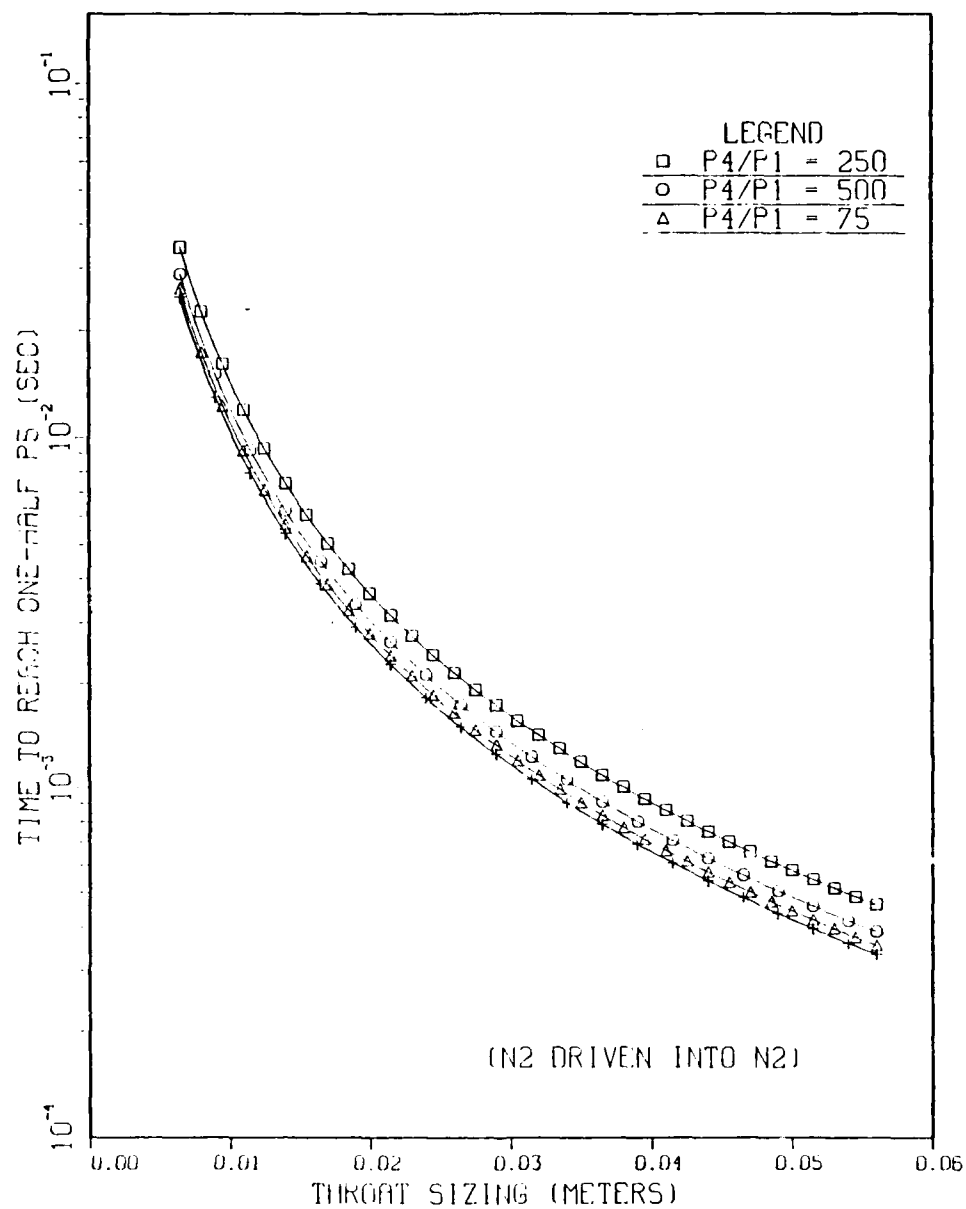
#### B. DUMP CHAMBER SIZE

The dump chamber requires a capacity such that the back pressure remains below the nozzle exit pressure for the duration of steady conditions in the driven tube. The



(a) Helium into Nitrogen

Figure 39. Time for Reflected Region Pressure to Drop to Half its Initial Value



(b) Nitrogen into Nitrogen

Figure 39 (CONTINUED)

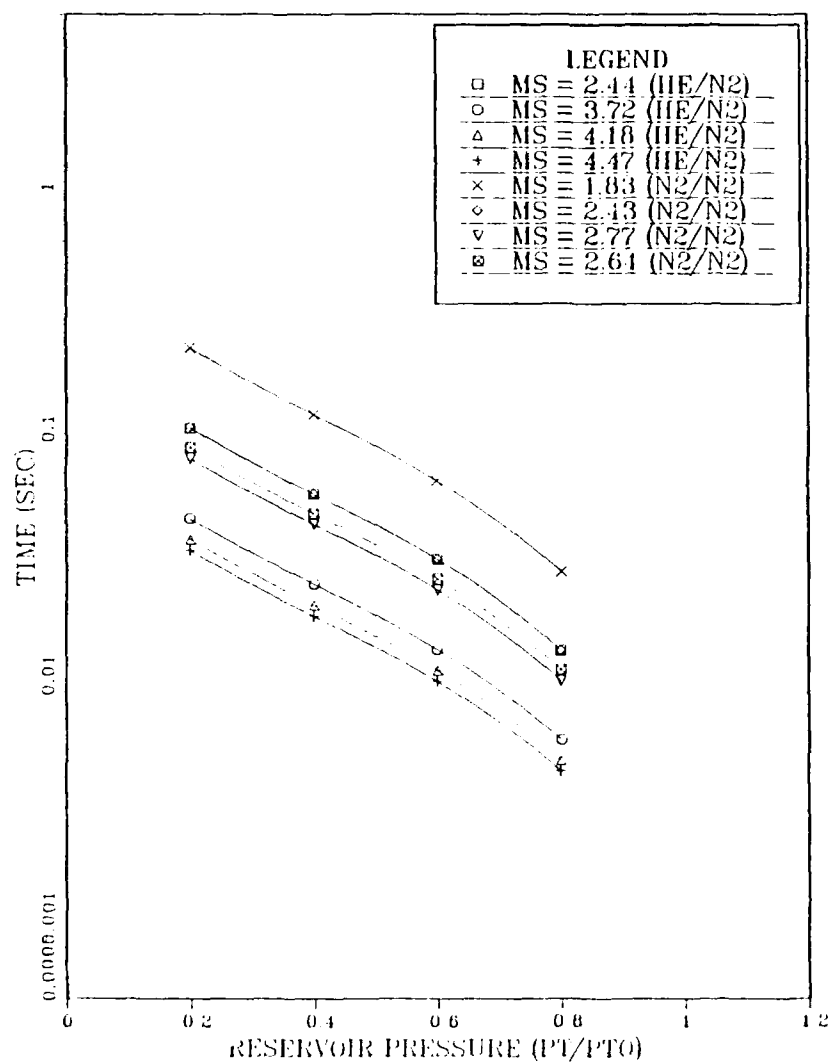


Figure 40. Calculated Time of Decay of Reflected Region Pressure for a 6.5mm Nozzle Throat

analysis in Appendix C gave the required ratio of dump chamber volume to reflected shock reservoir volume as

$$\frac{V_D}{V_0} = \left[ 1 + \frac{P_{D0}}{P_5} \frac{T_5}{T_D} \frac{V_D}{V_0} - \left( \frac{P_t}{P_5} \right)^{1/\gamma_5} \right] \frac{T_D \left[ 1 + \frac{\gamma_5 - 1}{2} M_e^2 \right]^{\frac{\gamma_5}{\gamma_5 - 1}}}{\frac{P_t}{P_5} T_5}$$

Examination reveals that the parameters which most influence the required dump chamber volume are the incident shock strength (which determines the reflected reservoir conditions), the desired test section Mach number, the driver gas selected, and the specified reflected region pressure ( $P_t/P_{t0}$ ) at which the flow breaks down. Since the pressure recovery is a function of which driver gas is selected, calculations were made for both nitrogen and helium. The results are shown in Figure 41. A mixture of the driver gases would be expected to fall between these two curves. Consistent with the finding above, the criterion that the dump chamber pressure becomes equal to the nozzle exit pressure when 20% of the stagnation pressure was exhausted, was taken to determine the necessary dump chamber volume. Shown in the figure are results obtained assuming the unknown temperature in the dump chamber to have its extreme maximum and minimum values; namely, initial reflected shock temperature and initial dump chamber temperature. From an examination of the results, a

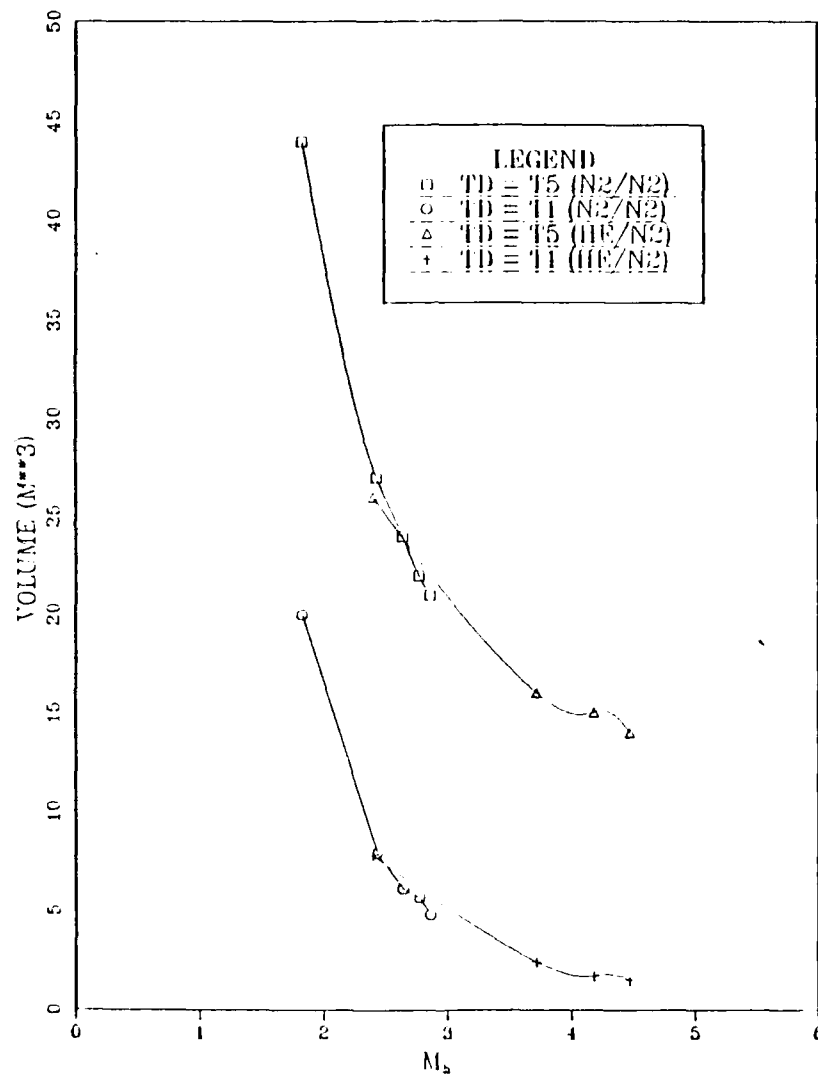


Figure 41. Dump Chamber Volume Requirements

conservative selection would be 15 cubic meters. This is a vessel approximately 6 feet in diameter and 15 feet long.

#### C. HIGH ENTHALPY MODIFICATION

Higher enthalpy flows can be generated using the free-piston arrangement shown in Figure 1. Stalker [Refs. 20,21] has carried out extensive experimental work in this area. A preliminary analysis shows that the NPS shock tube has the same internal diameter as Stalker's 1st generation free-piston tunnel, but has a thinner wall by 1/2". Structural limitations would prevent the full duplication of Stalker's tunnel but, with the published information on the design of free piston drivers, it should be possible to extend the present tube to an increased enthalpy level at which real gas effects of interest can be studied.

## VII. CONCLUSIONS AND RECOMMENDATIONS

The present study showed that:

- The existing shock-tube is straightforward and relatively inexpensive to operate, and gives repeatable test conditions;
- The existing shock tube can be used to drive a hypersonic shock tunnel to a Mach number of 12;
- Tailored operation can provide uniform stagnation conditions for periods of approximately 3.4 msec using Helium, and approximately 5 msec using a .7 He/.3N<sub>2</sub> mixture, as the driver gas;
- It is feasible to obtain both high speed movies and short duration spark flow visualization records of the test section flow field using currently available equipment;
- Contamination in the tube can lead to unwanted radiation (which must clearly be eliminated if real gas effects are the purpose of the experiment).

It is recommended that:

- The existing tube be serviced and its operating instrumentation be upgraded, as outlined in Appendix A;
- A Mach 10 nozzle, 15 cubic meters dump chamber and model support be designed and procured for operation with the current tube;
- Consideration be given to the addition of a free-piston tunnel to provide high enthalpy simulation.

Operation of a shock tunnel with the existing tube would provide a convenient and inexpensive facility for use in laboratory instruction. It would also provide a tool for thesis studies aimed at hypersonic CFD code validation.

Extension to a free-piston driver would provide an advanced tool for hypersonic research.

## APPENDIX A

### APPRAISAL OF THE PRESENT SHOCK TUBE

The NPS shock tube has been in operation since the late 1960's. This appendix provides a description of recommended improvements/enhancements of the existing system, which result from the experience gained in the reported program of tests.

#### A. O-RINGS

The planned relocation of the facility to the new Gas Dynamics Laboratory requires complete disassembly of the shock tube. Many O-rings are old and worn and they should be replaced at that time. Table 5 details the O-ring requirements.

#### B. THIN FILM GAUGES

The unavailability of replacement thin film gauges used to measure shock speed is unacceptable. Only the two installed gauges remain operational. The options are either to manufacture thin films in-house as detailed in Penaranda [Ref. 4] or to procure them commercially through the supply system.

TABLE 5

## O-RING REPLACEMENT GUIDE

<u>Location</u>	<u>Number Required</u>	<u>Width of Groove</u> (inches)	<u>Depth of Groove</u> (inches)	<u>Inside Diameter</u> (inches)	<u>Outside Diameter</u> (inches)
Driver Tube	1	$\frac{.100}{.106}$	$\frac{.157}{.163}$		$3.502 \pm .005$
Space/ Diaphragm	2	$\frac{.100}{.106}$	$\frac{.157}{.163}$		$\frac{4.000}{4.005}$
	2	$\frac{.100}{.106}$	$\frac{.157}{.163}$		$\frac{3.500}{3.505}$
Valve Body	1	$\frac{.101}{.105}$	$\frac{.157}{.163}$	$\frac{3.2485}{3.2495}$	
Tubing Sections	3	$\frac{.101}{.105}$	$\frac{.157}{.105}$	$\frac{3.2485}{3.2495}$	
Instrumentation Section	5	$\frac{.101}{.105}$	$\frac{.157}{.163}$	$\frac{3.2485}{3.2495}$	
Driver End Cap	1	$\frac{.101}{.105}$	$\frac{.157}{.163}$	$\frac{3.2470}{3.2460}$	

## C. PRESSURE TRANSDUCERS

### 1. Piezoelectric Transducer

The two Endevco Model 2501 transducers with Model 2642 M35 charge amplifiers should be returned to the manufacturer for calibration. Biased and unbiased responses should be checked. Unknown, but apparently unrealistic response characteristics made these transducers unusable for the reported experiments.

### 2. Piezoresistive Pressure Transducer

Procurement of a piezoresistive pressure measurement system, including a transducer and amplifier such as the Kistler Model 603B Series and Model 5004 Charge Amplifier, would provide continuous measurements of shock tube pressures.

A second transducer, to be used as a pitot probe for flow survey work in shock tunnel applications, is also required. Selection would be based on the selected nozzle Mach number and probe geometry. Cornell Aeronautical Laboratory publications by MacArther should be consulted.

## D. THIN FILM SIGNAL AMPLIFIER

The current thin film signal amplifier has no record of calibration for the past ten years. Voltage fluctuations are apparent and dial adjustment response is very poor. Prior to the next use the amplifier components should be tested and replaced as required.

#### E. DATA ACQUISITION

It is recommended that the Scientific Atlanta signal analyzer or its equivalent be used in all future testing. Post processing capability, and the availability of four channels with independent trigger adjustment provide a valuable experimental capability not available with the Tektronics 549 and 551 oscilloscopes.

#### F. DIAPHRAGMS

The existing brass diaphragms allow driver operation at a constant 600 psi level. Redesign to a higher operational level of approximately 700 psi would increase the range of reflected pressures available to drive a shock tunnel, with an associated cost of higher gas consumption. While not essential, this modification would reduce problems which would be expected in an extension to a shock tunnel with respect to the measurement of small aerodynamic forces.

Gaydon [Ref. 2:p. 91] and Glass [Ref. 18: pp. 503-511] provide valuable design insight into successful diaphragm material selection and preparation.

#### G. MISCELLANEOUS HARDWARE

Valve 7 and valve 11 located in the driven end of the tube [Ref. 4:Figure 2] exhibited some signs of leakage during the loading process. Repair or replacement of the valve seats is recommended.

## APPENDIX B

### ESTIMATION OF SHOCK TUNNEL NOZZLE THROAT AREA

In order to size a suitable nozzle to be driven by the high pressure and temperature in the reflected region, a simplified model was developed. The model was based on the following assumptions:

- A constant volume reservoir corresponding to the initial reflected shock conditions was available to drive the nozzle flow. The reservoir volume was defined by the diameter of the tube and the axial distance from the endplate of the tube to the point where the contact surface and reflected shock met (Fig. 3);
- The gas remaining in the reflected region expands isentropically to fill the constant volume;
- The flow through the nozzle throat was isentropic and always choked. (This implies that the evacuated dump chamber had sufficient volume, so as not to influence the nozzle flow.)

The total mass initially in the reflected reservoir is given by,

$$m_0 = \frac{P_5}{R_g T_5} V_0 \quad , \quad (B.1)$$

where

$$V_0 = \frac{\pi D^2 x_c}{4}$$

The mass at any later time is given by

$$m = \frac{P_t}{R_g T_t} \cdot V_0 \quad (B.2)$$

As the mass flows through the choked nozzle the rate of change of mass in the volume is equal to that which flows out through the nozzle, thus

$$-\frac{dm}{dt} = \frac{A^* P_t}{\sqrt{T_t}} C_1, \text{ where } C_1 = \sqrt{\frac{\gamma_5}{R_g}} \left[ \frac{\gamma_5 + 1}{2} \right]^{-\frac{\gamma_5 + 1}{2(\gamma_5 - 1)}} \quad (B.3)$$

Integrating

$$-\int_0^t dm = \int_0^t \frac{A^* P_t}{\sqrt{T_t}} C_1 dt \quad (B.4)$$

Since the expansion in the reservoir is assumed to be isentropic, the stagnation pressure and temperature are related according to

$$\frac{P_5}{T_5^{\frac{\gamma_5}{\gamma_5 - 1}}} = \frac{P_t}{T_t^{\frac{\gamma_5}{\gamma_5 - 1}}} \quad (B.5)$$

Taking the ratio of Equations B.1 and B.2 and substituting into Equation B.5,

$$\frac{m}{m_0} = \left( \frac{T_t}{T_5} \right)^{\frac{1}{\gamma_5 - 1}} = \left( \frac{P_t}{P_5} \right)^{1/\gamma_5} \quad (\text{B.6})$$

Substitution into Equation B.3 gives

$$- \frac{dm}{dt} = \frac{P_5}{\sqrt{T_5}} A^* \cdot C_1 \cdot \left( \frac{m}{m_0} \right)^{\frac{\gamma_5 + 1}{\gamma_5}} \quad (\text{B.7})$$

so that

$$- \int_1^{\frac{m}{m_0}} \left( \frac{m}{m_0} \right)^{-\frac{\gamma_5 + 1}{2}} d\left(\frac{m}{m_0}\right) = \frac{C_1 A^* P_5}{m_0 \sqrt{T_5}} \int_0^t dt \quad (\text{B.8})$$

On integrating, the variation of mass in the reflected reservoir with time is given by

$$t = \frac{m_0 \sqrt{T_5}}{C_1 A^* P_5} \left( \frac{2}{\gamma_5 - 1} \right) \left[ \left( \frac{m_0}{m} \right)^{\frac{\gamma_5 - 1}{2}} - 1 \right] \quad (\text{B.9})$$

and the variation of pressure in the reflected region with time is given by

$$t = \frac{m_0 \sqrt{T_5}}{C_1 A^* P_5} \left( \frac{2}{\gamma_5 - 1} \right) \left[ \frac{1}{\frac{\gamma_5 - 1}{2\gamma_5}} - 1 \right] \left[ \frac{P_t}{P_5} \right] \quad (\text{B.10})$$

To estimate a suitable nozzle throat, Equation B.10 was programmed and a ratio of  $P_t/P_s$  equal to one half was selected as the criterion for calculating the useful run time. Using throat area as a variable all other parameters were a function only of the incident shock strength and of the physical size of the tube. Thus Equation B.10 enabled the available time for steady flow through a given throat diameter to be estimated.

## APPENDIX C

### ESTIMATION OF THE REQUIRED DUMP CHAMBER VOLUME

In a shock tunnel application, the dump chamber pressure is required to remain below the nozzle exit static pressure for the useful duration of the reflected-shock supply conditions in the shock-tube. To aid in sizing a dump chamber for a Naval Postgraduate School shock tunnel the following analysis, based on a simplified model, was developed. The model assumes the pressure and temperature are uniform in the dump chamber, and that the velocity there is effectively zero. It is assumed that the flow to the exit of the nozzle is isentropic, and that the volume of the nozzle is negligible in comparison to that of the chamber. The volume of the dump chamber is given in terms of the initial mass contained and its properties, by

$$V_D = \frac{RT_D m_D}{P_D} \quad (C.1)$$

Dividing by the reflected reservoir volume, similarly written in terms of the initial mass contained and its properties, the ratio of dump chamber to reflected shock volume is given by

$$\frac{V_D}{V_0} = \frac{T_D}{T_5} \frac{P_5}{P_D} \frac{m_D}{m_0} \quad (C.2)$$

As the flow continues, the original reflected pressure ( $P_5$ ) decreases to lower values ( $P_t$ ). Since the nozzle area ratio is fixed, the pressure at the exit of the nozzle ( $P_e$ ) also steadily decreases. Meanwhile, the pressure in the dump chamber ( $P_D$ ) steadily increases until, at a point in time,  $P_D = P_e$ , and the useful test time is over. The ratio of the initial reflected pressure to dump chamber pressure is then given by

$$\frac{P_5}{P_D} = \frac{P_5}{P_t} \cdot \frac{P_t}{P_D} = \left(\frac{P_5}{P_t}\right) \left(\frac{P_t}{P_e}\right) \quad (C.3)$$

where

$$\frac{P_t}{P_e} = 1 + \frac{\gamma_5 - 1}{2} M_e^2 \frac{\gamma_5}{\gamma_5 - 1} \quad (C.4)$$

A mass balance gives

$$m_D = m_0 - m_i + m_{D0} \quad (C.5)$$

so that

$$\frac{m_D}{m_0} = 1 - \frac{m_i}{m_0} + \frac{m_{D0}}{m_0} \quad (C.6)$$

Using Equation B.6 from Appendix B

$$\frac{m_i}{m_0} = \frac{P_t}{P_5}^{1/\gamma_5} \quad (C.7)$$

and substituting in Equation C.6,

$$\frac{m_D}{m_0} = 1 - \left( \frac{P_t}{P_5} \right)^{1/\gamma_5} + \frac{m_{D0}}{m_0} \quad (C.8)$$

Using Equation C.2 applied to the initial conditions,

$$\frac{m_{D0}}{m_0} = \left( \frac{V_D}{V_0} \right) \left( \frac{P_{D0}}{P_5} \right) \left( \frac{T_5}{T_{D0}} \right) \quad (C.9)$$

Combining Equations C.2 through C.9

$$\frac{V_D}{V_0} = \left[ 1 + \left( \frac{P_{D0}}{P_5} \right) \left( \frac{T_5}{T_{D0}} \right) \left( \frac{V_D}{V_0} \right) - \left( \frac{P_t}{P_5} \right)^{1/\gamma_5} \right] T_D \frac{\left[ 1 + \frac{\gamma_5 - 1}{2} M_e^2 \right]^{\frac{\gamma_5}{\gamma_5 - 1}}}{\left( \frac{P_t}{P_5} \right) T_5} \quad (C.10)$$

Equation C.10 provides a relationship between  $V_D/V_0$  and the value of  $P_t/P_5$  which terminates the useful test time, in terms of given initial reflected reservoir and dump chamber conditions. Using an interval halving technique the dump chamber volume requirements were investigated using an assumption that the temperature in the dump chamber was equal to its initial value, and also with the worst-case assumption that it was equal to  $T_5$ . (It is noted that the temperature change can be included explicitly through the conservation of energy. However the complexity of doing so

is not warranted when an estimate of the needed volume is  
all that is required.)

APPENDIX D  
SUMMARY OF EXPERIMENTAL DATA

This appendix contains data taken using thin film gauges and the pressure transducer. First, in Figure 42, the measurements obtained of shock Mach number using oscilloscopes (preceeding Run 50) are shown. For all runs from Run 50 on, data were taken using the Scientific Atlanta SD380 signal analyzer. Tables 6 and 7 list data for runs using a mixture of helium and nitrogen and for runs using pure helium as a driver, respectively. For each run, trace A recorded the response of the thin film at location A, trace B recorded the response of the thin film response at station B, trace C recorded the response of the endplate pressure transducer. Delay times were programmed prior to each run. Traces B and C were delayed by the same time. Figure 43 provides definitions of items which appear on the SD380 screen and identifies the menu selections of interest.

The last 35 pages of the appendix contain printouts of the SD380 screen for the runs listed in Tables 6 and 7. Each printout can be interpreted with reference to Figure 43. Times were obtained for shock travel between transducers on traces A, B and C, using the time scale given on the printout, and the delay times listed in Tables 6 and 7. These results are included in the two tables.

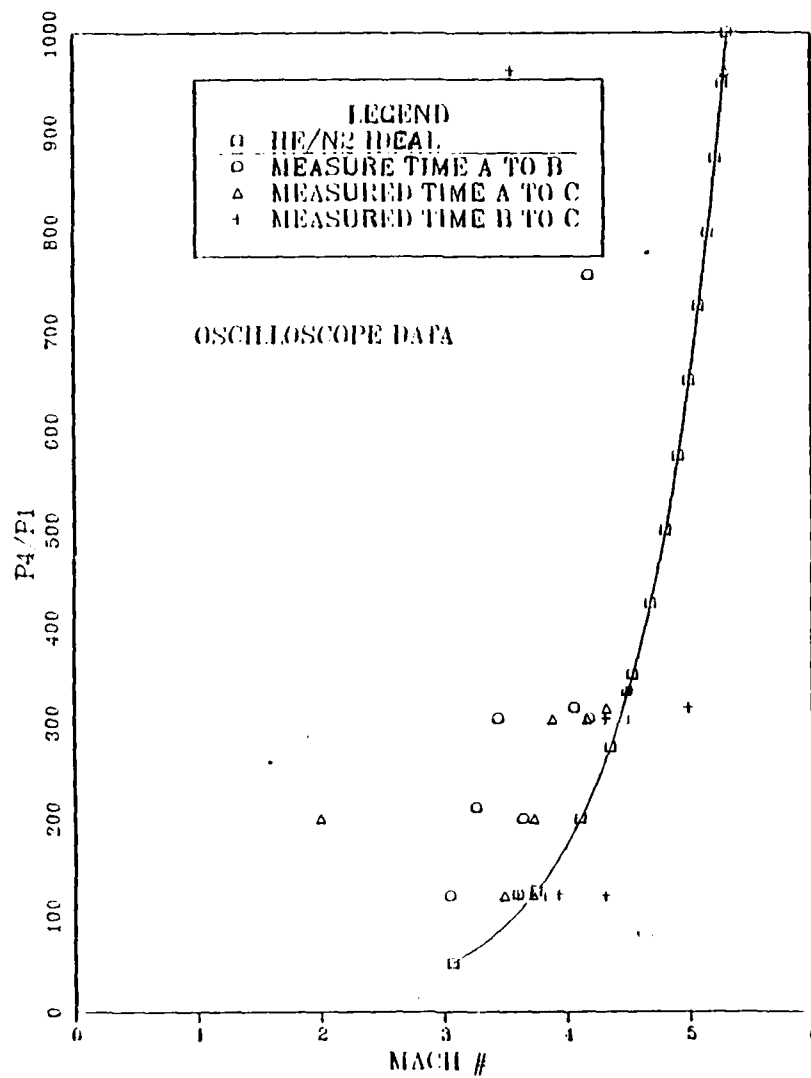


Figure 42. Shock Strength vs.  $P_4/P_1$  for Data Reduced from Polaroid

TABLE 6

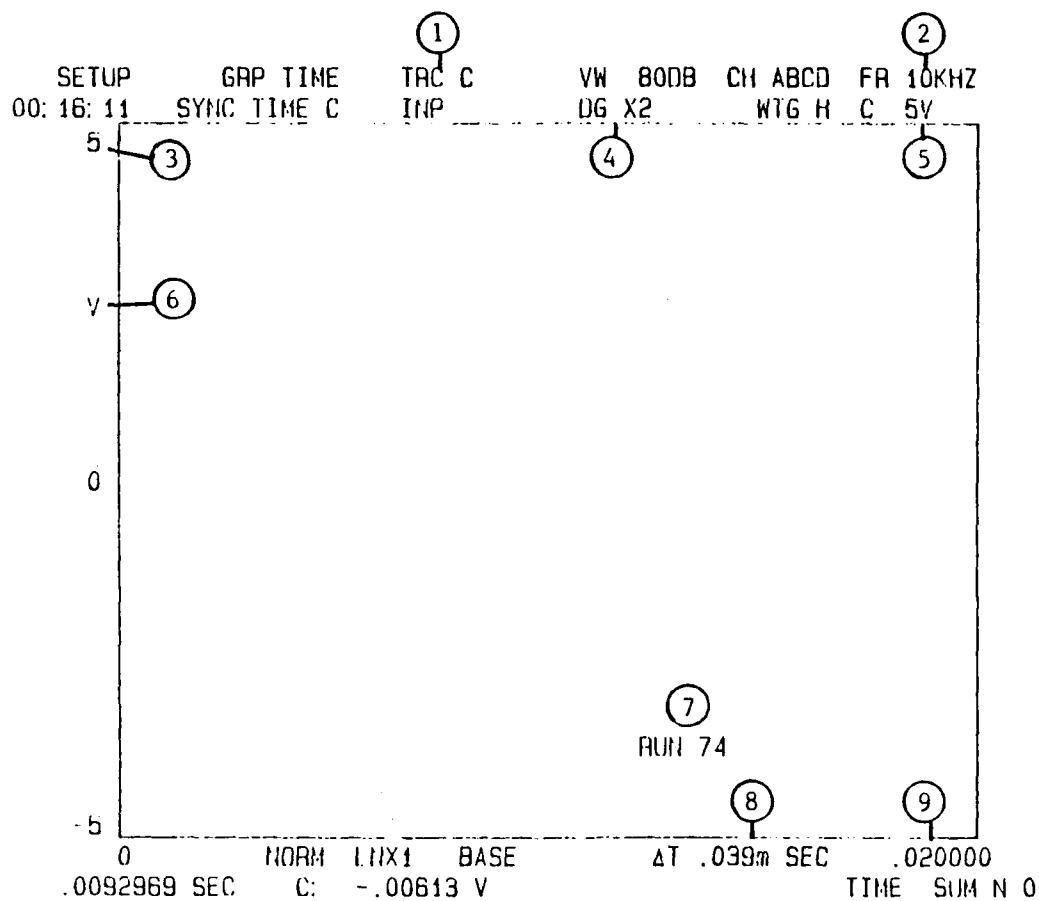
TIME MEASUREMENT  
(70% HELIUM 30% NITROGEN DRIVER/N<sub>2</sub> DRIVEN)

Run #	Temperature (F)	Delay A (msec)	Delay B (msec)	Time A to B (msec)	Time B to C (msec)	Time C to B (msec)
62	63	-1.01	0.00	2.84	1.67	3.63
63	65	-1.01	-1.01	1.77	1.77	1.72
69	64	-1.01	0.49	1.81	--	--
70	64	-1.01	0.51	1.36	1.83	3.86
71	64	-1.01	0.51	1.72	2.03	3.79
72	65	-1.01	0.51	1.76	2.03	3.82
73	64	-1.01	0.51	1.80	2.07	3.86

TABLE 7

TIME MEASUREMENT  
(HE DRIVER/N<sub>2</sub> DRIVEN)

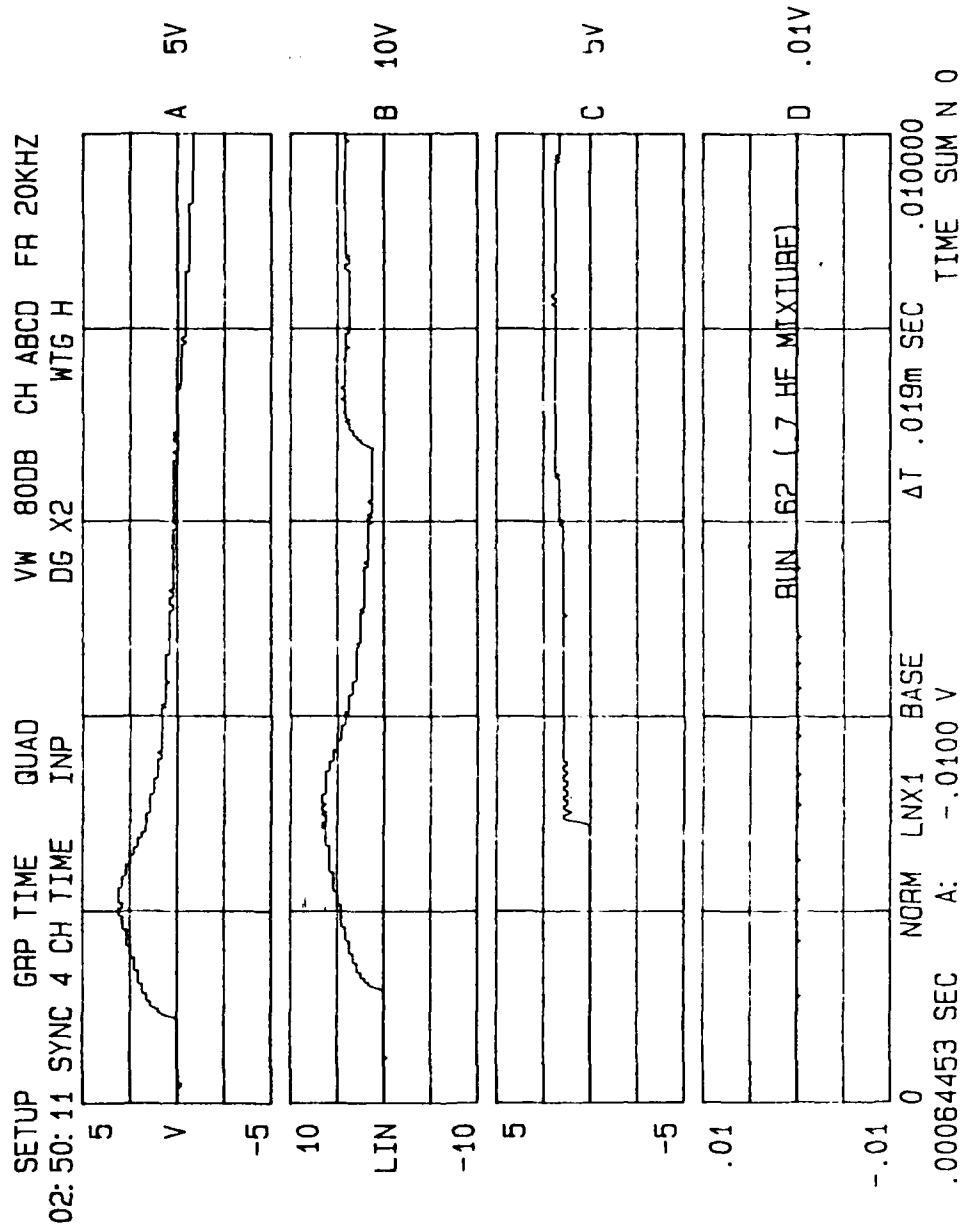
Run #	Temperature (F)	Delay A (msec)	Delay B (msec)	Time A to B (msec)	Time B to C (msec)	Time C to B (msec)
50	66	0.00	0.49	1.45	--	
51	66	0.00	0.49	1.64	0.94	2.50
52	62	-1.01	0.49	0.92	1.24	2.48
53	62	-1.01	0.49	1.30	0.92	2.55
57	62	-1.01	0.49	0.92	1.09	2.50
58	62	-1.01	0.49	1.19	1.13	2.48
59	62	-1.01	0.49	1.17	1.23	2.34
60	62	-1.01	0.49	1.32	1.11	2.44
61	62	--	--	1.15	--	
64	64	-1.01	0.49	1.23	--	
65	63	-1.01	0.49	1.30	--	
66	61	--	--	--	--	
67*	63	--	--	1.18	--	
68*	63	--	--	1.18	--	
74	67	-2.02	0.51	0.97	--	
75	67	--	--	--	--	



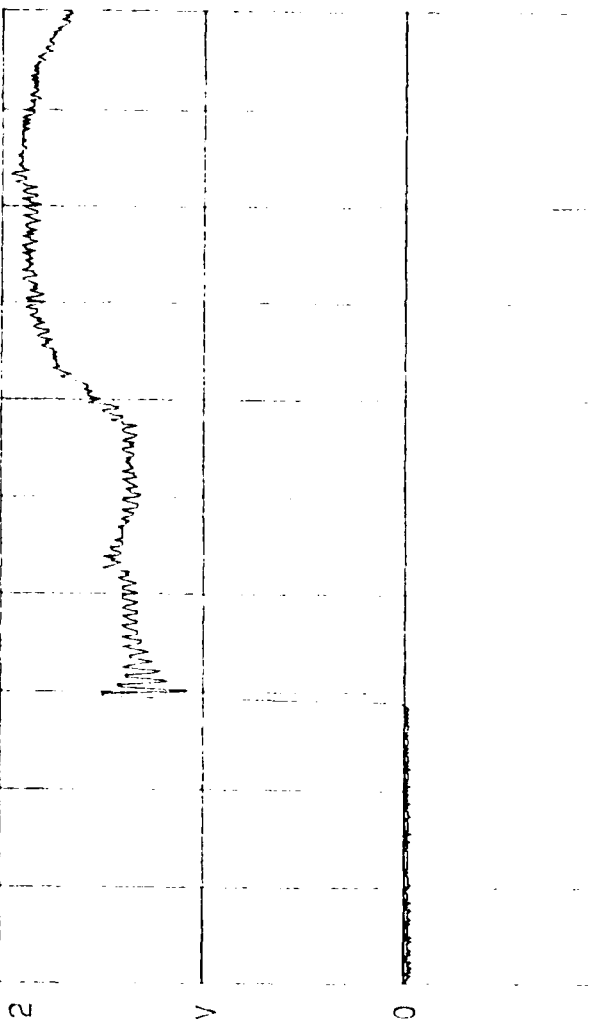
Menu Selections of Interest:

- |                             |                           |
|-----------------------------|---------------------------|
| 1 - DISPLAY TRACE SELECTION | 6 - Y AXIS UNITS          |
| 2 - FREQUENCY RANGE         | 7 - RUN NUMBER            |
| 3 - Y AXIS SCALING          | 8 - X AXIS UNITS          |
| 4 - DISPLAY GAIN            | 9 - X AXIS SCALING (msec) |
| 5 - INPUT LEVEL             |                           |

Figure 43. SD380 Menu Selection Items of Interest



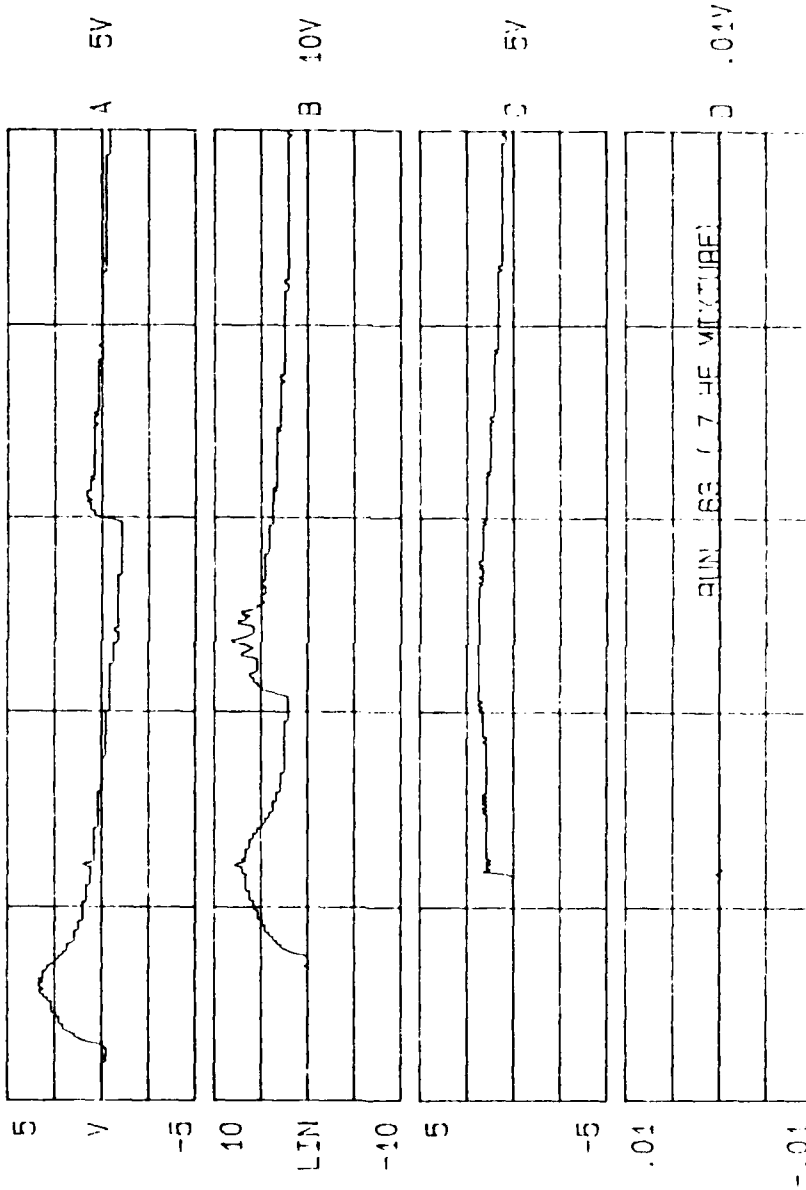
SETUP 02:53:52 GRP TIME TRC C VV 80C3 CH ABCD FR 20KHZ  
 SYNC TIME C INP DG X5 WTG H C 5V



RUN 62 (.7 HE MIXTURE)

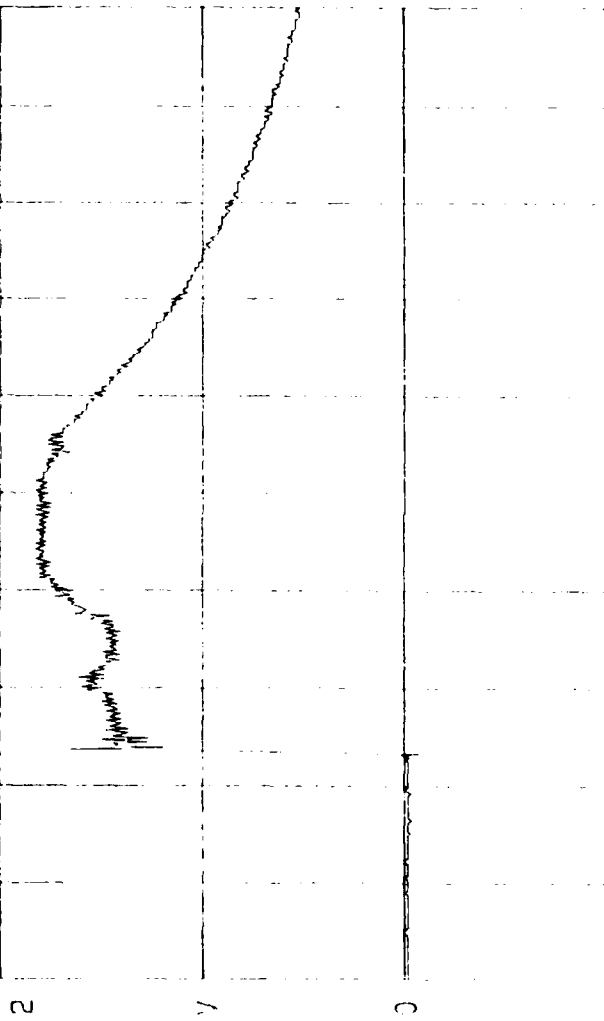
-2  
 0 NORM ENXI BASE LT .019m SEC .010000  
 .00064453 SEC 2: .0195 TIME SUM N J

SETUP 02:38:18 SYNC 4 CH TIME GRP TIME QUAD VV 8003 CH ABCD FR 10KHZ  
 DG X2 WTS 4



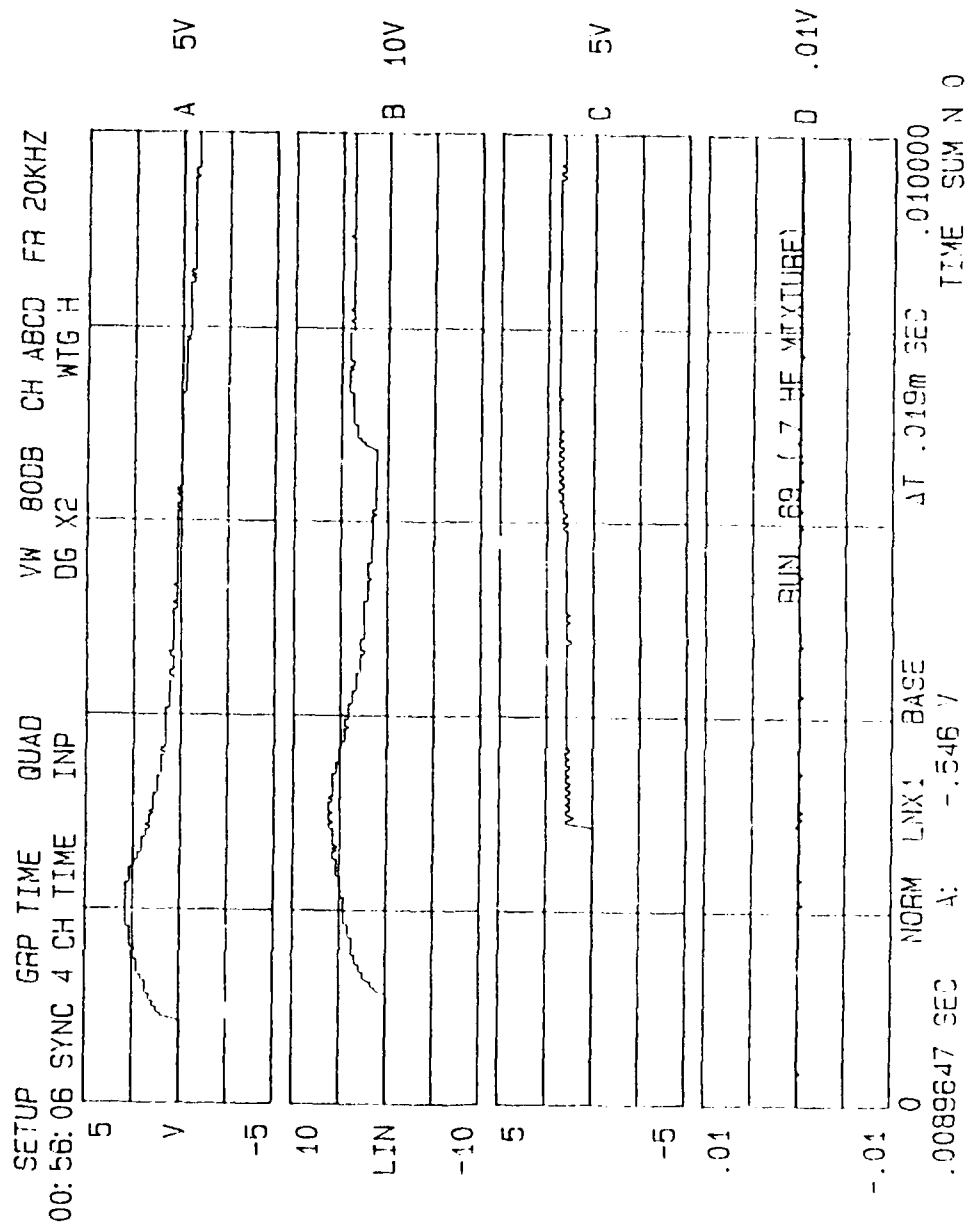
0 NORM LN1 BASE 0.00000  
 .0012891 SEC 4: 1.39 / TIME SUM 10

SETUP 02: 41: 38 GRP TIME TRC C YW 80DB CH ABCD FR 10KHZ  
 SYNC TIME C INP DG X5 WTG H C 5V

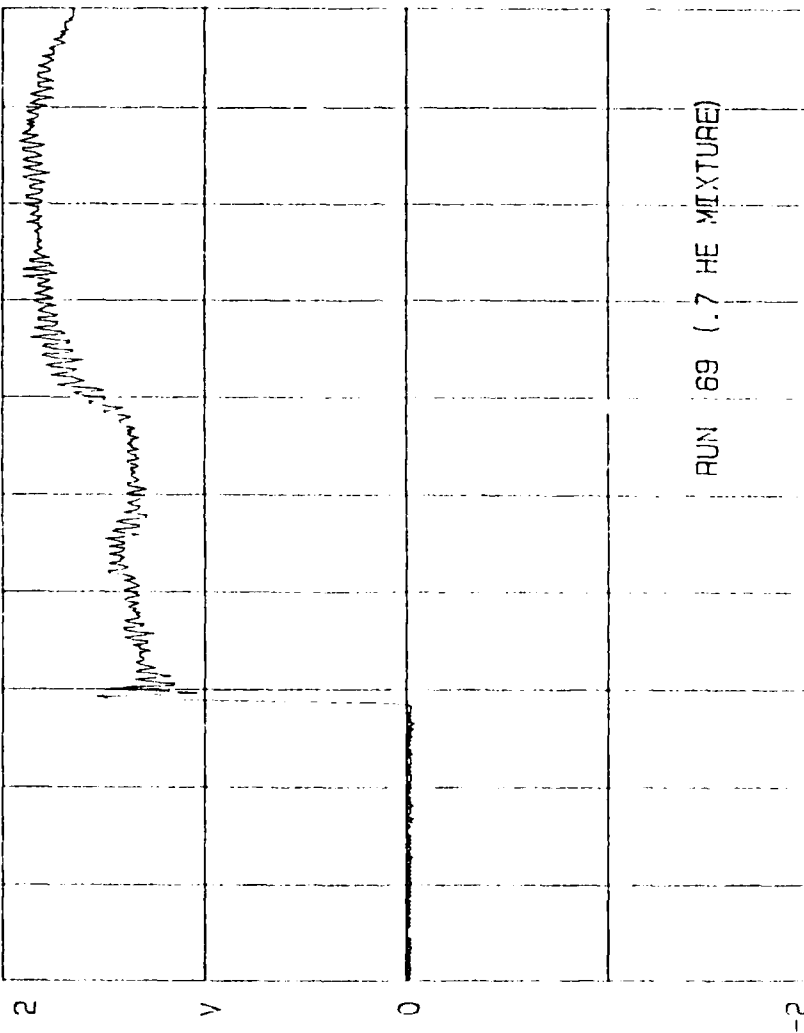


RUN 63 (.7 HE MIXTURE)

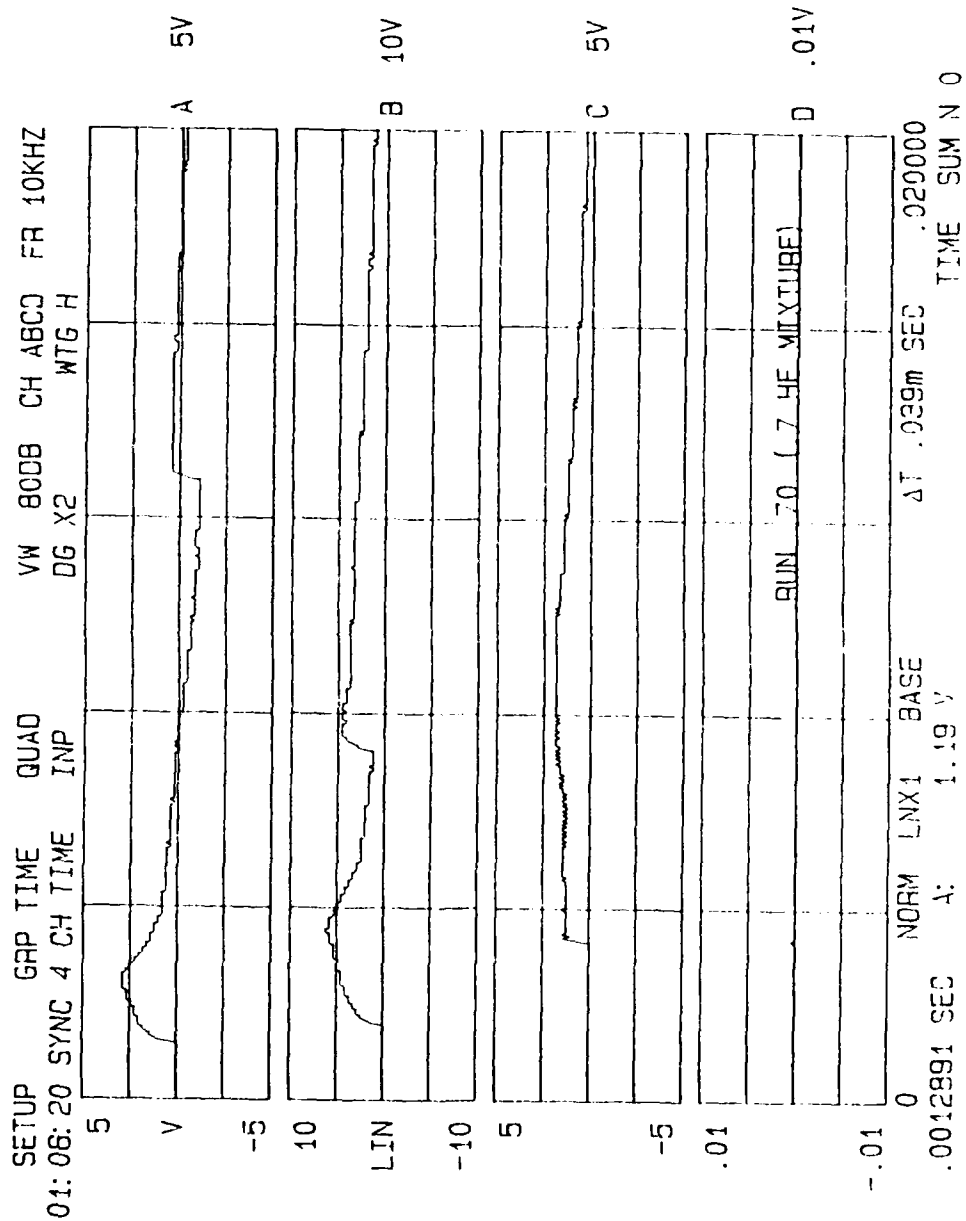
-2  
 0  
 .0053203 SEC C: 1.19 BASE  
 .020000  
 TIME SUM N 0



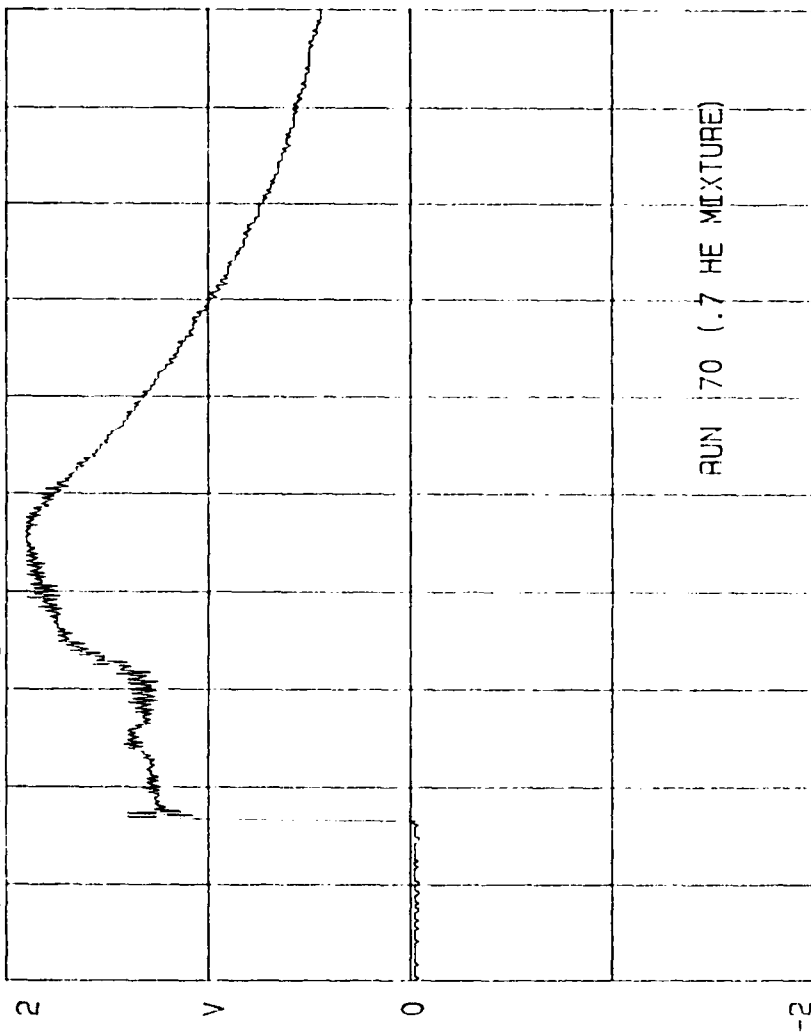
SETUP GRP TIME TRC C VW 8008 CH ABCD FR 20KHZ  
 00: 44: 12 SYNC TIME C INP DG X5 WTG H C 5V



0 NORM LNX1 BASE ΔT .019m SEC .01000  
 .0041502 SEC C: 1.41 V TIME SUM N 0

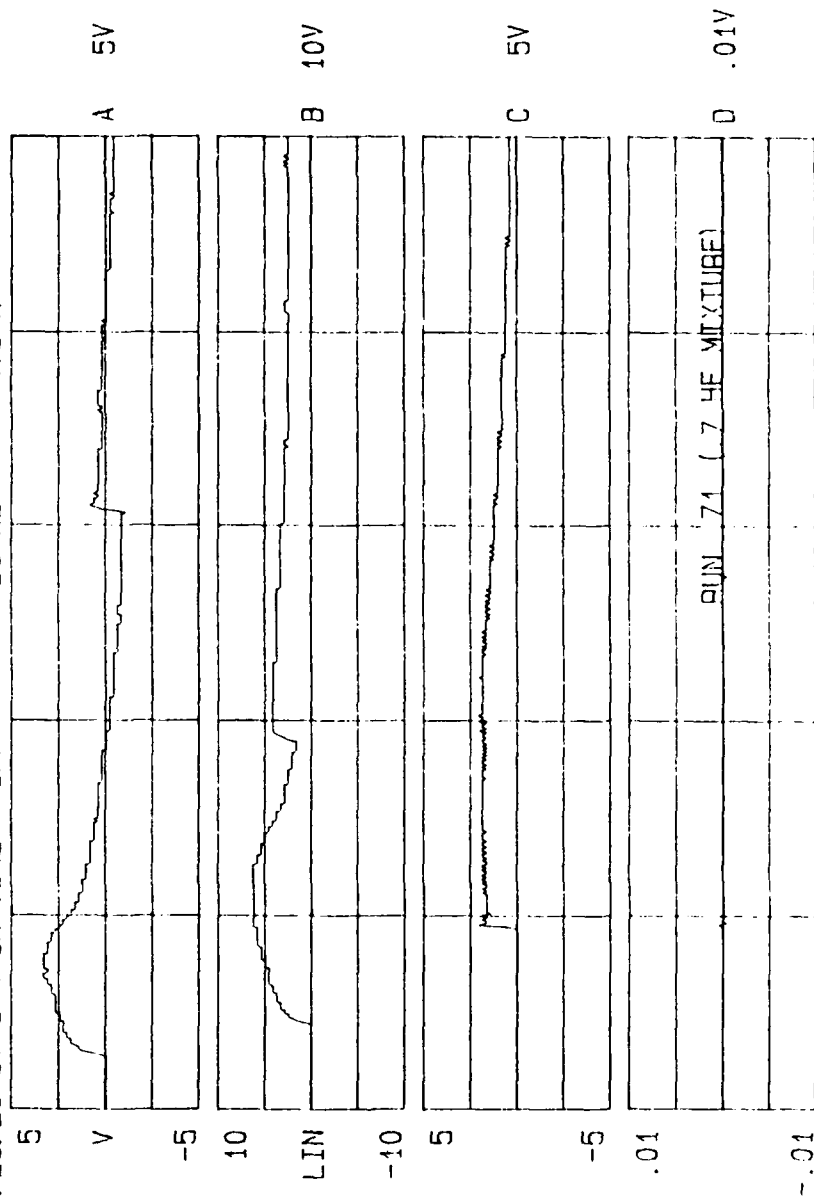


SETUP 00: 20: 48 GRP TIME TRC C VW 80DB CH ABCD FR 10KHZ  
 SYNC TIME C INP DG X5 WTG H C 5V



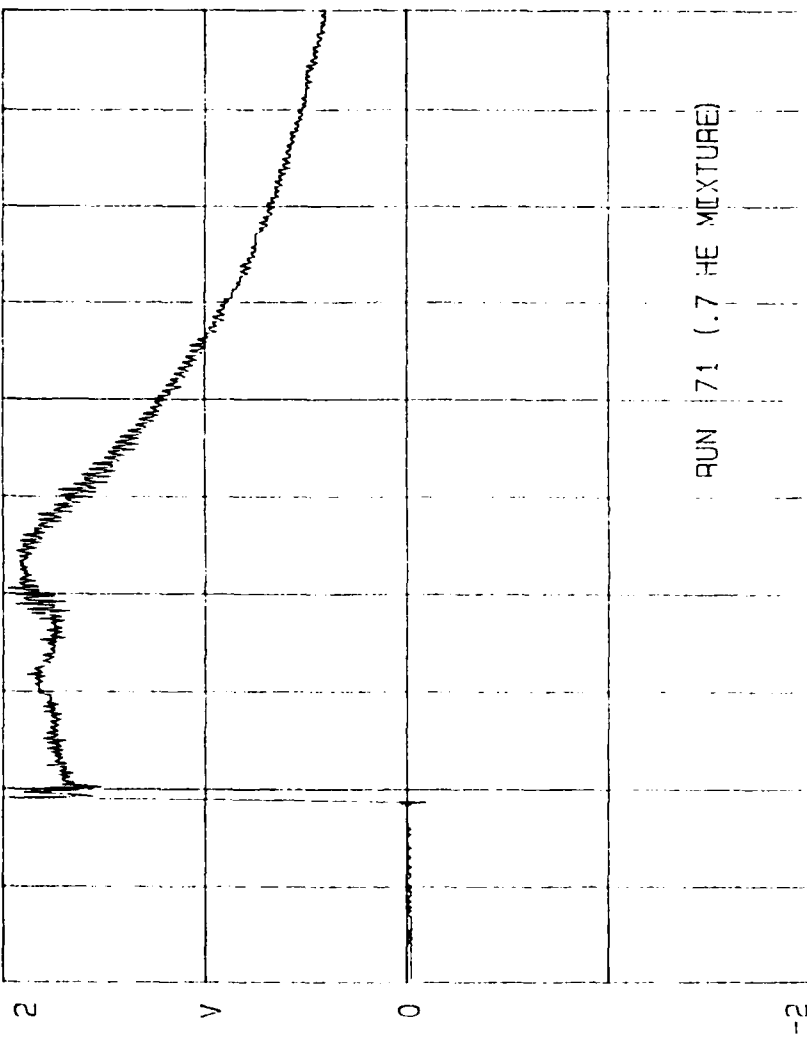
0 .0034374 SEC C: 1.40 V  
 ΔT .039m SEC TIME SUM N 0

SETUP GRP TIME QUAD VW BODB CH ABCD FR 10KHZ  
 01:26:25 SYNC 4 CH TIME INP DG X2 WTG H

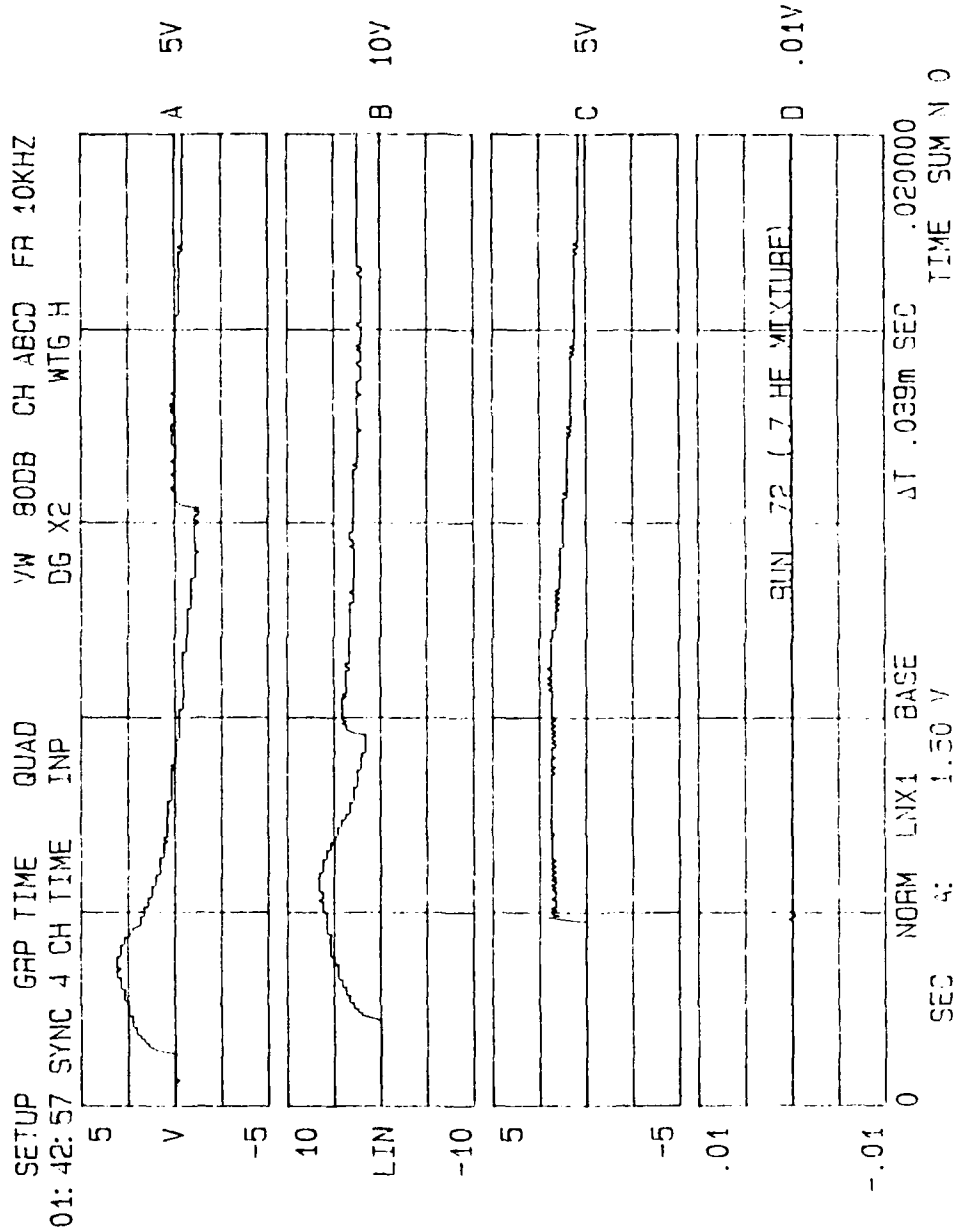


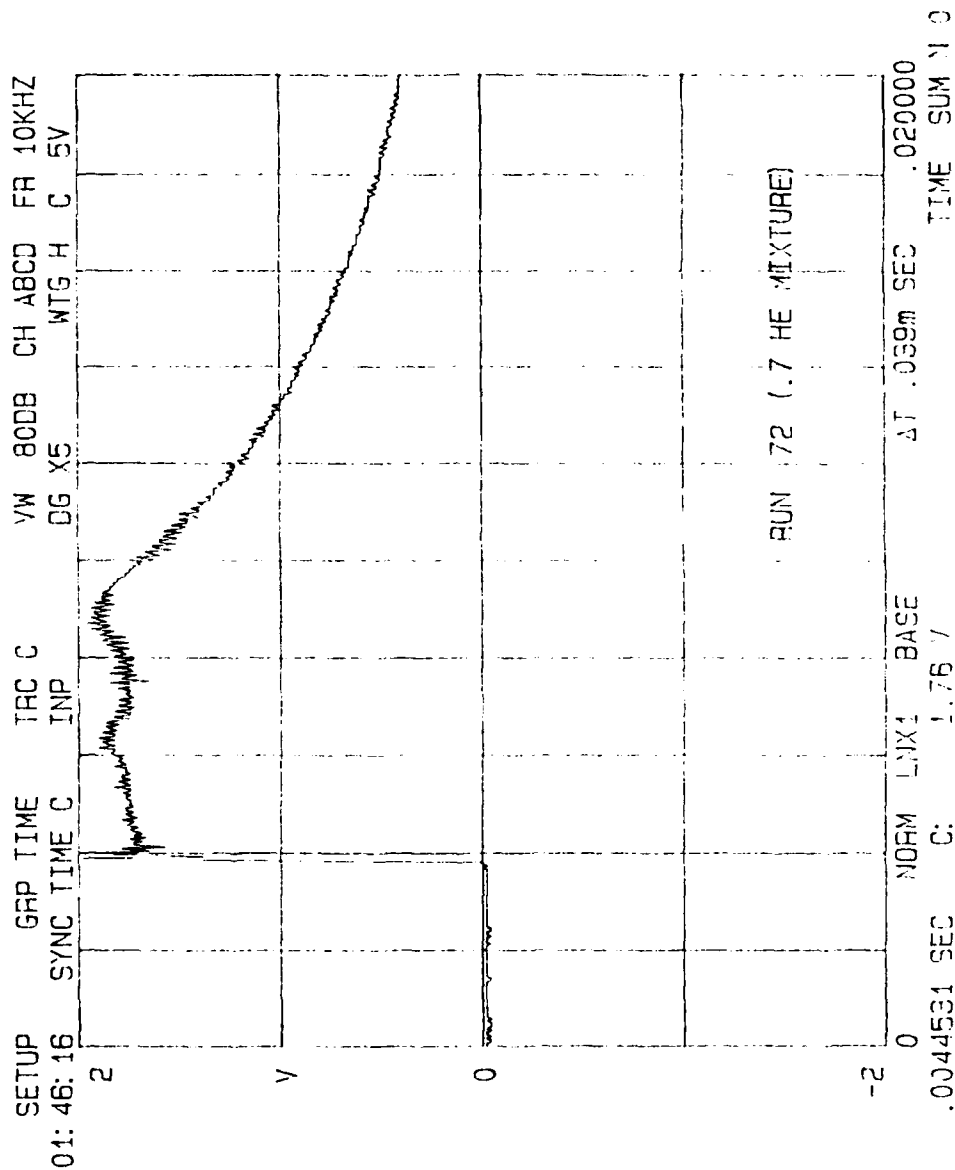
0 NORM LN1 BASE  
 .0015824 SEC A: 2.13 V  
 .020000  
 TIME SUM N 0

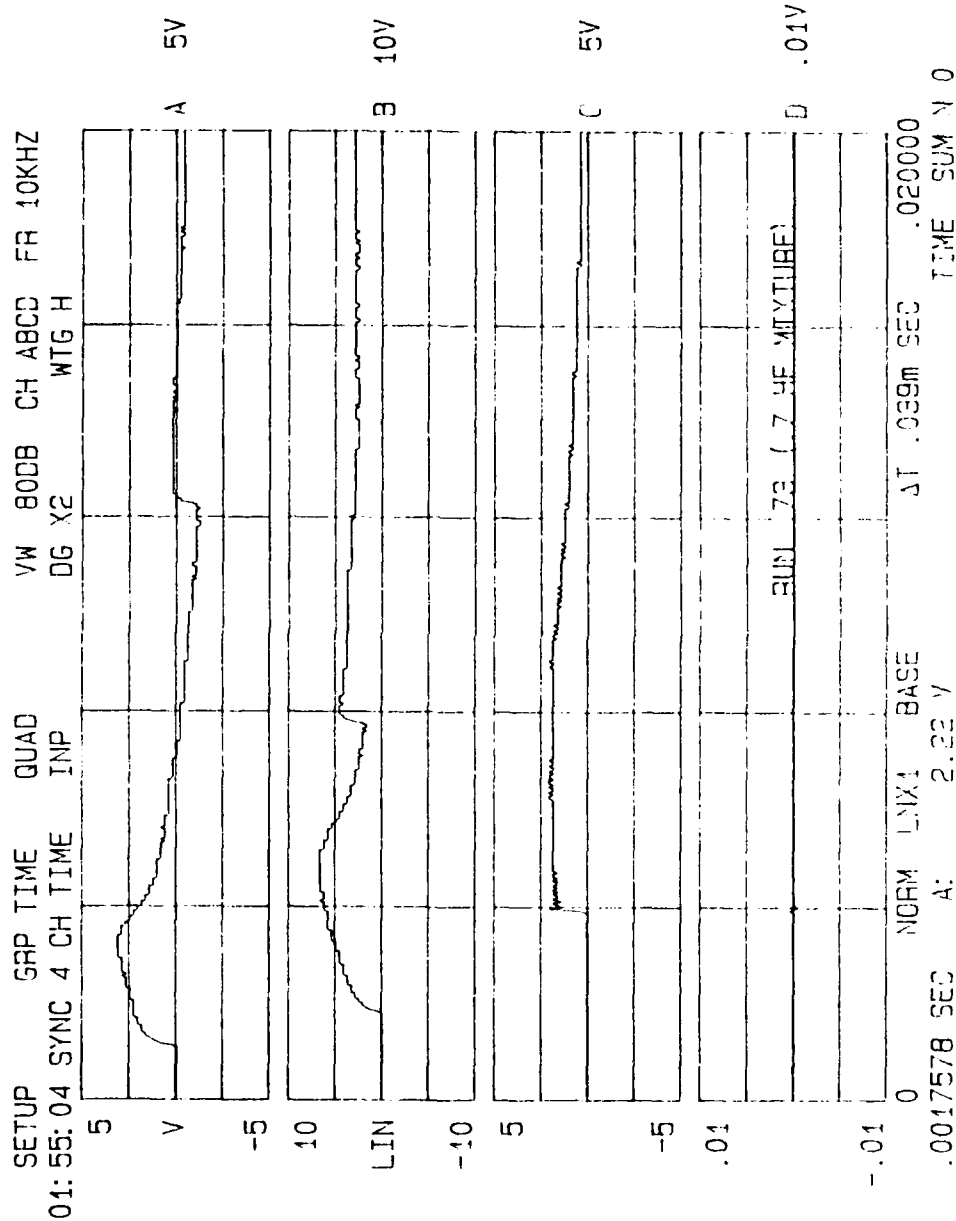
SETUP GRP TIME TRC C VW 800B CH ABCD FR 10KHZ  
 01:31:44 SYNC TIME C INP WTG H C 5V



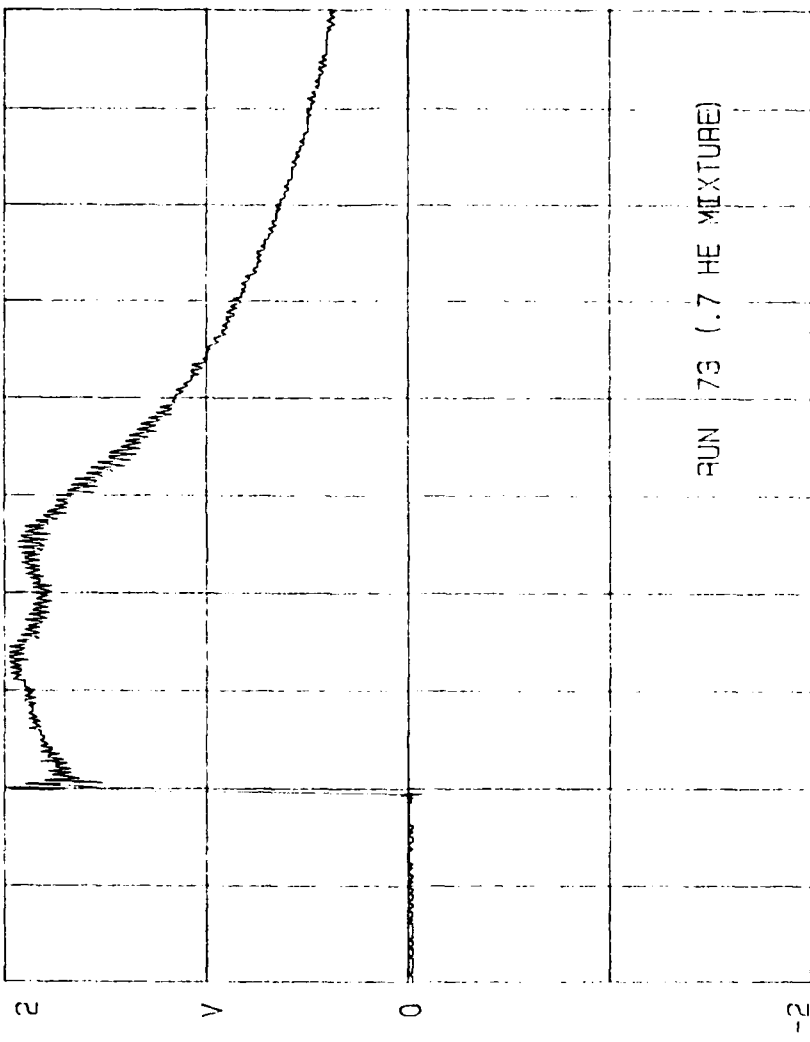
0 NORM LIN! BASE  
 .0058993 SEC C: 1.79 V  
 ΔT .039m SEC TIME SUM V 0



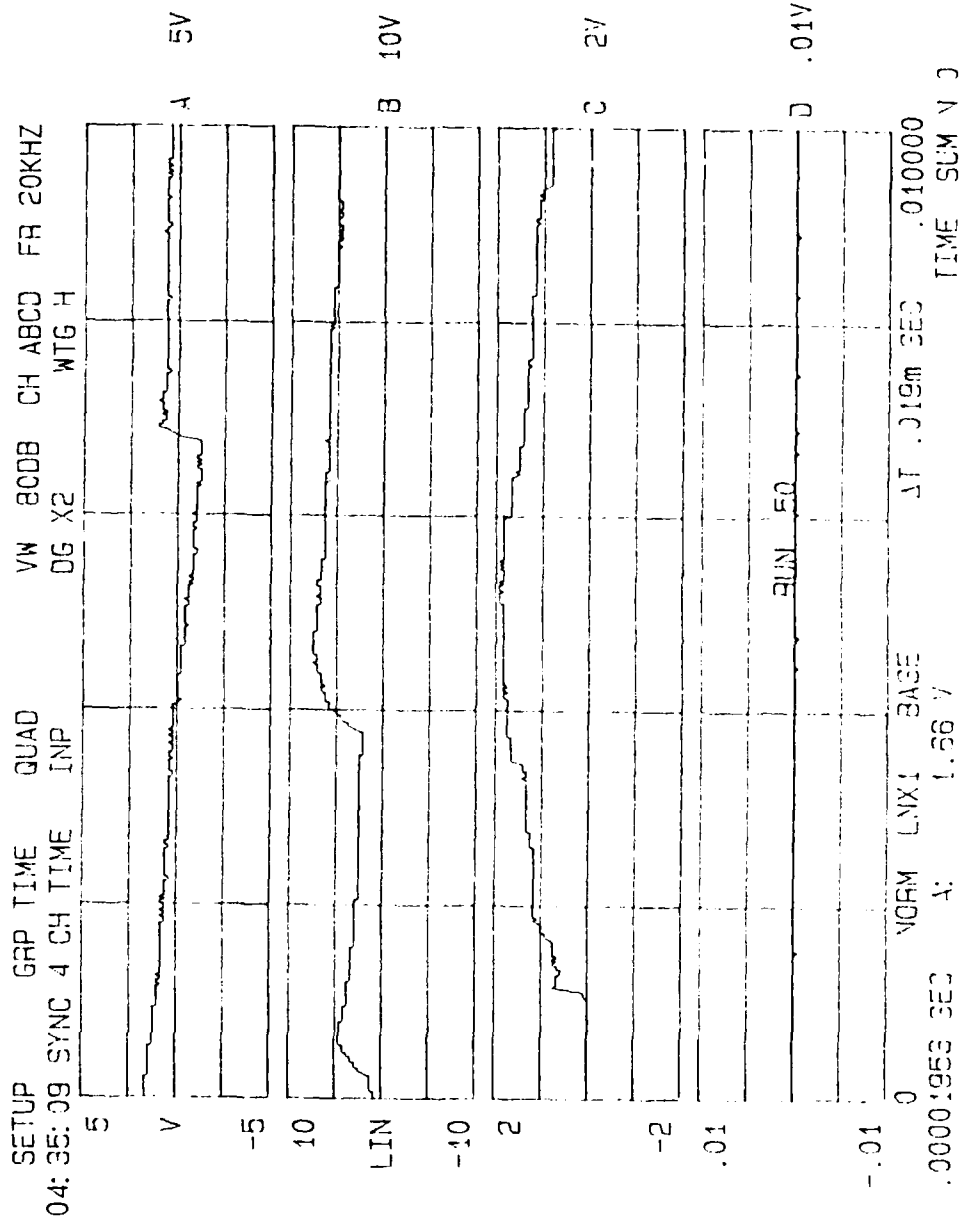




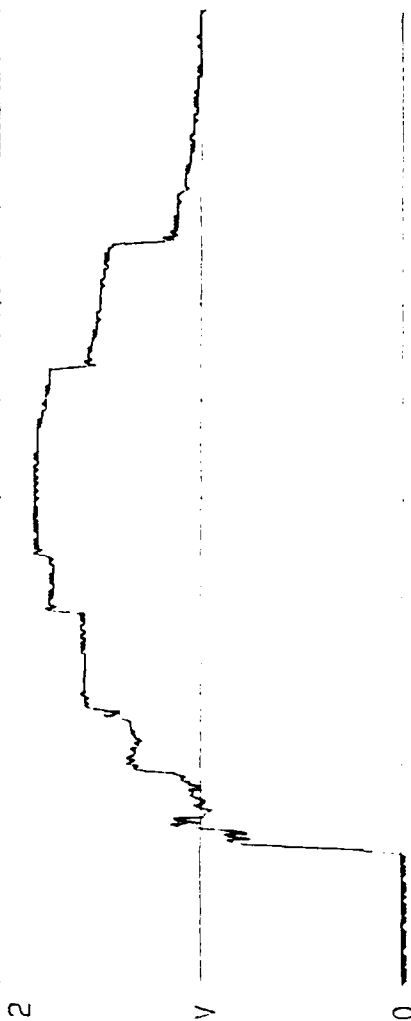
SETUP 01:58:33 GAP TIME TAC C TRC C VW 80DB CH ABCD FR 10KHZ  
 SYNC TIME C INP WTG H C 5V



0 .0066405 SEC C: .0066405 SEC AT .039m SEC .020000  
 TIME SUM N 0



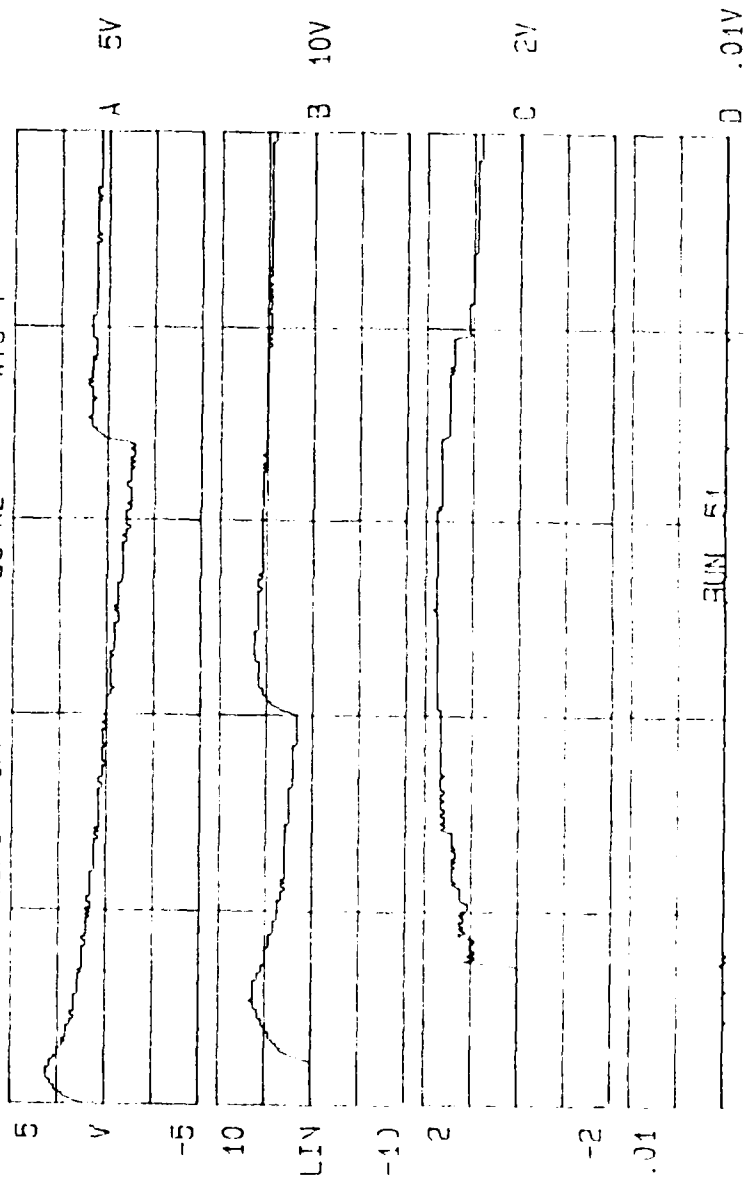
SETUP GRP TIME TRC C YW 80DB CH ABCD FR 20KHZ  
 02:10:25 SYNC TIME C INP DG X2 WTG H C 2V



RUN 50 PRESSURE  
 TRACE

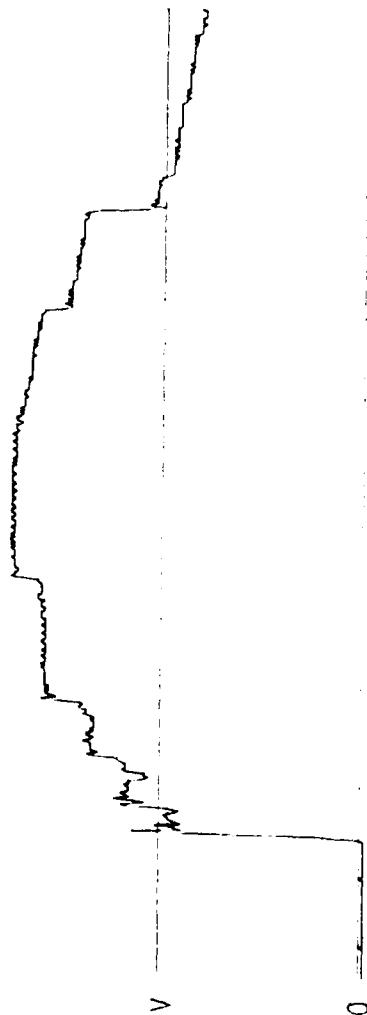
-2  
 0  
 .0016405 SEC C: 1.01 V  
 NORM LNX1 BASE  
 ΔT .019m SEC .010000  
 TIME SUM N 0

SETUP 04: 25: 27 SYNC 4 CH TIME QUAD INP VV 80DB CH ABCD FR 20KHZ  
 DG X2 WTG H



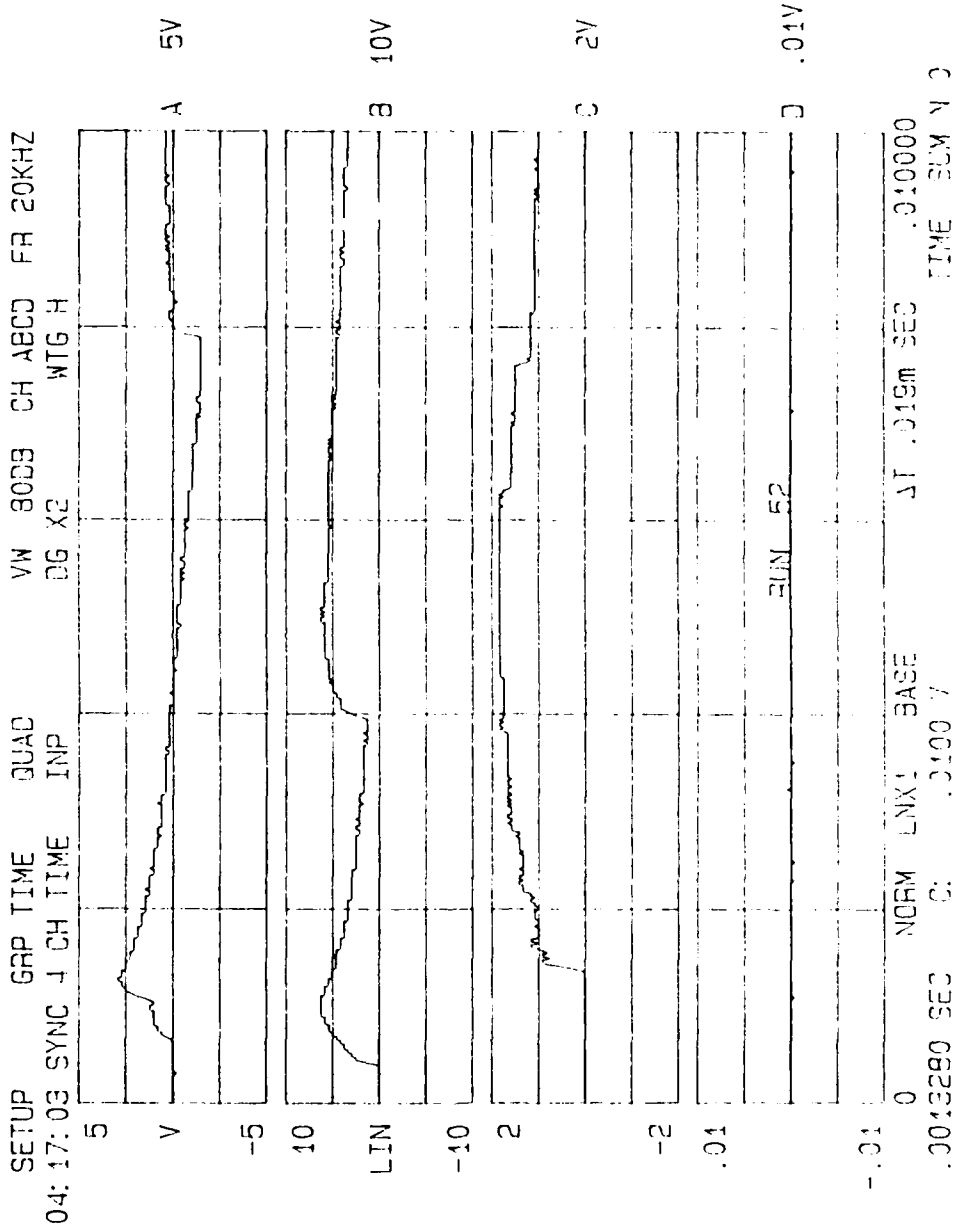
5  
 V  
 -5  
 10  
 LIN  
 -10  
 2  
 -2  
 .01  
 -.01  
 0  
 .0014257 SEC 2: .0179 /  
 .0014257 SEC 2: .0179 /  
 .010000  
 TIME SUM N 0

SETUP GAP TIME IRC C VW 80DB CH ABCJ FR 20KHZ  
 01:48:59 SYNC TIME C INP DG X2 WTG H C 2V  
 2

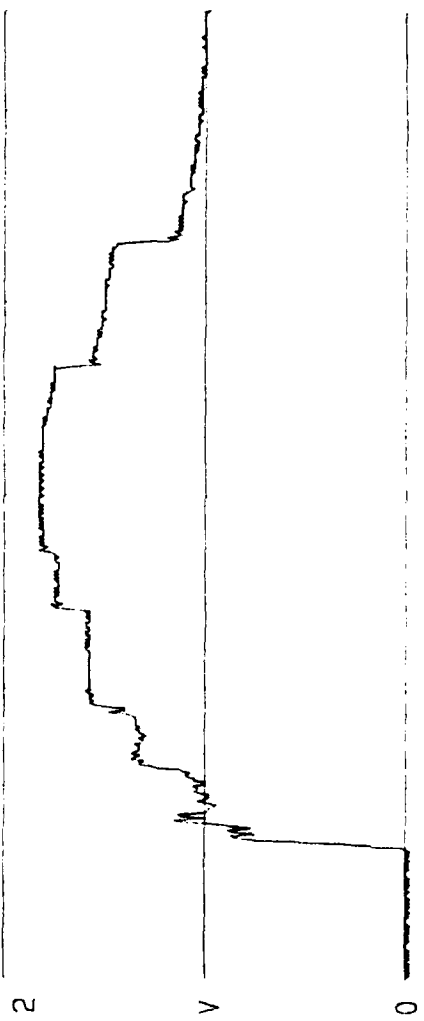


RUN 51 PRESSURE  
 TRACE

-2 0 NORM LIX: BASE  
 .0015430 SEC 2: 1.32 /  
 .010000  
 TIME SUM N 0

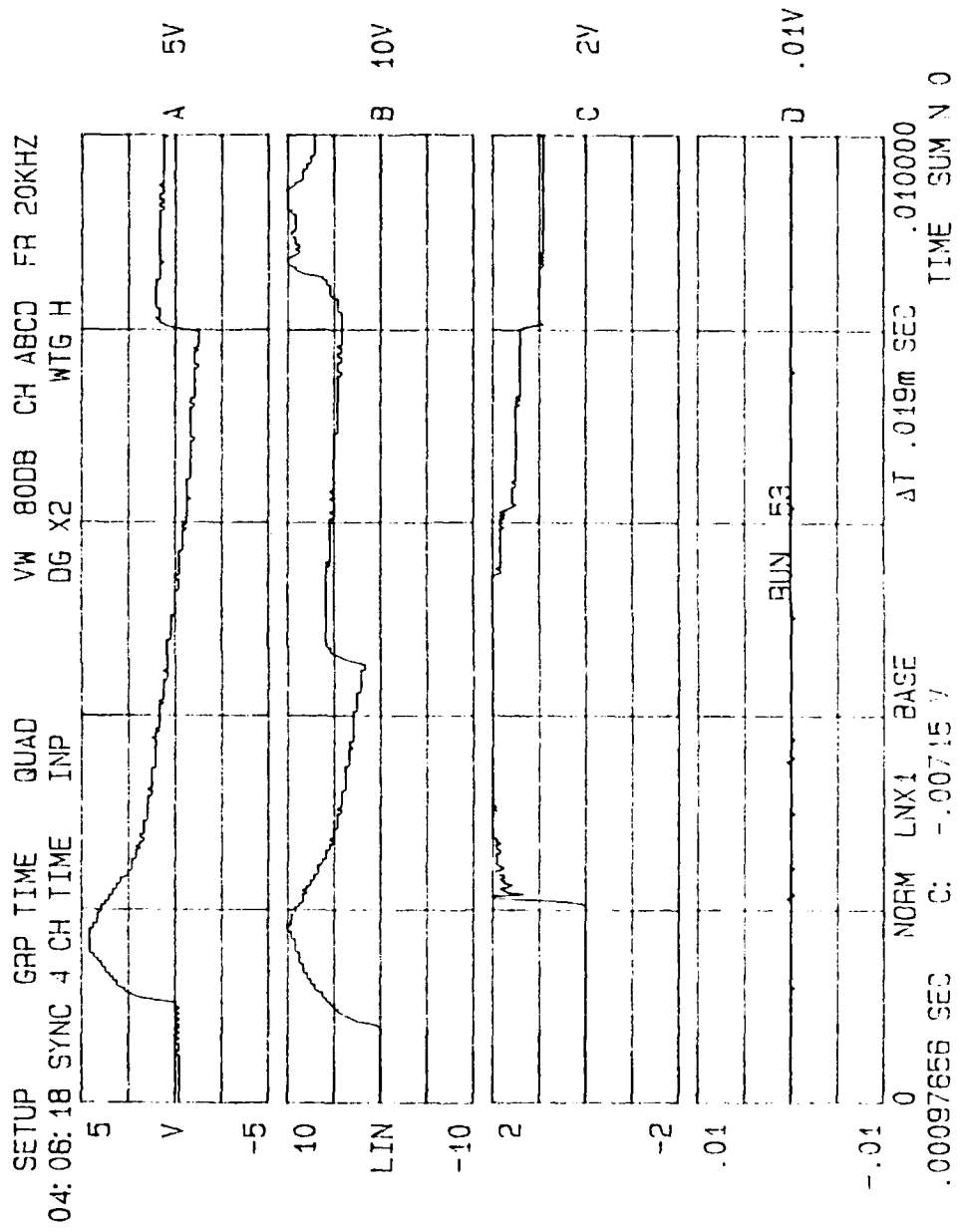


SETUP GRP TIME TRC C VW 800B CH ABCD FR 20KHZ  
 01:37:47 SYNC TIME C INP DG X2 WTG H C 2V

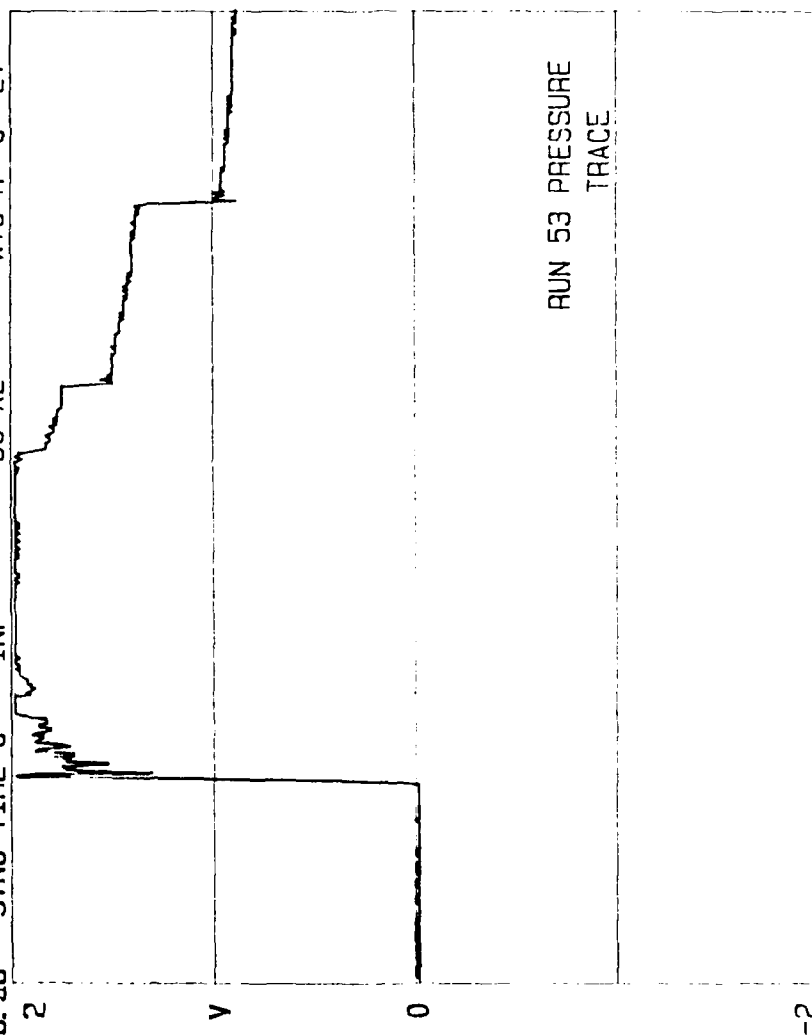


RUN 32 PRESSURE  
 TRACE

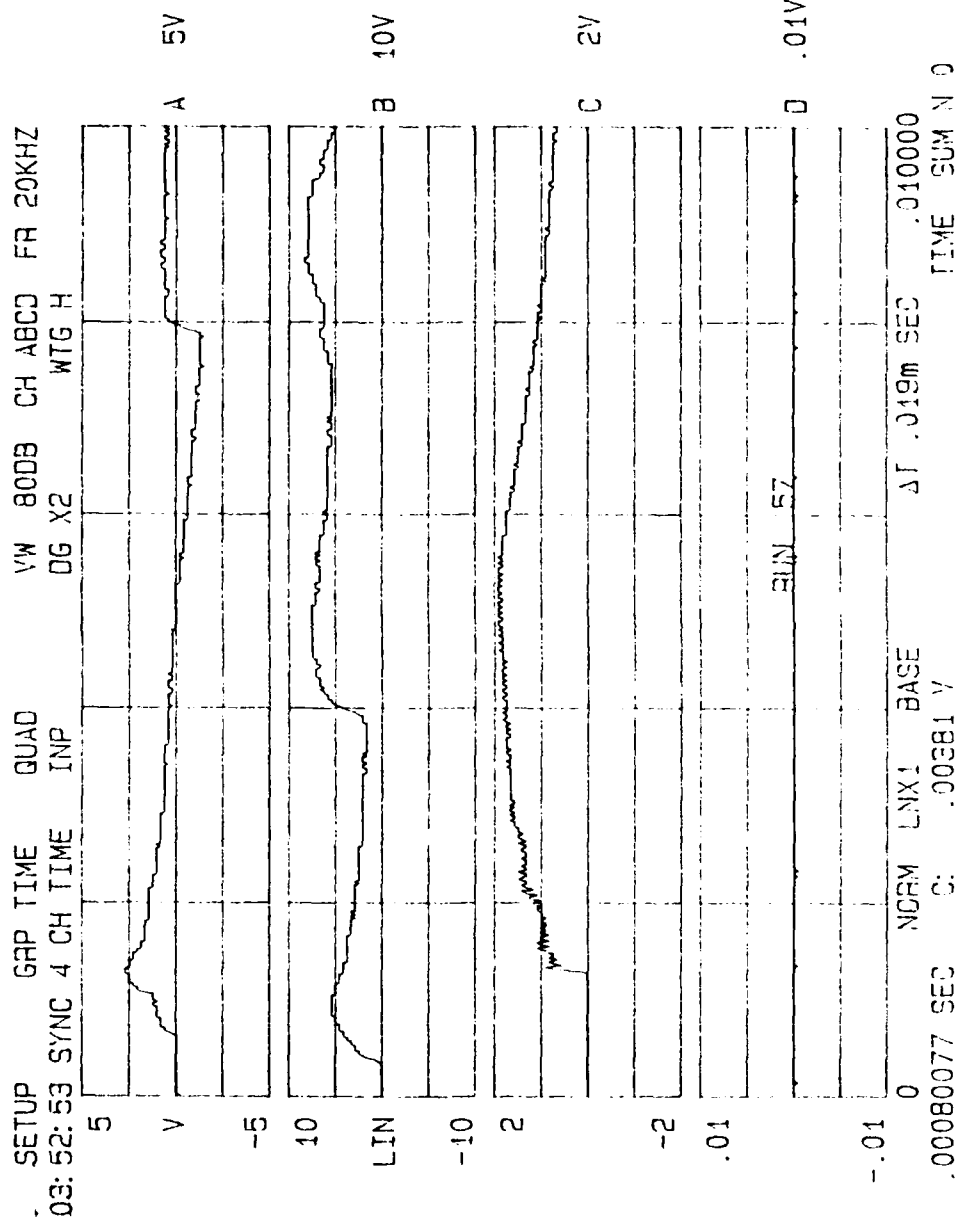
-2  
 0  
 .0014062 SEC C: NORM LNX1 BASE  
 .0109m SEC .010000  
 TIME SUM N 0

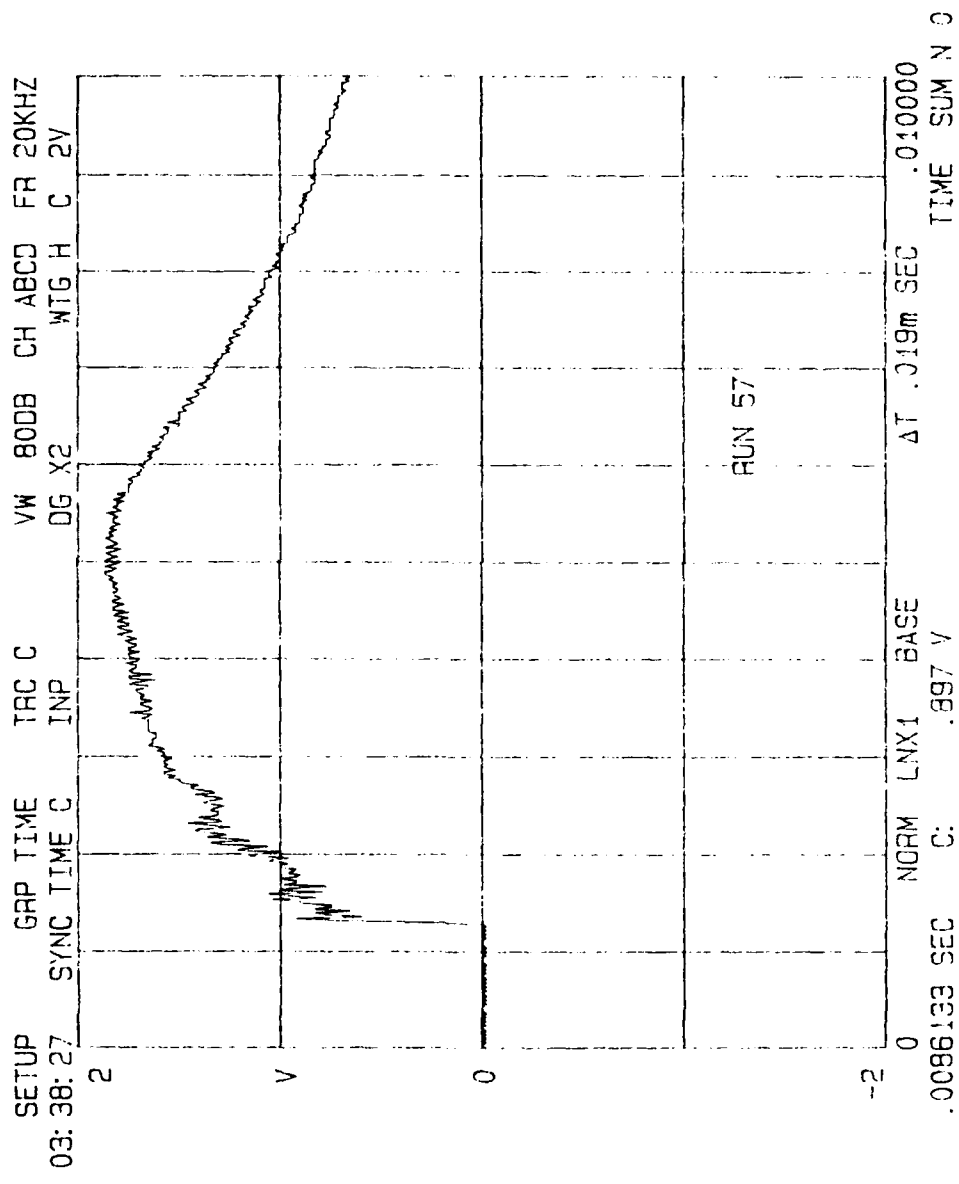


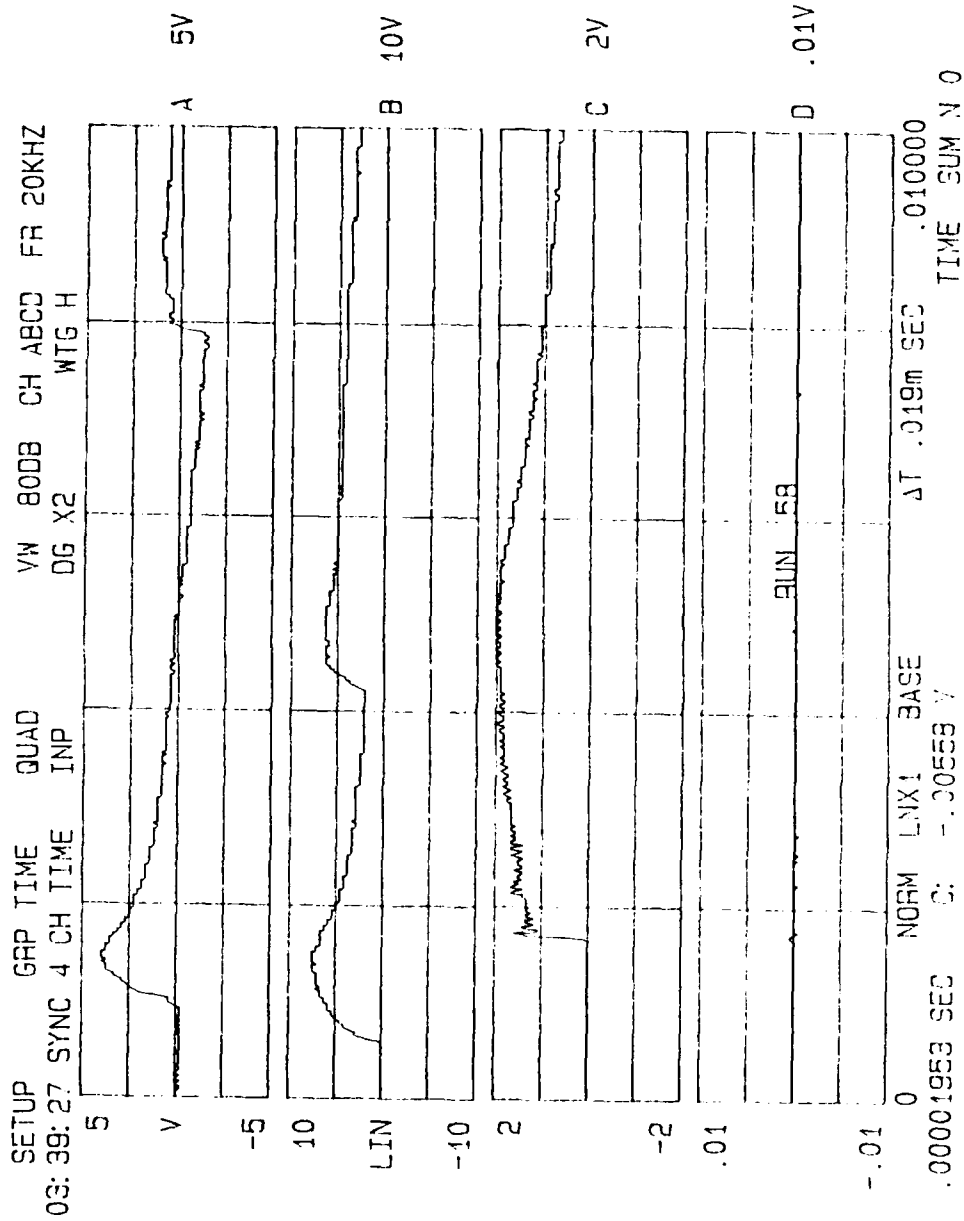
SETUP 01:28:38 GRP TIME TRC C VW 80DB CH ABCD FR 20KHZ  
 SYNC TIME C INP DG X2 WTG H C 2V

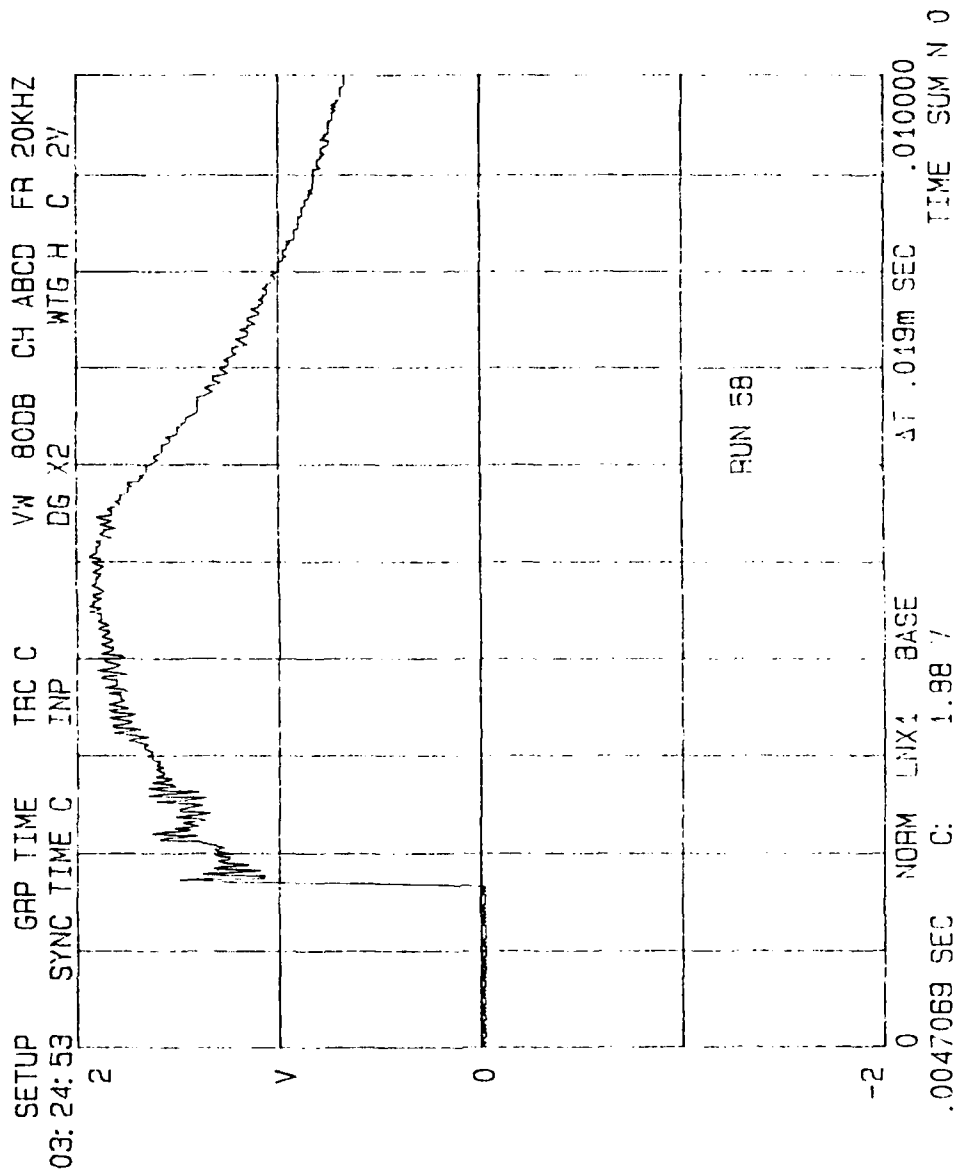


0 NORM LNX1 BASE ΔT .019m SEC .010000  
 SEC C: 1.98 V TIME SUM N 0

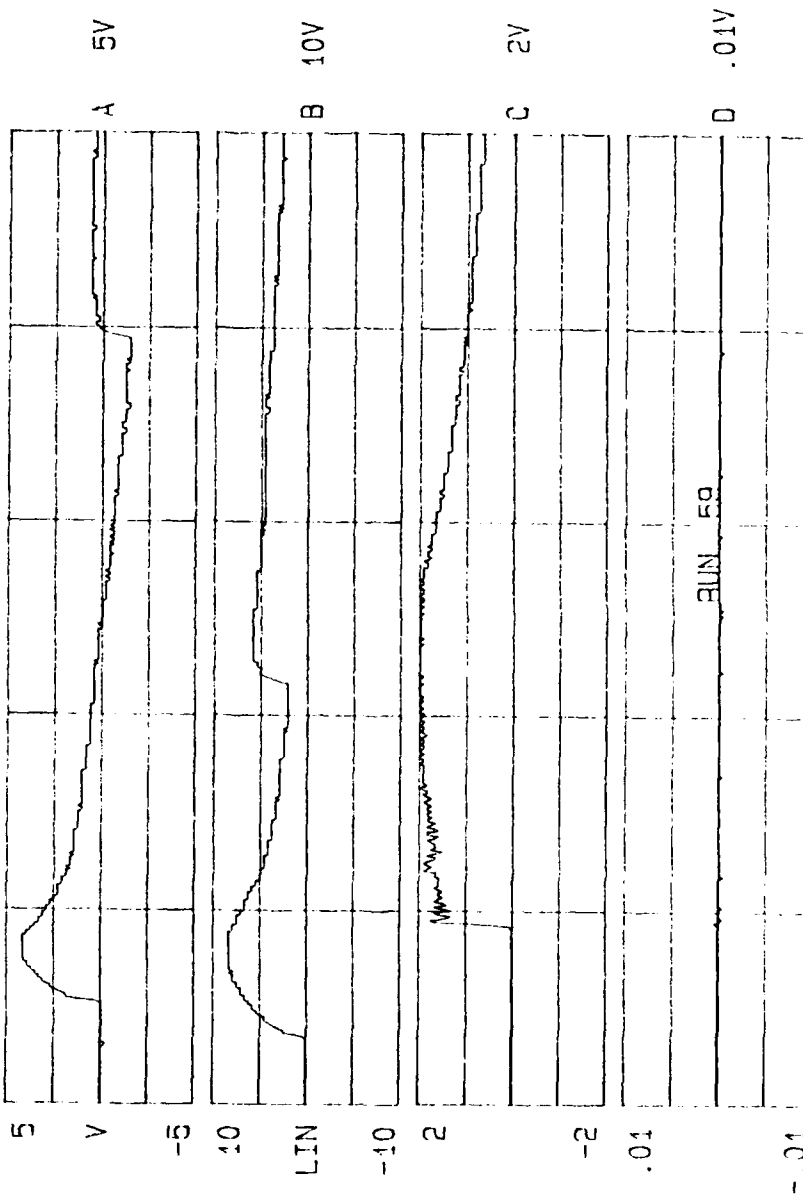




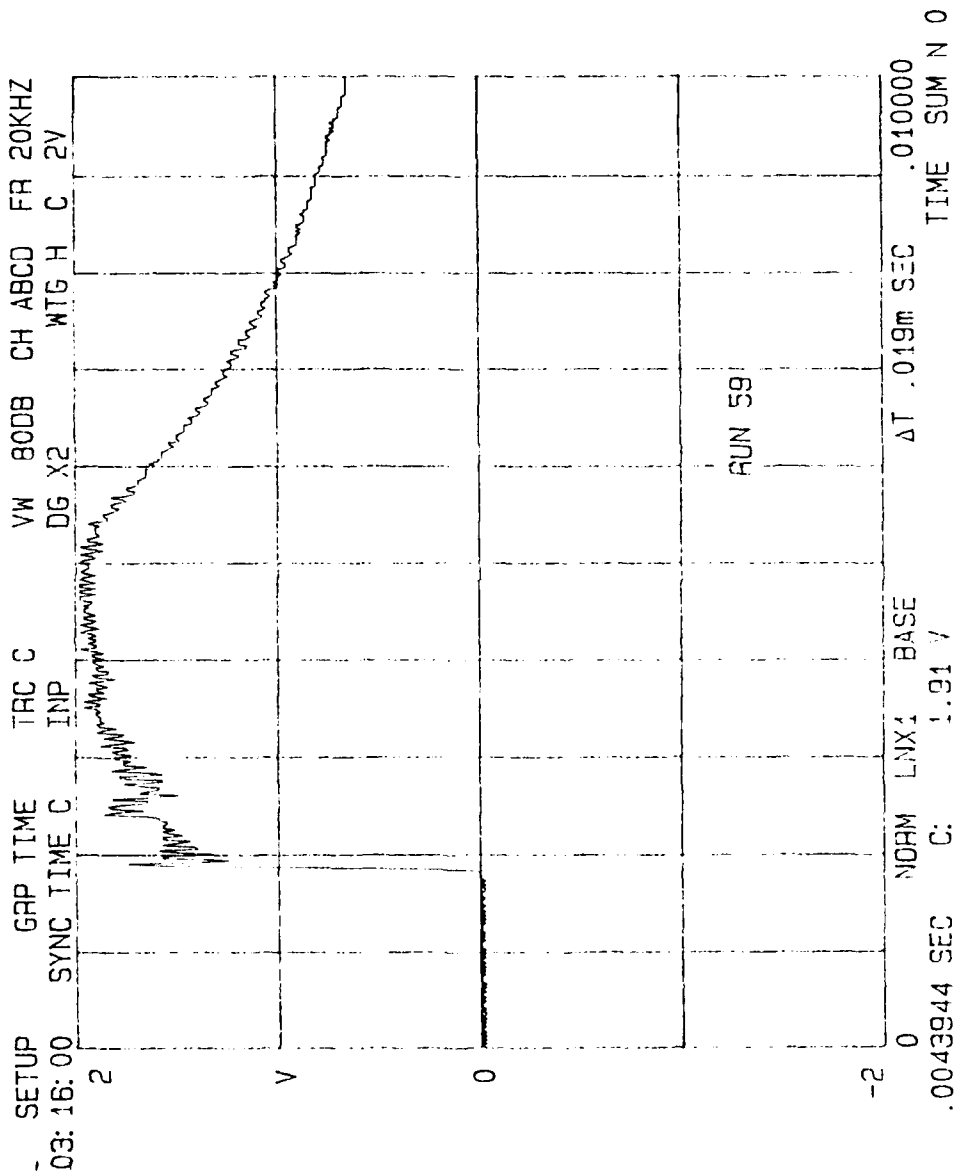


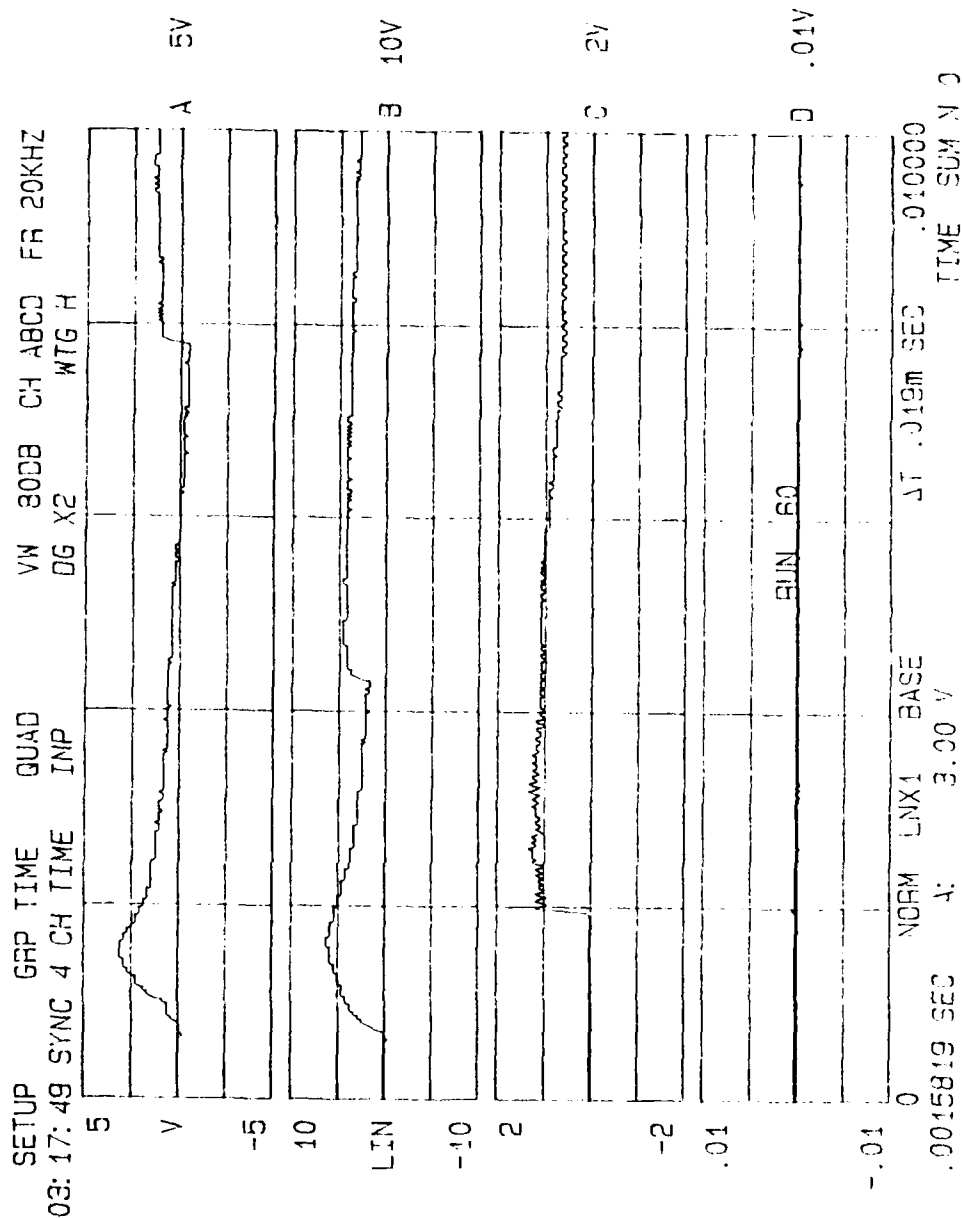


SETUP GRP TIME QUAD VV 80DB CH ABCD FR 20KHZ  
 03:26:53 SYNC 4 CH TIME INP DG X2 WTG H

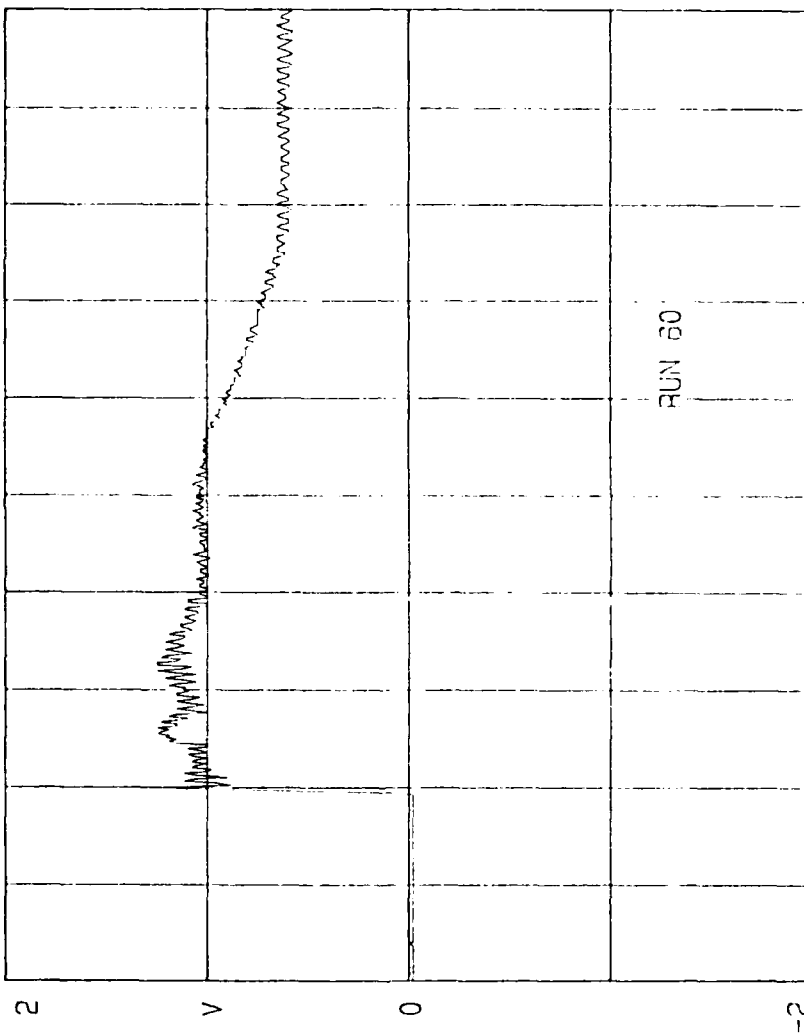


0 NORM LNX1 BASE  
 .00001953 SEC B: .0112 V  
 .010000  
 TIME SUM N 0

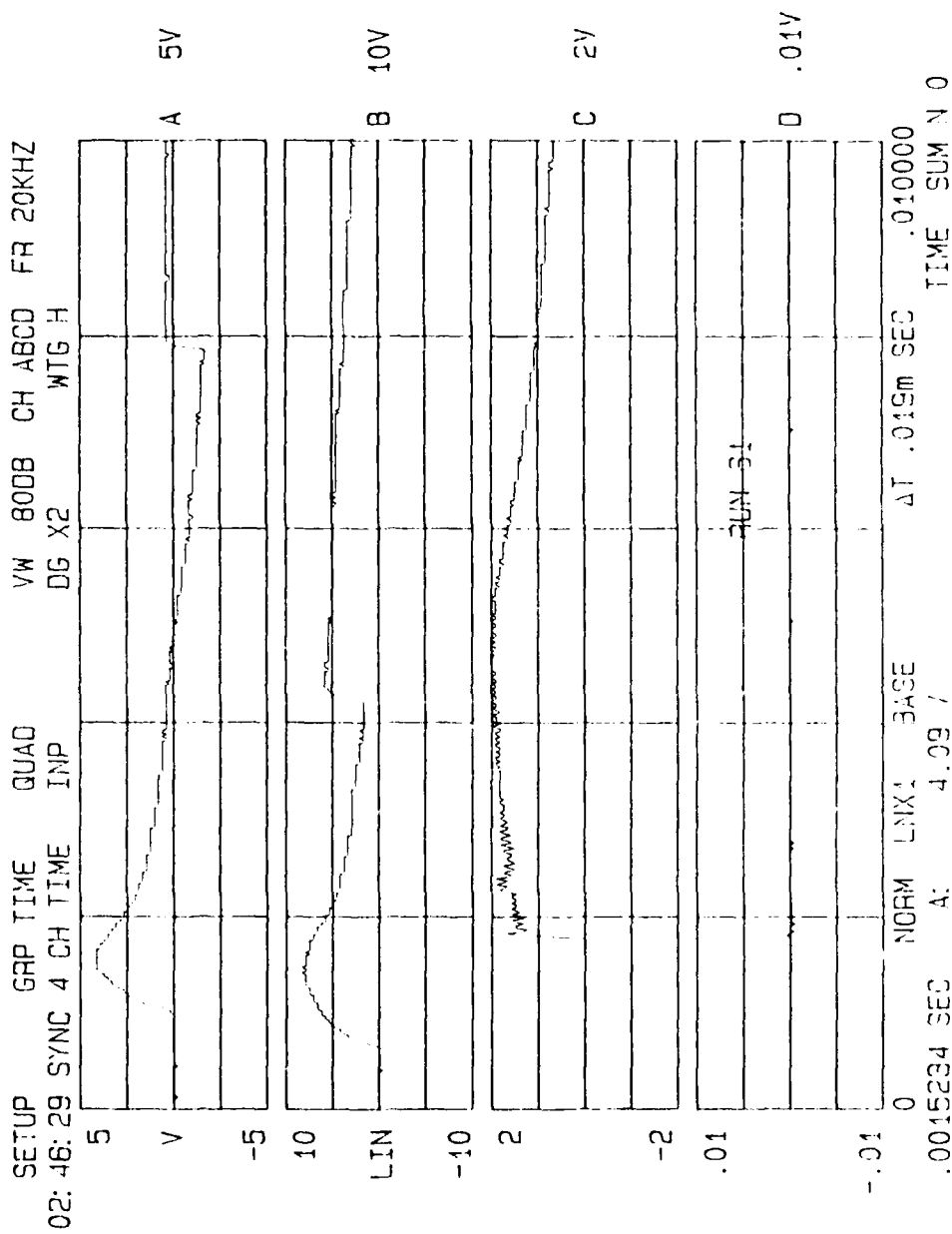


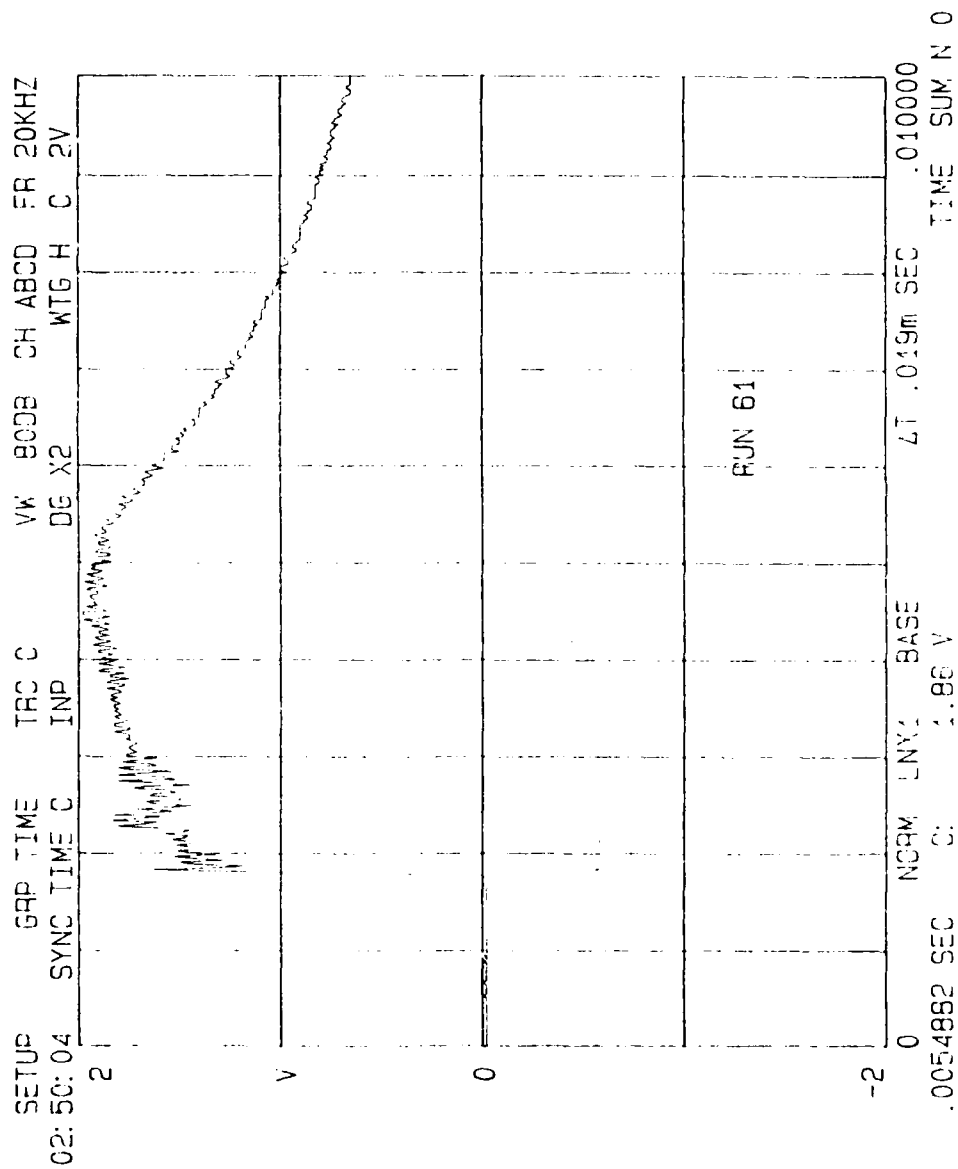


SETUP 03:06:06 GRP TIME TRC C VW 80DB CH ABCD FR 20KHZ  
 SYNC TIME C INP DG X2 WTG H C 2V

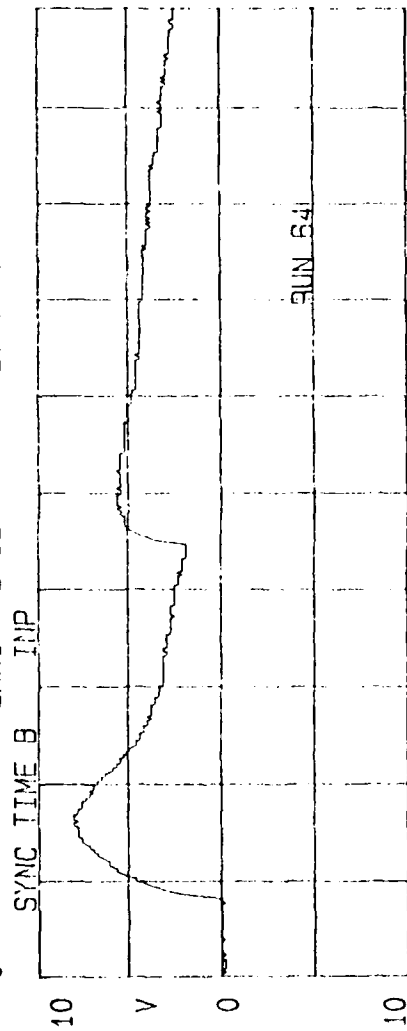
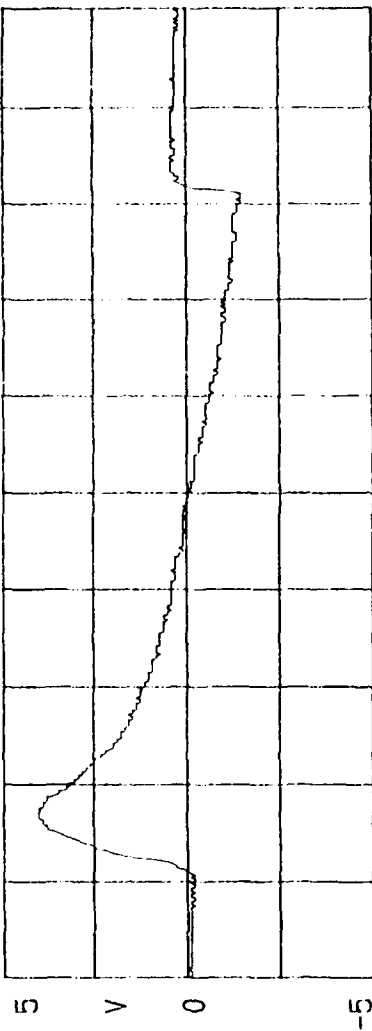


0 NORM LNX1 BASE ΔT .019m SEC .01000  
 .0028515 SEC C: 1.11 V TIME SUM N 0

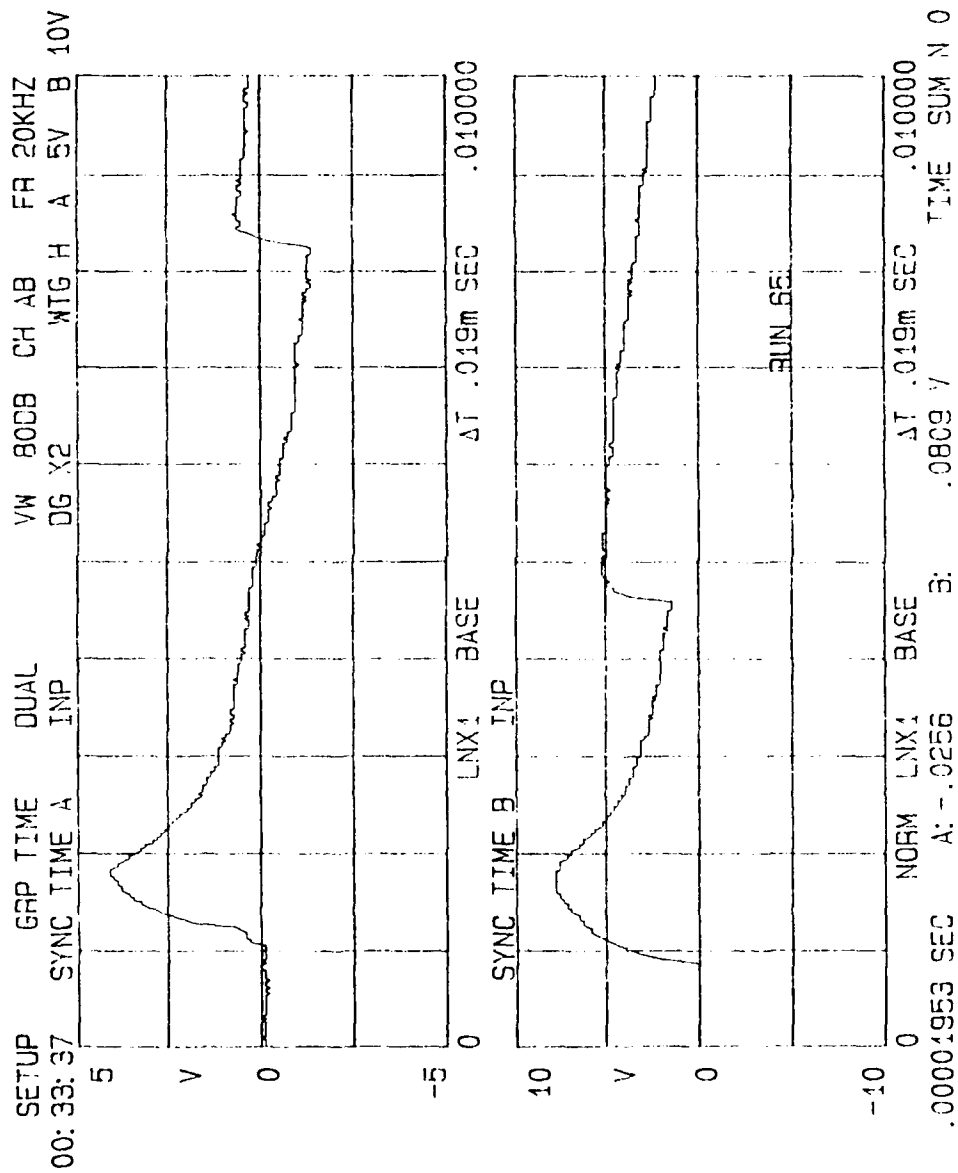




SETUP 00:25:39 GRP TIME SYNC TIME A DUAL LN1 BASE VW 80DB CH AB FR 20KHZ  
 00:25:39 SYNC TIME A INP WTG H A 5V B 10V



.00001953 SEC A: -.00147 B: .0451 V TIME SUM N 0



## APPENDIX E

### COMPUTER PROGRAM FOR SHOCK TUNNEL EVALUATION

The attached program was used for the evaluation of the NPS shock tube and shock tunnel. Sources of shock tube relationships are noted in the program were applicable. Output was tabulated by the program and graphical analysis was provided by the plotting routine 'EASYPLOT' installed on the NPS IBM computer.

```

CC      THIS PROGRAM CALCULATES THE IDEAL PERFORMANCE OF A SHOCK
CC      TUBE USING THE ANALYSIS PRESENTED IN THE 'FUNDAMENTALS
CC      OF GAS DYNAMICS' BY J. A. OMCZAREK PG 395-398 (FIG 8-22)
C       & 'THE SHOCK TUBE IN HIGH TEMPERATURE CHEMICAL PHYSICS' BY GRA
C       GRAYDON HURLE 1963.

```

```

C      IMPLICIT REAL * 4 (A-H,M,P-Z)
      REAL FCN,X1,X2,XTOL,FTOL,FCN1,FCN2,FCN3,FCN4
      INTEGER I,NLIM,J,I1,I2
      EXTERNAL FCN,FCN1,FCN2,FCN3,FCN4
      DIMENSION M1(200),M2(200),M3(200),P4P1(200),P2P1(200)
      DIMENSION P3P4(200),MS(200),US(200),T2(200),P5P2(200),P5P4(200)
      DIMENSION C3(200),C4(200),P4P3(200),T3(200),TC(200),XC(200)
      DIMENSION VC(200),P5P1(200),T5T1(200),UR(200),DELTIM(200)
      DIMENSION DIST(200),TCC(200),XC1(200),DELTA(200),PDI(8)
      DIMENSION XMS(200),XP2P1(200),XP5P2(200),XP3P4(200),XR02R1(200)
      DIMENSION XT2T1(200),URUS(200),TSTART(200),VDV0(8),VD(8),AA(8)
      DIMENSION P5(200),T5(200),DTHR(200),DI(200),MT(200),DTEST(200)
      DIMENSION PT(200),TT(200),T(200,4),TMASS(200),DTDTHR(5),P1(200)
      DIMENSION FT(4,10),PTPTO(10)
      COMMON /B/ R1,MM,C8,DTHR,T
      COMMON /A/ CONST,GAMMA1,GAMMA4,A4A1SQ,C1,C1SQ,CC3,CC4,C5,A4A1,C9
      COMMON /C/ ATASTR,MT,DTEST
      COMMON /E/ DTHR,T,MT,DTHRDT,MM,C8,R1
      COMMON /D/ P5,T5,T1,AA,PDI,J,I1,I2
      COMMON /F/ PTPTO,FT
      DATA X1,X2,XTOL,FTOL,I,NLIM/0.1,6.0,0.0001,0.00001,0.50/

```

```

C
C=====

```

\_\_\_\_\_

GAS	MW	GAMMA	SPEED OF SOUND
AIR	28.97	1.4	345 M/S
ARGON	39.94	1.67	321
HE	4	1.67	1062
N2	28.02	1.4	350
CO2	44.01	1.29	269

C  
C DRIVEN GAS CONSTANTS

R1=8314/28.02

T1=288

GAMMA1=1.4

C      P1=1.0E04

C  
C DRIVER GAS CONSTANTS

R4=8314/28.02

$$T_4 = 288$$

GAMMA4=1.40

P4=600\*6.8948E03

C            A   I S

A=100

C                      MM IS

MM=6

```

C =====
P4P1(1)=20

```

```
C
C      INPUT TUNNEL PARAMETERS(DRIVER LENGTH L1 & L4)
```

L1=6.453

$$L_4 = 2.375$$
$$DT1 = 3 \times .0254$$

C TO EVALUATE TEST CONDITIONS SET FL2=1

THR1 = .0065

FL1=0

```

C      FL2 CALCULATES TEST SECTION MACH #

```

FL2=1

C FL3 IS FOR NOZZLE SIZING CALCULATIONS

FL3=0

C CALCULATES TEST SECTION CONDITIONS

CALCO  
E14E1

11

FILE: SHOCK2 FORTRAN A1

```

C      FL6 EXPERIMENT OUTPUT RUNS
      FL6=0
C      FL7=1 PRINTS MISC RELATIONSHIPS
      FL7=0
C      FL8=1 EVALUATES PT/PTO RATIOS FOR GIVEN THROAT
      FL8=1
C      EVALUATE SPEED OF SOUND CONSTANTS
      A1=SQRT(GAMMA1*R1*T1)
      A4=SQRT(GAMMA4*R4*T4)
      A4A1=A4/A1
      A4A1SQ=A4A1**2
C
C=====
C      EVALUATE CONSTANTS USED COMMONLY USED
      C1=(GAMMA1+1)/(2*GAMMA1)
      C1SQ=C1**2
      C5=(-2*GAMMA4)/(GAMMA4-1)
      C6=(GAMMA4-1)/(2*GAMMA4)
      C7=(GAMMA4+1)/(4*GAMMA4)
      C8=(GAMMA1-1)/(2*GAMMA1)*(1)
      C9=(GAMMA1+1)/(2*(GAMMA1-1))
      C10=(GAMMA1/(GAMMA1-1))
C=====
C      THIS LOOP INCREMENTS PRESSURE P4/P1 BY A AND THEN
C      USES INTERVAL HALVING TO DETERMINE M3.
C
      DO 1 J=1,MM,1
        CONST=P4P1(J)
        CALL INTHV(FCH,X1,X2,XR,XTOL,FTOL,NLIM,I)
        M3(J)=XR
        C3(J)=CC3
        C4(J)=CC4
        X1=XR
        X2=6.0
        I=0
C      THE ROOT HAS BEEN FOUND AT XR IF I EQUALS 1 OR 2
        K=J+1
        P4P1(K)=P4P1(J)+A
1      CONTINUE
C
C      THIS LOOP USES P4/P1 & M3 TO DETERMINE P2,P1,MS,M2,US,P3P4
C
      DO 5 I=1,MM,1
        FIND P2/P1 (EQN 8-57)
C
        P2P1(I)=P4P1(I)/C4(I)
        M2(I)=SQRT(2*(P2P1(I)+(1/P2P1(I))-2)/(GAMMA1*(GAMMA1-1)*
&((GAMMA1+1)/(GAMMA1-1)+P2P1(I))))
C      FIND MS & SPEED OF SHOCK (EQN 8-51)
        MS(I)=SQRT((P2P1(I)-1)*C1+1)
        US(I)=MS(I)*A1
C      FIND P3/P4
        P3P4(I)=C3(I)**C5
        P4P3(I)=1/P3P4(I)
C      EVALUATE MAXIMUM DURATION OF UNIFORM FLOW IN THE REGION
C      BETWEEN THE SHOCK WAVE AND THE CONTACT SURFACE.
C      REFERENCE PAGE 433 PROBLEM
C
        T2(I)=(2/(P3P4(I)**C7))-((4*A4*(1-P3P4(I)**C6)*(1/P3P4(I))**C7)/
&((GAMMA4-1)*A1*SQRT(1+(GAMMA1+1)*(P2P1(I)-1)/
&(2*GAMMA1))))*L4/A4
C
C      T3 IS THE THEORITICAL MAXIMUM DURATION OF UNIFORM FLOW
C      IN THE REGION BETWEEN THE CONTACT SURFACE AND THE TAIL OF
C      CENTERED EXPANSION WAVE (REGION 3). (PG 433 PBLM 8-6)
C
        T3(I)=(L4/A4)*((GAMMA4-1)/2)*((P4P3(I)**(3-GAMMA4))
&**((1/(GAMMA4*4)))/(1-(P3P4(I)**C6)))
C
C      TC & XC ARE THE TIME AND DISTANCE AT WHICH THE WAVE FORMED BY

```

FILE: SHOCK2 FORTRAN A1

```

C      THE REFLECTION OF THE CENTERED EXPANSION WAVE OVERTAKES THE
C      CONTACT SURFACE. (REF PG433 PBLM 8-7)
C
C      TC(I)=(L4/A4)*2*(P4P3(I)**C7)
C      XC(I)=(L4*4/(GAMMA4-1))*(1-(P3P4(I)**C6)/(P4P3(I)**C7)))
C
C=====
C
C      CALCULATION OF REFLECTED REGION PARAMETERS ACCORDING TO REF 2
C
C      VELOCITY OF CONTACT SURFACE VC
C      VC(I)=2*A1/(GAMMA1+1)*(MS(I)-1/MS(I))
C      PRESSURE AND TEMPERATURE IN REFLECTED REGION 5 (EQN 2.31)
C      P5P1(I)=((2*(GAMMA1+1)*MS(I)**2-(GAMMA1-1))/(GAMMA1+1))
C      &*(((3*(GAMMA1-1)*MS(I)**2-2*(GAMMA1-1))/(GAMMA1-1)*MS(I)**2+2))
C      T5T1(I)=((2*(GAMMA1-1)*MS(I)**2+(3-GAMMA1))
C      &*(((3*(GAMMA1-1)*MS(I)**2-2*(GAMMA1-1))/(GAMMA1+1)*MS(I)**2))
C      CALCULATE VELOCITY OF REFLECTED SHOCK UR (EQN 2.38)
C      UR(I)=US(I)*((2+(2/(GAMMA1-1))*(1/P2P1(I)))/
C      &((GAMMA1+1)/(GAMMA1-1)-1/P2P1(I)))
C      OBSERVATION TIME AND DISTANCE IN REFLECTED SHOCK
C      DELTIM(I)=L1*(US(I)-VC(I))/(US(I)*(UR(I)+VC(I)))
C      DIST(I)=DELTIM(I)*UR(I)
C      TIME TO EXPANSION WAVE REACH CONTACT SURFACE (EQN 4.7)
C      C=((GAMMA4+1)/(2*(GAMMA4-1)))
C      TCC(I)=2*L4*(1+(GAMMA4-1)*M3(I)/2)**C/A4
C      XC1(I)=TCC(I)*((2*A1*(MS(I)**2-1))/(GAMMA1+1)*MS(I))
C      TEST TIME BETWEEN CONTACT SURFACE AND SHOCK
C      DELTA(I)=TCC(I)*(1-2*(MS(I)**2-1)/((GAMMA1+1)*MS(I)**2))
C      P5P2(I)=P5P1(I)/P2P1(I)
C
C      5      CONTINUE
C
C=====
C=====
C      SECOND METHOD OF CALCULATIONS
C      X1=.1
C      X2=6.0
C      XTOL=0.0001
C      FTOL=0.00001
C      I=0
C      HLIM=50
C      XR=.5
C      DO 2 J=1,MM,1
C      CONST=P4P1(J)
C      CALL INTHV(FCN1,X1,X2,XR,XTOL,FTOL,HLIM,I)
C      XMS(J)=XR
C      XP2P1(J)=(2*(GAMMA1+1)*XMS(J)**2-(GAMMA1-1))/(GAMMA1+1)
C      XP3P4(J)=1/(P4P1(J)/XP2P1(J))
C      XR02R1(J)=((GAMMA1+1)*XMS(J)**2)/((GAMMA1-1)*XMS(J)**2+2)
C      XT2T1(J)=((GAMMA1+1)*XMS(J)**2-(GAMMA1-1)/2)/((GAMMA1-1)/2*XMS(J)**
C      &2+1)/(((GAMMA1+1)/2)**2*XMS(J)**2)
C      XP2P1(J)=(2*(GAMMA1+1)*XMS(J)**2-(GAMMA1-1))/(GAMMA1+1)
C      XP5P2(J)=(((GAMMA1+1)/(GAMMA1-1))+2-1/XP2P1(J))/
C      &(1+(GAMMA1+1)/(GAMMA1-1)*1/XP2P1(J))
C      XP3P4(J)=1/(P4P1(J)/XP2P1(J))
C      XR02R1(J)=((GAMMA1+1)*XMS(J)**2)/((GAMMA1-1)*XMS(J)**2+2)
C      XT2T1(J)=((GAMMA1+1)*XMS(J)**2-(GAMMA1-1)/2)/((GAMMA1-1)/2*XMS(J)**
C      &2+1)/(((GAMMA1+1)/2)**2*XMS(J)**2)
C      X1=XR
C      X2=6.0
C      I=0
C      M3 HAS BEEN DETERMINED BY INTERVAL HALVING
C      DATA X1,X2,XTOL,FTOL,I,HLIM/XR,5.0,0.0001,0.00001,0,50/
C      URUS(J)=UR(J)/US(J)
C      P5P4(J)=P5P1(J)/P4P1(J)
C      P5(J)=P5P1(J)*P1
C      P5(J)=P5P4(J)*P4
C      P1(J)=P4/P4P1(J)
C      T5(J)=T5T1(J)*T1
C      WRITE(*,*) P5P1(J),P4P1(J),P1(J),UR(J),DELTIM(J)
C      2      CONTINUE

```

```

C=====
C      IF (FL3.EQ.0)GO TO 36
C      THIS SECTION DETERMINES P5 T5 AND DETERMINES TESTIME AS A
C      FUNCTION OF NOZZLE THROAT DIAMETER.
C      NN=1
C      DO 3 I=1,MM
C      REFLECTED MO AVAILABLE TO DRIVE NOZZLE
C      C=SQRT(GAMMA1/R1)*(1-(GAMMA1-1)/2)**(-1*C9)
C      TMASS(I)=P5(I)*(UR(I)*DELTIM(I))*3.1417*DT1**2/(R1*T5(I)*4)
C      WRITE(*,*) P5P1(I),P5(I),T5(I),NN,TMASS(I)
C      CALL NOZZLE(P5(I),T5(I),NN,TMASS(I),C,FL3)
C601  FORMAT('P4P1=',D9.3,2X,'P1=',D9.3,2X,'TOTAL MASS MO=',D9.4,2X,
C      &'RUN =',I5/)
C      NN=NN+1
C      3  CONTINUE
C      DO 309 I=1,100
C      WRITE(8,602) DTHR(I),T(I,1),T(I,2),T(I,3),T(I,4)
C602  FORMAT(5(E9.3,2X))
C201  FORMAT('P5=',E9.2,2X,'T5=',E9.2,2X,'NN=',I1
C      &,2X,'TOTAL MASS MO=',E9.2)
C      309 CONTINUE
C      WRITE(8,603)
C603  FORMAT(/,'THROAT DIAM',2X,'RUN1',6X,'RUN2',7X,'RUN3',7X,'RUN4',/)
C      WRITE(8,601) (P4P1(I),P1(I),TMASS(I),I,I=1,4)
C=====
C      36  IF (FL8.EQ.0)GO TO 37
C      THIS SECTION DETERMINES P5 T5 AND DETERMINES TESTIME AS A
C      FUNCTION OF PT/PTO FOR A GIVEN THROAT DIAMETER
C      NN=1
C      DO 82 I=1,MM
C      REFLECTED MO AVAILABLE TO DRIVE NOZZLE
C      C=SQRT(GAMMA1/R1)*(1-(GAMMA1-1)/2)**(-1*C9)
C      TMASS(I)=P5(I)*(UR(I)*DELTIM(I))*3.1417*DT1**2/(R1*T5(I)*4)
C      CALL NOZZLE2(P5(I),T5(I),NN,TMASS(I),C,FL3)
C      NN=NN+1
C      82  CONTINUE
C      DO 89 I=1,MM
C      WRITE(8,802) PTPTO(I),FT(I,1),FT(I,2),FT(I,3),FT(I,4)
C802  FORMAT(5(E9.3,2X))
C      89  CONTINUE
C      WRITE(8,803) (P4P1(I),I=1,MM)
C803  FORMAT(/,4('P4P1=',E9.3,2X))
C=====
C      37  IF (FL2.EQ.0)GO TO 133
C      DETERMINE TEST SECTION MACH # AS FUNCTION OF THROAT
C      CALL EXPAN(THR1,DT1)
C      SUBROUTINE EXPAN(THR1,DT1)
C      REAL X1,X2,XTOL,FTOL,DT1,THR1
C      INTEGER I,NLIM,J
C      DIMENSION MT(200),DTEST(200),DTDTHR(5)
C      COMMON /A/ CONST,GAMMA1,GAMMA4,A4A1SQ,C1,C1SQ,CC3,CC4,C5,A4A1
C      COMMON /C/ ATASTR,MT,DTEST,C9,DTDTHR
C      WRITE(8,300)
C      DTEST(1)=DT1
C      X1=.10
C      XR=50
C      DO 30 J=1,8
C      X2=100
C      XTOL=0.0001
C      FTOL=0.00001
C      I=0
C      NLIM=50
C      ATASTR=(DTEST(J)/THR1)**2
C      WRITE(*,*) THR1,DTEST(J),ATASTR,C9
C      CALL INTHV(FCH3,X1,X2,XR,XTOL,FTOL,NLIM,I)
C      MT(J)=XR
C      X1=XR
C      X2=100
C      K=J+1

```

FILE: SHOCK2 FORTRAN A1

```

      DTEST(K)=(DTEST(J)+DT1*.5)
      DTDTHR(J)=DTEST(J)/DT1
      PRINT *, 'HELP'
      WRITE(8,301) MT(J), DTDTHR(J), DTEST(J), ATASTR, THR1, DT1
300  FORMAT(/, 4X, 'MTEST', 1X, 'DTEST/DTUBE', 1X, 'DTEST', 2X, 'ATASTR'
      &, 4X, 'DTHROAT', 3X, 'DTUBE')
301  FORMAT(4(F9.3), 2(2X, E9.3))
30  CONTINUE
C=====
133  IF (FL4.EQ.0) GO TO 105
C    THIS SECTION EVALUATES TEST CONDITIONS FOR VARIOUS
C    TEST CHAMBER AREAS GIVEN A FIXED NOZZLE THROAT DIAMETER
C    OUTER LOOP IS FOR P4P1 CHANGE, INNER LOOP EVALUATE CH AREA
      DO 22 J=1, MM
      WRITE(8,400)
      DO 21 I=1, 8
      WRITE(*,*) C10
      WRITE(*,405) MT(I), P5(J), T5(J), PT(I), TT(I), C10
C406  FORMAT(2X, 'MACH', 6X, 'P5 =', 6X, 'PT', 5X, 'T5', 8X, 'TT', 5X, 'TSTART')
C405  FORMAT(6(D9.2))
      CALL TCOND(MT(I), P5(J), T5(J), PT(I), TT(I), TSTART(I), THR1, C10)
      WRITE(8,401) MT(I), P5(J), PT(I), T5(J), TT(I), MS(J), P4P1(J), P1(J)
      &, TSTART(I)
400  FORMAT(/, 'TEST MACH', 5X, 'P5', 4X, 'TEST P', 4X, 'T5', 4X,
      & 'TEST TEMP', 3X, 'MS', 4X, 'P4P1', 6X, 'P1', 7X, 'TSTART')
401  FORMAT(9(E8.3, 1X), E6.1)
21  CONTINUE
C    DUMP CHAMBER SIZING EVALUATION
      WRITE(8,411)
      DO 461 II=1, 1
      DO 460 I1=1, 1
      AA(I1)=.1*I1
C    AA(I1)=.8
      PDI(I1)=.013332
      X1=-10000
      XR=50
      X2=100000
      XTOL=.0001
      FTOL=.000001
      I=0
      NLIM=200
C    WRITE(8,*) AA(I1), PDI(I1)
      CALL INTHV(FCH4, X1, X2, XR, XTOL, FTOL, NLIM, I)
      VDVO(I1)=XR
C    WRITE(8,*) AA(I1), PDI(I1), VDVO(I1)
      X1=XR
      X2=10
      VD(I1)=VDVO(I1)*(UR(J)*DELTIM(J)*3.1417*DT1**2/4)
      WRITE(8,412) P5(J), T5(J), VDVO(I1), VD(I1), AA(I1)
411  FORMAT(/, 3X, 'P5', 8X, 'T5', 8X, 'VDVO', 7X, 'VD', 8X, 'PIPT0',
      &6X)
412  FORMAT(5(E9.2, 1X))
460  CONTINUE
461  CONTINUE
      WRITE(8,402) DELTIM(J), T(1, J)
402  FORMAT(/, 'TEST TIME OF SHOCK TUBE =', D9.4, /
      &, 'TIME FOR .5*P5 OUT OF NOZZLE =', D9.4)
C    &, 'TIME TO START NOZZLE (EMPERICAL ESTIMATE)', D9.4)
22  CONTINUE
C=====
105  K=MM
      IF (FL6.EQ.0) GO TO 699
      WRITE(8,695)
      WRITE(8,696) (P4P1(J), MS(J), US(J), VC(J), URUS(J), T5(J)
      &, P5(J), J=1, K)
695  FORMAT(2X, 'XP4P1', 7X, 'MS', 9X, 'VS', 9X, 'VC', 9X, 'URUS',
      &5X, 'P5', 8X, 'T5')
696  FORMAT(6(F9.3, 2X), E9.3)
C=====
699  IF (FL1.EQ.0) GO TO 108
      WRITE(8,201)

```

FILE: SHOCK2 FORTRAN A1

```

      WRITE(8,200) (P4P1(J),MS(J),XP2P1(J),XP5P2(J),XP3P4(J)
&.XR02P1(J),XT2T1(J),XMS(J),URUS(J),J=1,K)
200   FORMAT(9(F11.3,2X))
201   FORMAT(2X,'XP4P1',7X,'MS',8X,'XP2P1',8X,'XP5P2',6X,'XP3P4'
&,4X,'ROU2/ROU1',4X,'XT2/T1',6X,'XMS',6X,'UR/US')
      WRITE(8,203) (P4P1(J),MS(J),XT2T1(J),T5T1(J),P2P1(J)
&,P5P4(J),DELTIM(J),J=1,K)
203   FORMAT(7(D9.4,2X))
108   WRITE(8,204)
      WRITE(8,205) R1,T1,GAMMA1,R4,T4,GAMMA4
204   FORMAT(3X,'P4P1',8X,'MS',8X,'XT2T1',7X,'T5T1',7X,'P2P1'
&,7X,'P5P4',5X,'DELTIM')
205   FORMAT('R1=',F9.2,2X,'T1=',F9.2,2X,'GAMMA1=',F9.2,
&/, 'R4=',F9.2,2X,'T4=',F9.2,2X,'GAMMA4=',F9.2)
C=====
      IF (FL7.EQ.0) GOTO 109
C      OUTPUT DATA TO A FILE
      WRITE(8,103)
      WRITE(8,100) (P4P1(I),MS(I),M2(I),M3(I),A4A1,
&P5P1(I),T5T1(I),P3P4(I),P2P1(I),P5P2(I),DELTIM(I),I=1,K)
C      WRITE(8,106)
C      WRITE(8,107) (P4P1(I),UR(I),DIST(I),XC1(I),TCC(I),DELTIM(I),
&DELTA(I),T2(I),I=1,K)
C 106   FORMAT(4X,'P4P1',2X,'VEL REFL',4X,'DIS REFL',4X,
&'EXP POS',4X,'EXP TIME',4X,'DEL TIM',5X,'DELTA',8X,'T2')
C      WRITE(8,104)
C 107   FORMAT(8(F9.4,2X))
C      WRITE(8,105) (P4P1(I),T2(I),T3(I),TC(I),XC(I),I=1,K)
100   FORMAT(11(F9.4,1X))
C 102   FORMAT(4X,'P4P1',8X,'T2',8X,'P3P4',6X,'P2P1')
103   FORMAT(4X,'P4P1',6X,'MS',
&9X,'M2',6X,'M3',8X,'A4A1',6X,'P5P1'
&,6X,'T5T1',6X,
&1X,'P3P4',6X,'P2P1',6X,'P5P2',6X,'TESTTIME')
C 104   FORMAT(2X,'P4P1',12X,'T2',8X,'T3',10X,'TC',9X,'XC')
C 105   FORMAT(5(F10.4,2X))
109   X=1
      STOP
      END

C
C
C
C
C      REAL FUNCTION FCN(X)
      REAL X
      COMMON/A/ CONST,GAMMA1,GAMMA4,A4A1SQ,C1,C1SQ,CC3,CC4,C5,A4A1,C9
      CC3=(1+(GAMMA4-1)*X/2)
      CC4=(CC3**((2*(GAMMA4))**((1/(GAMMA4-1))
      FCN=(1+(.5*A4A1SQ)*((GAMMA1*X/CC3)**2)
&*(C1+SQRT((C1SQ+4/(A4A1SQ*(GAMMA1*X/CC3)**2))))))
&CC4-CONST
C      WRITE(8,200) FCN,GAMMA1,GAMMA4,A4A1SQ,CC3,CC4,CONST
C 200   FORMAT(7(F8.2))
      RETURN
      END

C
C      REAL FUNCTION FCH1(Y)
      REAL Y
      COMMON/A/ CONST,GAMMA1,GAMMA4,A4A1SQ,C1,C1SQ,CC3,CC4,C5,A4A1,C9
      FCH1=((2*(GAMMA1*Y**2-GAMMA1+1)/(GAMMA1+1))*((1-((GAMMA4-1)/(A4A1
&(GAMMA1+1))*(Y-1/Y))))**C5-CONST
C      PRINT*,FCH1,CONST,A4A1,C5
      RETURN
      END

C
C
C      REAL FUNCTION FCN3(Z)
      REAL Z
      COMMON /C/ ATASTR,MT,DTEST
      COMMON /A/ CONST,GAMMA1,GAMMA4,A4A1SQ,C1,C1SQ,CC3,CC4,C5,A4A1,C9

```

FILE: SHOCK2    FORTRAN    A1

```

C      WRITE(*,*) ATASTR,GAMMA1,Z,C9
      FCN3=ATASTR-1/Z*(2*(1+(GAMMA1-1)/2*Z**2)
      &/((GAMMA1+1)))**C9
C      WRITE(*,*) ATASTR,GAMMA1,Z,FCN3
      RETURN
      END

C      REAL FUNCTION FCN4(W)
      REAL W
C      INTEGER J,I2,I1
      DIMENSION P5(200),T5(200),AA(8),PDI(8),MT(200)
      COMMON/C/ ATASTR,MT,DTEST
      COMMON/D/ P5,T5,T1,AA,PDI,J,I1,I2
      FCN4=W-(1+PDI(I1)*T5(J)*W/(P5(J)*T1)-AA(I1)**.714)*T1*
      &(1+.2*100)**3.5/(AA(I1)*T5(J))
C      WRITE(8,131) AA(I1),PDI(I1),P5(J),W,T5(J),J,I1
C 131  FORMAT('A=',E9.2,'PDI=',E9.2,'P5=',E9.2,
C      &'W=',E9.2,1X,E9.2,1X,F4.1,1X,F4.1)
      RETURN
      END

C
C      SUBROUTINE NOZZLE(X,Y,NN,MTOTAL,CONST2,FL3)
C      THIS ROUTINE DETERMINES TIME FOR NOZZLE FLOW FOR A GIVEN THROAT
C      DIAMETER.
      REAL *8 X,Y,MTOTAL,CONST2,PI
      INTEGER NN,FL3
      DIMENSION DTHR(200),T(200,4)
      COMMON /A/ CONST,GAMMA1,GAMMA4,A4A1SQ,C1,C1SQ,CC3,CC4,C5,A4A1,C9
C      COMMON /B/ P5,T5,R1,MM,C8,DTHR,DTHRDT,T
      COMMON /B/ R1,MM,C8,DTHR,T
      PI=3.1416
      DTHR(1)=.0065
      DO 30 I=1,100,1
      T(I,NN)=MTOTAL*DSQRT(Y)*2*(1/.5**C8-1)/(CONST2*PI*DTHR(I)**2/4*X
      &*(GAMMA1-1))
      J=I+1
      DTHR(J)=DTHR(I)+.0005
C      WRITE(8,200) DTHR(I),T(I,NN)
C200  FORMAT(2(E9.3,2X))
C201  FORMAT('P5=',E9.2,2X,'T5=',E9.2,2X,'NN=',I1
C      &,2X,'TOTAL MASS MO=',E9.2)
C 30  CONTINUE
C      WRITE(8,201) X,Y,NN,MTOTAL
      RETURN
      END

C
C      SUBROUTINE NOZZLE2(X,Y,NN,MTOTAL,CONST2,FL3)
C      THIS ROUTINE DETERMINES TIME FOR NOZZLE FLOW FOR A GIVEN THROAT
C      DIAMETER WITH VARIATION OF PT/PT0
      REAL *8 X,Y,MTOTAL,CONST2,PI
      INTEGER NN,FL3
      DIMENSION DTHR(200),T(200,4),PTPTO(10),FT(4,10)
      COMMON /A/ CONST,GAMMA1,GAMMA4,A4A1SQ,C1,C1SQ,CC3,CC4,C5,A4A1,C9
C      COMMON /B/ P5,T5,R1,MM,C8,DTHR,DTHRDT,T
      COMMON /B/ R1,MM,C8,DTHR,T
      COMMON /F/ PTPTO,FT
      PI=3.1416
      DTHR(1)=.0065
      PTPTO(1)=.2
      DO 80 I=1,4
      FT(I,NN)=MTOTAL*DSQRT(Y)*2*(1/PTPTO(I)**C8-1)
      &/((CONST2*PI*DTHR(1)**2/4*X
      &*(GAMMA1-1))
      J=I+1
      PTPTO(J)=PTPTO(I)+.2
C 80  CONTINUE
      RETURN
      END

C
C      SUBROUTINE EXPAN(THR1,DT1)

```

FILE: SHOCK2    FORTRAN    A1

```

C      REAL X1,X2,XTOL,FTOL,DT1,THR1
C      INTEGER I,NLIM,J
C      DIMENSION MT(200),DTEST(200),DTDTHR(5)
C      COMMON /A/ CONST,GAMMA1,GAMMA4,A4A1SQ,C1,C1SQ,CC3,CC4,C5,A4A1,C9
C      COMMON /C/ ATASTR,MT,DTEST,C9,DTDTHR
C      DTEST(1)=DT1
C      X1=1.0
C      XR=2
C      DO 30 J=1,2
C      X2=10
C      XTOL=0.001
C      FTOL=0.0001
C      I=0
C      NLIM=50
C      ATASTR=(DTEST(J)/THR1)**2
C      WRITE(*,*) THR1,DTEST(J),ATASTR
C      CALL INTHV(FCN3,X1,X2,XR,XTOL,FTOL,NLIM,I)
C      MT(I)=XR
C      X1=XR
C      K=J+1
C      DTEST(K)=(DTEST(J)+DT1)
C      DTDTHR(J)=DTEST(J)/DT1
C      WRITE(8,301) MT(J),DTDTHR(J),DTEST(J)
C300  FORMAT(2X,'MTEST',2X,'DTEST/DIUBE',2X,'DTEST')
C      WRITE(8,300)
C301  FORMAT(3(F9.2))
C 30  CONTINUE
C      RETURN
C      END

C
C      SUBROUTINE TCOND(Z1,P5,T5,PT,TT,TIME,THR1,C10)
C      REAL *8 P5,T5,TT,TIME,Z1,THR1,B,C10
C      COMMON /A/ CONST,GAMMA1,GAMMA4,A4A1SQ,C1,C1SQ,CC3,CC4,C5,A4A1,C9
C      COMMON /E/ DTRH(200),T(200),MT,DTHRDT,MM,C8
C      COMMON /B/ R1,MM,C8,DTHR,T
C      WRITE(*,403)
C      WRITE(*,404) Z1,P5,PT,T5,TT,C10
C      WRITE(*,*) C10
C      A5=SQRT(GAMMA1*R1*T5)
C      PT=P5/(1+(GAMMA1-1)/2*Z1**2)**C10
C      TT=T5/(1+(GAMMA1-1)/2*Z1**2)
C      B IS THE ANGLE OUT OF THE THROAT 30 DEGREES
C      B=TAN(15*3.1416/180)
C      TIME=0
C      TIME=.76*THR1/(2*B*A5)*((DSQRT(Z1))*(1-1/Z1)
C      &+1/15*((DSQRT(Z1))**3-1)+1/25*((DSQRT(Z1))**5-1))
C403  FORMAT(2X,'MACH',6X,'P5 =',6X,'PT',5X,'T5',8X,'TT',5X,'TSTART')
C      WRITE(*,404) Z1,P5,PT,T5,TT,C10,TIME
C404  FORMAT(7(D9.2))
C      RETURN
C      END

C      -----
C
C      SUBROUTINE INTHV(FCN,X1,X2,XR,XTOL,FTOL,NLIM,I)
C
C      -----
C      THIS ROUTINE WAS DEVELOPED BY PROF. MILLER DEPT AERONAUTICS
C      SUBROUTINE INTHV :
C      THIS SUBROUTINE FINDS THE ROOTS OF A FUNCTION ,
C      F(X) = 0, BY INTERVAL HALVING.
C
C      -----
C
C      PARAMETERS ARE :
C      FCN      -FUNCTION THAT COMPUTES VALUES FOR F(X).MUST BE DECLARED
C                EXTERNAL IN CALLING PROGRAM.IT HAS ONE ARGUMENT, X.

```

FILE: SHOCK2    FORTRAN    A1

```
C    X1,X2        -INITIALS VALUES OF X.F(X) MUST CHANGE SIGN AT THESE PTS
C    XR          -RETURNS THE ROOT TO THE MAIN PROGRAM.
C    XTOL,FTOL    -TOLERANCE VALUES FOR X,F(X) TO TERMINATE ITERATIONS.
C    NLM         -LIMIT TO NUMBER OF ITERATIONS.
C    I            -A SIGNAL FOR HOW ROUTINE TERMINATED.
C        I=1       MEETS TOLERANCE FOR X VALUES.
C        I=2       MEETS TOLERANCE FOR F(X)
C        I=-1      NLM EXCEEDED.
C        I=-2      F(X1) NOT OPPOSITE IN SIGN TO F(X2)
C    WHEN THE SUBROUTINE IS CALLED,THE VALUE OF I INDICATES WHETHER TO
C    PRINT EACH VALUE OR NOT.I=0 MEANS PRINT THEM,I.NE.0 MEANS DON'T.
```

```
C    -----
C                REAL FCH,X1,X2,XR,XTOL,FTOL
C                INTEGER NLM,I,J
C                REAL F1,F2,FR,XERR
```

```
C    -----
C    CHECK THAT F(X1) & F(X2) DIFFER IN SIGN.
```

```
C                F1 = FCH(X1)
C                F2 = FCH(X2)
C                IF (F1*F2 .GT. 0.0) THEN
C                    I=-2
C                    PRINT 201
C                    RETURN
C                END IF
```

```
C    -----
C    COMPUTE SEQUENCE OF POINTS CONVERGING TO THE ROOT
```

```
C                DO 20 J=1,NLM
C                XR = (X1+X2)/2.0
C                FR = FCH(XR)
C                XERR = ABS(X1-X2)/2.0
C                IF (I .EQ. 0.0) THEN
C                    PRINT 199, J,XR,FR
C                END IF
```

```
C    -----
C    CHECK ON STOPPING CRITERIA
```

```
C                IF ( XERR .LE. XTOL) THEN
C                    I=1
C                    PRINT 202, J,XR,FR
C                    RETURN
C                END IF
```

```
C                IF ( ABS(FR) .LE. FTOL ) THEN
C                    I=2
C                    PRINT 203, J,XR,FR
C                    RETURN
C                END IF
```

```
C    -----
C    COMPUTE NEXT X
```

```
C                IF ( FR*F1 .GT. 0.0 ) THEN
C                    X1=XR
C                    F1=FR
C                ELSE
C                    X2=XR
C                    F2=FR
C                END IF
C                20 CONTINUE
```

FILE: SHOCK2    FORTRAN   A1

```
C -----
C
C WHEN LOOP IS NORMALLY COMPLETED,NLIM IS EXCEEDED
C
C      I=-1
C      PRINT 200, NLIM,XR,FR
C      RETURN
C -----
C
C 199  FORMAT(' AT ITERATION',I3,3X,' X=',E12.5,4X,' F(X) =',E12.5)
C 200  FORMAT(/' TOLERANCE NOT MET AFTER ',I4,' ITERATIONS  X =',
C      1      E12.5,' F(X) = ',E12.5)
C 201  FORMAT(/' FUNCTION HAS THE SAME SIGN AT X1&X2')
C 202  FORMAT(/' TOLERANCE MET IN ',I4,' ITERATIONS  X =',E12.5,
C      1      ' F(X) = ',E12.5)
C 203  FORMAT(/' F TOLERANCE MET IN  ',I4,' ITERATIONS X = ',E12.5,
C      1      ' F(X) =',E12.5)
C      END
C -----
C
```

### LIST OF REFERENCES

1. Dunn, M.G. and Lori, "AIAA-89-0184 Facility Requirements for Hypersonic Propulsion System Testing," paper presented at 27th Aerospace Meeting, Reno, Nevada, 9-12 January 1989.
2. Gaydon, A.G., and Hurle, J.R., The Shock Tube in High Temperature Chemical Physics, Reinhold Publishing Corporation, 1963.
3. Owezarck, J.A., Fundamentals of Gas Dynamics, International Textbook Company, 1964, pp. 395-398.
4. Penaranda, F.A., Shock Tube Investigation of Thermal Conductivity in Noble Gases, Master's Thesis, Naval Postgraduate School, Monterey, California, April 1969.
5. Cornell Aeronautical Laboratory, Inc., Report No. AD-1052-A-12, Summary of Shock Tunnel Development and Applications to Hypersonic Research, July 1961.
6. Cornell Aeronautical Laboratory, Inc., Report No. AD-1052-A-7, Modification of the Basic Shock Tube to Improve Its Performance, by A. Russo and A. Hertzberg, August 1968.
7. AVCO Research Laboratory, Hypersonic Gas Dynamic Charts for Equilibrium Air, by S. Feldman, May 9, 1957, pp. 93,96.
8. Smith, E., "The Starting Process of a Hypersonic Nozzle," Journal of Fluid Mechanics, Vol. 24, pp. 625-640.
9. Baum, F.L., and Gyarmathy, G., "Condensation of Air and Nitrogen in Hypersonic Wind Tunnels," AIAA Journal, Vol. 6, No. 3, p. 460.
10. Ministry of Aviation Aeronautical Research Council Reports and Memoranda R&M No. 3398, The Change in Shock-Tunnel Tailoring Mach Numbers Due to Driver Gas Mixtures of Helium and Nitrogen, by L. Pennelegion and P.J. Gough, Her Majesty's Stationery Office, 1965.
11. PCB Piezontronics, Inc., Transducer Instrumentation Model 124A Water Cooled Pressure Transducer Operating Instructions, 1968.

12. Kistler Instrument Corporation, Model 504A Dial Gain Charge Amplifier, March 1968.
13. Tektronix, Inc., Instruction Manual Type 549 Storage Oscilloscope, 1975.
14. Tektronics, Inc., Instruction Manual Type 551 Dual Beam Oscilloscope, 1975.
15. Scientific Atlantic Spectral Dynamics Division, Operator's Manual SD380A Signal Analyzer P/N 22088100, June 1986.
16. Aerolabs, Operating Instructions for Aerolab Schlieren System for Naval Postgraduate School, Naval Postgraduate School, Monterey, California, 1981.
17. Red Lake Laboratories, Inc., Hycam Instruction Manual, Morgan Hill, California, 1968.
18. NAVORD Report 1488 (Vol. 6), Handbook of Supersonic Aerodynamics, Section 18, Shock Tubes, by I.I. Glass and J.G. Hall, December 1959.
19. Aeronautical Research Council Report 22.778, Tabulated Solutions of Equilibrium Gas Properties Behind the Incident and Reflected Normal Shock-Wave in a Shock Tube, I--Nitrogen, II--Oxygen, by L. Bernstein, 4 April 1961. UNCLASSIFIED
20. Stalker, R.J., "A Study of the Free-Piston Shock Tunnel," AIAA Journal, Vol. 5, pp. 2160-2167, 1967.
21. Stalker, R.J., "The Free-Piston Shock Tube," The Aeronautical Quarterly, November 1966, pp. 351-369.
22. Stalker, R.S., "Development of a Hypervelocity Wind Tunnel," Aeronautical Journal, June 1972, pp. 374-381.

INITIAL DISTRIBUTION LIST

	No. Copies
1. Defense Technical Information Center Cameron Station Alexandria, Virginia 22304-6145	2
2. Library, Code 0142 Naval Postgraduate School Monterey, California 93943-5002	2
3. Commander, Naval Air Systems Command Naval Air Systems Command Headquarters Propulsion and Power Division (AIR-5362) Washington, D.C. 20361-5360	2
4. Chairman, Code 67 Department of Aeronautics and Astronautics Naval Postgraduate School Monterey, California 93943-5000	1
5. Prof. David Netzer, Code 67Nt Naval Postgraduate School Monterey, California 93943-5000	1
6. Prof. Raymond Shreeve, Code 67Sf Naval Postgraduate School Monterey, California 93943-5000	6
7. Prof. Daniel Collins, Code 67Co Naval Postgraduate School Monterey, California 93943-5000	1
8. Prof. Richard Wood, Code 67Wr Naval Postgraduate School Monterey, California 93943-5000	1
9. Michael H. Sherman 3004 Fairhill Road Fairfax, Virginia 22031	3
10. Mr. Jack King, Code 67Jk Naval Postgraduate School Monterey, California 93943-5000	1